AUTOMATED OPTIMUM DESIGN AND RELIABILITY ANALYSIS OF MACHINE TOOL STRUCTURES

A Thesis Submitted
in partial Fulfilment of the Requirements
for the Degree of

DOCTOR OF PHILOSOPHY

By

CHALLA PAPI REDDY

to the

DEPARTMENT OF MECHANICAL ENGINEERING

INDIAN INSTITUTE OF TECHNOLOGY KANPUR

DECEMBER, 1975

IN MEMORY OF

MY MOTHER

ME-1975-D-RED-AUT

30/12/75

CERTIFICATE

This is to certify that the thesis entitled AUTOMATED OPTIMUM DESIGN AND RELIABILITY ANALYSIS OF MACHINE TOOL STRUCTURES by Mr. Challa Papi Reddy for the award of the degree of Doctor of Philosophy is a record of bonafide research work carried out by him under my supervision, and has not been submitted elsewhere for a degree.

S S Rao

(Dr. S. S. Rao)
Assistant Professor
Department of Mechanical Engineering
Indian Institute of Technology
Kanpur

December, 1975

ACKNOWLEDGEMENTS

The author expresses his appreciation and deep sense of gratitude to his advisor, Dr. S.S. Rao, for his able guidance, inspiration and constant encouragement throughout this investigation.

The author also expresses his appreciation and gratitude to Prof. A. Ghosh for his valuable suggestions in connection with chatter stability analysis in machine tools.

The author thanks Dr. M. Hariharan, Dr. C.P. Vendhan and Sri P. K. Nath for their helpful discussions. He thanks many of his colleagues and friends for their help during computation and thesis preparation.

The author is grateful to Regional Engineering College, Warangal for sponsoring him to I.I.T. Kanpur under the Quality Improvement Programme of Govt. of India.

The computer programs were perfected in the IBM 7044 computer at I.I.T. Kanpur. The authorities at I.I.T. Kanpur readily gave the permission to obtain the final results in the IBM 370/155 system at IIT Madras.

Finally, the author thanks his wife, Vijaya and his daughters, Sucharitha and Sunita, for their understanding, patience and encouragement.

CHALLA PAPI REDDY

CONTENTS

LIST OF TABLES

LIST OF FIGURES

LIST OF IMPORTANT SYMBOLS

B	:	Width of engagement
B_{LIM}	:	Limiting chip width
c	:	Cutter centre location
d	:	Depth of cut
d_c	:	Maximum deflection of the cutter centre
d_L	:	Angle of twist of lathe bed
$d_c^{(u)}$	:	Upper bound on maximum deflection of cutter centre
$d_L^{(u)}$	:	Upper bound on the angle of twist of lathe bed
D	:	Diameter of the milling cutter
E	:	Young's modulus
f	:	Objective function
$\bar{f}$	:	Mean value of the objective function
F_T	:	Tangential force on the milling cutter
F_R	:	Radial force on the milling cutter
F_H	:	Horizontal force on the milling cutter
F_V	:	Vertical force on the milling cutter
F_A	:	Axial force on the milling cutter
F_A	:	Feed force on lathe tool
F_N	:	Cutting force on the lathe tool
g_j	:	j^{th} inequality constraint
G	:	imphase cross-receptance

G_{MIN}	:	Minimum negative inphase cross receptance of cutter centre relative to table
$\lvert G_{MIN}^{(u)} \rvert$	:	Upper bound on absolute value of G_{MIN}
H	:	Imaginary component of cross receptance
$[H_i]$	:	Symmetric positive definite matrix in variable metric method
[I]	:	Identity matrix
k	:	constant in milling
[K]	:	elemental stiffness matrix
$[K]_p$	:	In plane stiffness matrix
$[K]_b$	:	Bending stiffness matrix
$[\bar{K}]$	:	Master stiffness matrix
$[\tilde{K}]$	:	Generalized stiffness matrix in Ritz coordinates
L	:	Load
[L]	:	Transformation matrix
m	:	Number of constraints
$[\bar{M}]$	:	Master stiffness matrix
$[\tilde{M}]$	:	Generalized stiffness matrix in Ritz coordinates
n	:	Number of design variables
N	:	Number of degrees of freedom
N_p	:	Number of plate elements
N_F	:	Number of frame elements
p	:	Number of first few modes
P	:	Load
$P_T\rvert_{avg}$	:	Average tengential force in plain milling

$\vec{P}$: Load vector

P_f : Probability of failure

$P_{f_{ij}}$: Probability of failure of i^{th} member due to j^{th} load

r : Coupling constant

r_{LIM} : Limiting value of r

r_k : k^{th} penalty parameter

R : Strength

$\bar{R}$: Mean value of R

R_o : Reliability of the system

$(R_o)_{overall}$: Overall reliability of the system

s_t : Feed per tooth in plain milling

$\vec{s}_i$: i^{th} search vector

s : Number of random variables

t : Thickness of plate element

t_m : Maximum undeformed dip thickness

t_{avg} : Average uncut chip thickness in plain milling

u : displacement in x-direction

$[\bar{U}]$: $[\bar{M}]$-orthonormal model matrix

v : feed rate

v : displacement in x-direction

V_j : Volume of j^{th} element

V : Cutting velocity

V_{x_i} : Coefficient of variation of i^{th} design parameter

w : Displacement in z-direction

x, y, z: Cortesian coordinates

$\bar{x}_i$: Mean value of i^{th} random variable

X_j : j^{th} design variable

$\vec{X}_i$: i^{th} design vector

$\vec{Y}$: Displacement vector

$\vec{Y}, \vec{Y}_i$: Eigen vector

Z : Number of teeth on milling cutter

Z_i : Number of teeth in engagement

ρ_j : Density of j^{th} element

ρ : Density

ζ_i : Damping factor

ω_i : i^{th} natural frequency of vibration

θ : Helix angle of milling cutter

ψ : The angle of engagement

ψ_i : Angle of engagement of i^{th} tooth

ψ_{yi} : Angle between the i^{th} tooth and normal to the cut surface

λ : Friction angle

λ : Eigen value

$[\lambda]$: Transformation matrix

γ : Normal rake angle

ϕ : Shear angle

ϕ : Penalty function

Φ : Absolute cross-receptance

τ_s : Dynamic shear stress

$\vec{\eta}$: Modal coordinates

ν : Poisson's ratio

σ_R : Standard deviation of R.

SYNOPSIS

CHALLA PAPI REDDY
Ph.D.
Department of Mechanical Engineering
Indian Institute of Technology Kanpur
December 1975

AUTOMATED OPTIMUM DESIGN AND RELIABILITY ANALYSIS OF MACHINE TOOL STRUCTURES

A computational capability for the automated optimum design of complex machine tool structures to satisfy static rigidity, natural frequency and regenerative chatter stability requirements is developed in the present work. More specifically, the minimum weight design of Warren type lathe bed and horizontal knee type milling machine structures using finite element idealization is considered in this exploratory study. The Warren type lathe bed is optimized to satisfy torsional rigidity and natural frequency requirements, whereas, the milling machine structure is optimized with static rigidity of the cutter centre, natural frequency and regenerative chatter stability constraints.

A survey of the available literature indicates that the use of computers in the machine tool manufacturing industry has up to the present time been confined to the implementation of finite element technique for the purpose of static and dynamic analysis only and the potentialities of optimization techniques have not yet been exploited by the machine tool structural designers.

In designing these structures, the most unfavourable cutting conditions and sizes of work piece are taken into account. The torsional deflections and the first two natural frequencies of vibration are the behavior constraints in the design of lathe beds. In the design of horizontal milling machine structures, the maximum deflection of cutter centre in any direction, the natural frequencies of vibration and the minimum negative inphase cross-receptances of cutter centre relative to the table (G_{MIN}) are the behavior constraints. The constraint on G_{MIN} is for regenerative chatter stability of the milling machine.

In the design of lathe bed, the thickness of the main members, thickness of the lacing diagonals, the width and the thickness of the flanges (stiffeners) on the main members and lacing diagonals and the width of the bed are considered as design variables. In the case of milling machine, the thickness of over-arm, the thickness of column and table, the depth of the column at the base, the depth of the column at the top end, the width of the machine, and the cross sectional area of ribs on the over-arm and its joint with the column are taken as design variables.

The idealisation using triangular plate elements with a 3-term in-plane and a 9-term transverse displacement model and frame elements has been found to be efficient. The triangular plate elements are used to idealise the main members and lacing diagonals of lathe bed, and the column, over-arm and table of

milling machine structures. The frame elements are used to idealise the carriage guides (guides on the lathe bed), stiffeners on the main members and the lacing diagonals of lathe bed. In the case of milling machine, the frame elements are used to model the ribs on the over-arm, the over-arm joint with the column, the arbor and the arbor support. The grouping of identical and identically disposed finite elements (having the same transformation matrix from elemental to global coordinate system) has resulted in savings of about 20% to 80% of the computer time in generating the global stiffness and mass matrices.

The cholesky decomposition of symmetric banded matrices has efficiently been applied in solving the equilibrium equations and in obtaining a partial solution of the eigenvalue problem by Rayleigh-Ritz sub-space iteration algorithm. This algorithm solves the eigenvalue problem directly without a transformation to the standard form. This method is the most efficient one for solving a partial eigen solution of large structural systems. The receptances of the cutter centre relative to the table of horizontal milling machines have been obtained by using modal coordinates taking the damping matrix as a linear combination of the stiffness and mass matrices.

The constrained optimum design problem is cast as a non-linear mathematical programming problem. The interior penalty function method, with a variable metric unconstrained minimization

technique, is used to solve the minimum weight design problems. The computation of the gradient and the slope of the ϕ-function has been carried out by a finite difference method which incorporates the rates of change of the response quantities with respect to the design variables. The computational experience shows that the approximate methods used in the reanalysis cycle of optimization have been quite efficient and reliable.

In the design of horizontal milling machine structures, the value of the minimum negative inphase cross receptance of the cutter centre relative to the table (G_{MIN}) has been computed for the most common range of cutting conditions.

The coupling constants for plain milling operation (for the most common cutting range) have been computed both by using the basic theory of metal cutting and by using an empirical formula, suggested by Vulf, which computes the average tangential force in plain milling. A close agreement is found between the values obtained from the two methods. The critical value of the coupling constant (r_{LIM}) has been selected from this analysis to obtain a bound on G_{MIN}.

The design examples of lathe bed indicate that the thicknesses of both the main members and lacing diagonals assume their minimum permissible values at the optimum point. The widths and thicknesses of the flanges on the main members and lacing diagonals also

decreased from the starting design. This establishes that in this type of structures, thin walled structures are preferable. The width of the lathe bed increased such that the corresponding lacing angle became 53.5° at the optimum. This value of lacing angle at optimum agrees very well with the results obtained by Badauri, Moshin and Thornly who analysed and tested a number of Warren type beams under static torsional loads.

The optimization results of horizontal milling machine show that the thickness of the over-arm, the column and the table decreased as the optimization progressed. Therefore the results indicate that even in milling machines, thin walled structures are preferable. The cross sectional dimensions of ribs on the over-arm and its joint with the column also decreased. At the optimum, the over-all dimensions of the milling machine are: depth at the base of the column is 50.12 cm. depth at the top of the column is 41.5 cm. and the width of the machine is 28.8 cm. In the design of horizontal milling machines these over-all dimensions are very important.

At initial and optimum designs, the reliability study of milling machine structures is made against the three response quantities i.e., deflection of cutter centre (d_c), first natural frequency of vibration (ω_1), and G_{MIN}. The average height of the table (h), the position of the cutter centre (c), modal damping factors (ζ_i), Young's modulus and the load on the machine (P) are taken as probabilistic quantities. A comparison of reliability results at initial and optimum designs is made. A sensitivity of the reliabilities with respect to the coefficient of variation of the various random design parameters is also conducted. A method of including reliability analysis in the optimum design procedure is also indicated.

CHAPTER 1

INTRODUCTION

It is customary to base the structural design of any machine tool primarily upon the requirements of static rigidity and minimum natural frequency of vibration. The effects of different machining parameters like cutting speed, feed and depth of cut as well as the size of the work piece also have to be kept in mind by a machine tool-structural designer. For a tentative design, the machine tool is analysed for various natural frequencies, dynamic rigidity and chatter stability. Based on the results of this analysis, suitable modifications are made, by a process of trial and error, to satisfy the design requirements. This procedure of trial and error is adopted mainly because of the complex nature of machine tool structures and also because of the lack of a suitable design procedure that can handle all the requirements simultaneously. Moreover, the modifications to satisfy the design requirements are often not very extensive. This is mainly because of the fact that the designers seek minor improvements over the existing designs. On the other hand, if altogether new design specifications have to be satisfied, these trial and error methods are not useful and only unified procedures like the automated optimum design methods are applicable in such situations. Hence it becomes necessary to develop design procedures that can consider all the design requirements simultaneously.

The dynamic stiffness of any machine tool structure has an important influence upon both surface finish and metal removal rate. Thus to achieve a high quality surface finish, forced vibration amplitudes must be controlled whilst in the interests of high metal removal rate the machine should have high dynamic stiffness to resist the onset of self excited vibrations, commonly known as chatter.

The aim of the present work is to develop a capability for the automated optimum design of machine tool structures to satisfy static rigidity, natural frequencies and chatter stability requirements. Since the cutting conditions vary substantially in a machine tool, the necessity of analysing its structural reliability becomes important. Hence the reliability analysis of machine tool structures is also considered in the present work.

1.1 REVIEW OF LITERATURE

Since the present work deals with the machine tool structural analysis, structural optimization and reliability analysis, a brief review of the available literature in each of these fields is given in the following sections.

1.1.1 Machine Tool Structural Analysis

The use of computers in the machine tool manufacturing industry has up to the present time been confined to the implementation of finite element technique for the purpose of static

and dynamic analysis only. The first publication describing a formalised digital computer method for calculating the deformation of machine tool structures appeared in 1964[1]. In this paper, Taylor and Tobias described the application of a finite element program involving the use of slender beams to represent the structural parts of a radial arm drill and a lathe. Since then a number of such applications have appeared in the literature. By idealizing the structure by frame elements, Cowley and Fawcett[2] analysed a plane milling machine for static deflections, natural frequencies and mode shapes. The authors have studied the effect of flexibilities between joints on natural frequencies and mode shapes. They found that for those mode shapes for which substantial deformation between joints is involved, the effect of joint flexibility is maximum. The static analysis of Warren type lathe beds was made by Badauri, Moshin and Thornley[3]. The authors have studied, both analytically and experimentally, the effects of breadth-to-depth ratios and lacing angles. They investigated the possibility of obtaining optimum stiffness-to-weight ratios of the Warren beams from their results. In reference 4, Thornley and Howes studied the static and dynamic behavior of Warren type beams by experimental methods.

As a co-operative programme during the period January 1970 to March 1971, a model milling machine was analysed for deflections, natural frequencies and modal shapes by a C.I.R.P. group (International

Institution for Production Engineering Research) in which professors from several European universities and one Japanese university participated[5,6]. They have used various types of finite elements like frame, triangular, rectangular and prismatic elements in analysing a milling machine structure. The primary objective of the collaboration was to compare the results obtained by using different finite element idealizations.

In the year 1960, Koenigsberger and Said[7] concluded that the danger of self excited vibrations would appear to be slight in the milling machine, but resonance vibrations due to fundamental frequency of cutting or any of its harmonics (forced vibration) would have to be carefully watched. Two years later, in 1962, working on a very similar type of machine, Andrews and Tobias[8] have come to precisely the opposite conclusion, namely, that self excited vibration was a significant limitation in horizontal milling, but forced vibration was relatively unimportant. The authors distinguished between forced vibration and chatter during horizontal milling. They found that forced vibration amplitude is proportional to the force fluctuation amplitude, while the onset of chatter depends on the force variation for a given amplitude of surface wave.

In reference 9, Taylor described a technique for predicting from design drawings the chatter stability of machine tool structures by computing responses to excitation from computed modes of

vibration and assumed damping constants. Out of several theories available for relating chatter stability to response loci[10,11,12], the author used regenerative chatter theory with penetration rate effects neglected[10]. This process is illustrated with reference to a lathe model and three versions of a milling machine. The authors established the superiority of machines with box type over-arm over those with bar type over-arm, as characterized by higher values of minimum stability under all cutting conditions.

Tlusty and Polacek, in reference 13, analysed the role of vibration of machine tool structures on the process of chatter with a scope to increase their stabilities for all possible cutting conditions. With reference to horizontal milling machines, these authors recognized the "weak links" of the structure and recommended maximum rigidity for the over-arm and its joint with the coloumn. They also recommended that the natural frequency of vibration corresponding to the vertical mode should be slightly higher than the one corresponding to the horizontal mode. The satisfaction of this requirement ensures a good stability in down-milling because of the advantageous interaction of both the modes. The effect of certain design features of horizontal milling machines was also investigated by Said[14]. Koenigsberger and Tlusty gave a state of art discussion of the machine tool structural design in 1971[15].

Yoshimura and Hoshi[16] developed computer program for the computation of structural dynamics and dynamic optimization of machine tool structures. Based on the energy equations of a

mechanical system at resonance, the authors developed an approach to the optimum design of a planar-type milling machine.

1.1.2 Structural Optimization

During the last few years, several optimization investigations have been reported in the fields of civil engineering and aircraft structural design. Using the method of feasible directions, Fox and Kapoor[17] reported a capability for the minimum weight optimum design of planar truss-frame structures with inequality constraints on the maximum dynamic displacement, stress and natural frequencies. McCart, Hang and Strecter[18] developed a steepest-descent boundary value method for the design of structures with constraints on strength and natural frequency. In reference 19, Turner attempted to minimize the mass of a structure with a specific natural frequency. Zarghamee[20] presented a method for the minimization of the lowest natural frequency of a structural system of given weight by varying the stiffness of its component elements. The author used the equations developed by Fox and Kapoor[21], to express the rates of changes of frequency with respect to the design parameters. In reference 22, Zarghamee considered the problem of the minimum weight design of a planar-truss structure with a general stability constraint. In this work, the gradient projection method of Rosen, in conjunction with the steepest-descent and alternate steps method of Schmit, was used for the optimum design of the descretized structure.

In the field of aircraft structural design, Schmit and Thornton[23], Giles[24] and Stroud, Dexter and Stein[25] attempted to solve various optimization problems. The automated minimum weight design of supersonic aircraft wings was attempted by Rao[26] by placing limitations on the natural frequencies, flutter mach number, the elastic deflection at the tip of the wing and the stresses induced in the skin at the root of the wing. In reference 27, Farshi and Schmit presented a method for the minimum weight design of stress and size limited trusses under multiple load conditions. When applied to a limited class of structures and a limited number of failure modes, the authors have achieved an acceptable efficiency with an opportunity to find a global minimum. Narasingam and Sridhar Rao[28] obtained a minimum weight design of linear elastic cantilever and simply supported trusses by solving a sequence of convex programming problems. The authors used linear constraints involving a smaller number of design variables instead of solving one mathematical programming problem with non linear constraints in a larger number of design variables. In reference 29, Twisdale and Kachaturian presented a generalized dynamic programming approach for the optimization of planar structural systems.

1.1.3 Reliability Analysis of Structures

When the parameters affecting the strength of a structure and the loads acting on it are statistical in nature, the conventional

design approaches based on the concept of "factor of safety" cannot be used to maintain a proper degree of safety. A more rational criterion, in the presence of random design parameters, will be to base the structural design on the concept of reliability or probability of failure. Reliability analyses in structural engineering recognize that both loads and strengths have statistical frequency distributions that must be considered in evaluating safety. Since the design parameters like cutting conditions, dimensions of the work piece and the location of the tool are random in nature in machine tools, an analysis, based on the principles of reliability, becomes important.

Freudenthal[30], in the year 1956, explained that the most rational way of describing the overall safety of structures is in terms of reliability or probability of failure. In reference 31, Moses and Kinser have demonstrated that an overall level of structural safety can be prescribed in terms of a rational criterion like probability of failure, and minimum weight structures can be designed to meet the prescribed safety level. In the year 1970, Moses and Stevenson[32] considered the subject of sensitivity of statistical parameters and presented methods of incorporating reliability analysis into optimum design of trusses and frames. Since then a number of such applications have appeared in literature[33,34,35] which show that a probabilistic design is a practical possibility.

Recently, the probabilistic design concepts have also been applied in the design of mechanical systems. Mischke[36] presented a formal relationship between the reliability and the factor of safety of a mechanical element. By treating the factor of safety as a random variable, he used Bienayme-Chabyshev and Camp-Meidell theorems to derive expressions for the mean and the variance of the factor of safety for any specified value of reliability. In reference 37, Rao has developed a probability based design method for the design of mechanical power transmission systems like gear trains. By idealizing the transmission system as a weakest-link kinematic chain (similar to a weakest-link structure), the design has been made to achieve a specified reliability with respect to bending and surface wear modes of failure.

1.2 OBJECTIVE AND SCOPE OF THE PRESENT WORK

It can be seen from the available literature that the potentialities of optimization techniques have not yet been exploited by the machine tool structural designers. This might be because of the complex nature of machine tool structures and the troublesome behavior constraints that arise due to the wide range of operating conditions in machine tools. In the present work, the automated minimum weight design of Warren type lathe bed and horizontal knee-type milling machine structures is considered. In designing these structures, the most unfavourable cutting conditions and sizes of the

work piece are taken into account. The torsional deflections and the natural frequencies are the behavior constraints in the design of lathe beds. In the case of design of milling machine structures, limitations are placed on the maximum cutter centre deflection, the natural frequencies of vibration and the minimum negative inphase cross receptance of the cutter centre relative to the table.

In order to predict the static and dynamic characteristics of a machine tool structure accurately and consistently, the structure has to be represented by a suitable model. The model must be simple enough from computational point of view for embedment into the iterative design-analysis loop of the optimization procedure.

In the present work, the finite element displacement method is used to model the machine tool structures. There are several ways of modelling the structure by the finite element method. Therefore it becomes necessary to make a comparative study of the various finite element idealizations to determine a suitable model for use in the optimization work. In this work, a study is undertaken to find the relative efficiencies of two different finite element idealizations for modelling machine tool structures. The idealization using triangular plate elements with a 3-term in-plane and a 9-term transverse displacement model[38,39,40] and frame elements has been found to be efficient. The triangular plate elements are used to idealize the main members and lacing diagonals of lathe beds,

and the coloumn, over-arm and table of milling machine structures. The frame elements are used to idealize the carriage guides stiffeners on the main members and on the lacing diagonals of lathe beds. In the case of milling machines, the frame elements are used to model the ribs on the over-arm, the over-arm joint with the coloumn, the arbor and the arbor support. In the present work, identically oriented finite elements of the same size and shape (having the same transformation matrix between local and global coordinate systems) are grouped together in generating element stiffness and mass matrices. This resulted in savings of about 20 to 80 percent of the computer time in generating the global stiffness and mass matrices.

For the dynamic optimization of large structures using finite element method, a designer is generally confronted with two problems, namely, the computer storage and the computer time. The eigen value problem has been solved by using one of the most efficient solution techniques developed by Bathe and Wilson for large structural systems[41]. In this technique the Rayleigh-Ritz sub-space iteration algorithm, which solves the eigen value problem directly without a transformation to the standard form, has been used. In this work, the Cholesky decomposition of symmetric banded matrices, storing only the upper triangular matrix, is used for solving the equilibrium equations. By using a judicious descretization and node numbering scheme, it has been possible to reduce the band width of the stiffness

matrix of the structure. A smaller band width, apart from reducing the computer storage, considerably reduces the computer time for static and eigen solutions.

The frequency response of the structure has been obtained by using modal coordinates, and by taking the damping matrix proportional to a linear combination of stiffness and mass matrices. Since the present day knowledge is not sufficient to estimate the modal damping factors from the blue prints of a given structure, the values of damping factors have to be obtained from experimental results on similar structures. In the present work, equal modal damping factors of value 0.06 have been used for the first few modes.

In machine tools, chatter occurs due to the interation of the cutting forces and the machine tool structural dynamics. To derive the limits of chatter stability for the machine tool and the cutting system, it is necessary to assume a force relationship for the cutting process and relate this to the machine dynamics. In this work, a simple dynamic cutting force relationship, assuming a direct proportionality between the force and the undeformed chip thickness, is taken. No definite criterion has been established so far for taking the critical proportionality constants between the force and the undeformed chip thickness in plain milling operation. In the present work, a study of proportionality constants in plain milling has been made to choose a critical value for incorporating in the chatter stability constraint. A method of including the

minimum negative inphase cross-receptance of cutter centre relative to table (in the design) is also developed in this work.

The constrained optimum design problem is cast as a nonlinear mathematical programming problem. The interior penalty function method, with a variable metric unconstrained minimization technique, is used to solve the minimum weight design problem. The minimizing step lengths in the unconstrained minimization are determined by the cubic interpolation method. The computation of the gradient and the slope of ϕ-function has been carried out by a finite-difference method which incorporates the rates of changes of the response quantities with respect to the design variables. In the design of the lathe bed, the main dimensions of the lathe bed, the thickness of the main members and lacing diagonals, and the cross sectional areas of their stiffeners are taken as design variables. In the case of milling machine, the overall dimensions and thickness of the column and the over-arm, and the cross sectional dimensions of ribs on the over-arm and on its joint with the column are assumed to be the design variables. The optimum design of a lathe bed and a milling machine structure are considered to illustrate the effectiveness of the method proposed.

In the optimum design of machine tool structures, all the design parameters have been assumed to be deterministic. However, in actual practice, most of the design parameters like the cutting conditions, the material and the structural properties vary considerably.

Hence the development of a more relastic analysis procedure, which takes the variability of the design parameters into account, becomes important. The present work aims at developing a method for the reliability analysis of machine tool structures by considering the various design parameters as random variables with known probability distributions. The reliability against any specified criterion like static rigidity, frequencies and dynamic response of the machine tool structures has been analysed by treating the machine tool structure as a single member acted on by a single load. All the random variables are assumed to be normally distributed for simplicity. The linearization using Taylor's series expansion (about the mean values of the random variables) has been used in deriving the expected value and the variance of a function of several random variables. The reliability analysis of the milling machine structure, considered in the optimization work, has been presented to illustrate the method developed.

1.3 ORGANIZATION OF THE THESIS

The thesis is organized into 9 chapters and 2 appendices. The formulation of the optimization problem is given in Chapter 2. Chapter 3 deals with a comparative study of two different finite element idealizations for modelling different machine tool structures. The static and eigen value results obtained for different structures have been compared with those available in

the literature. The idealization, for which the results compared closely with the known results, has been finally selected for use in the optimization program .

The expressions for the cutting forces developed in lathe and horizontal milling machines are derived in Chapter 4. This chapter gives a discussion of the regenerative chatter stability in horizontal milling machines. A method of including the regenerative chatter stability constraint in the optimization problem has also been developed in this chapter. Chapter 5 deals with the static and the dynamic analysis of machine tool structures. The algorithm used for the eigen value analysis is discussed in some detail.

Chapter 6 gives a discussion of the optimization algorithm used in the present work. The computation of the gradients of the response quantities along with the results of the approximate analyses are presented in this chapter. Some illustrative examples are given in Chapter 7 to demonstrate the effectiveness of the present approach for the design of machine tool structures under static and dynamic constraints.

The reliability analysis of machine tool structures is the subject matter of Chapter 8. A method of incorporating the reliability constraint in the optimum design of machine tool structures is indicated in this chapter. Finally, the conclusions

drawn from the present study and the recommendations for future research are given in Chapter 9.

The generation of the stiffness and mass matrices of a triangular plate bending element in the global coordinate system, by considering both in plane and bending actions, is described in appendix A. Appendix B contains the description and other details of computer program.

CHAPTER 2

FORMULATION OF THE DESIGN PROBLEM

When a means for predicting the behavior of any design is available, when limitations on the performance and other external constraints on the design can be stated and when some acceptance critaria can be established, a design modification problem can be cast as a mathematical programming problem.

2.1 DESIGN PHILOSOPHY

Any structural design problem can be formulated and solved according to either deterministic or probabilistic design philosophy. If all the quantities affecting the design problem are deterministic, the design problem can be solved according to the deterministic design philosophy. On the other hand, if some of the design parameters are random in nature, the design problem has to be solved according to the probabilistic design philosophy.

In the deterministic design philosophy, a general mathematical programming problem can be stated as follows :

Minimize a multivariable function $f(\vec{X})$ subject to the constraints

$$\left.\begin{array}{l} g_j(\vec{X}) \leq 0, \; j = 1,m \\ \text{where } \vec{X} \text{ is a n-dimensional vector consisting of the variables } X_1, X_2, \ldots, X_n. \end{array}\right\} \qquad (2.1)$$

In the probabilistic design philosophy, a general mathematical programming problem can be stated as follows :

$$\left.\begin{array}{l} \text{Minimize a multivariable function } \bar{f}(\vec{X},\vec{Y}) \\ \text{Subject to the probabilistic constraints} \\ P\,[g_j(\vec{X},\vec{Y}) \leq 0] \geq p_j, \qquad j = 1,2,\ldots,m. \end{array}\right\} \tag{2.2}$$

where $\vec{X}$ is the vector of design variables, and $\vec{Y}$ is the vector of other parameters affecting the design problem. Here the components of $\vec{X}$ and $\vec{Y}$ are assumed to be random variables. In equation 2.2, $\bar{f}$ represents the mean value of the objective function, and $P\,[g_j(\vec{X},\vec{Y}) \leq 0] \geq p_j$ denotes that the j^{th} constraint has to be satisfied with a probability of greater than or equal to some specified quantity, p_j $(j = 1,2,\ldots,m)$, where $0 \leq p_j \leq 1$.

In the present work, only the deterministic design philosophy is used for the optimization of machine tool structures.

2.2 OBJECTIVE FUNCTION

The function $f(\vec{X})$ in equation 2.1 is called the objective or criterion function and its choice is governed by the nature of the problem. The objective of any structural optimization problem is generally taken as minimization of weight or cost. The minimization of weight is more frequently taken as the objective since weight can be easily quantified and it reflects the material costs and, in some cases, the manufacturing and the transportation costs. The minimization of the weight of the structure is taken as the objective in the design of Warren type lathe bed and horizontal knee-type milling machine structures. The maximization of static rigidity or natural frequency of vibration or dynamic

rigidity of the machine tool structure can also be taken as objective function in some cases.

Although, only the deterministic design philosophy is used for the optimization of machine tool structures, an attempt is made to analyse the behavior of milling machine structures by taking the following quantities as probabilistic :

i) the cutting conditions, ii) the material properties of the structure iii) the modal damping factors, iv) the position of the cutter and v) the position of the table. Suggestions are given for incorporating the probabilistic analysis for designing machine tool structures according to the probabilistic design philosophy.

2.3 DESIGN CONSTRAINTS

The design requirements to be satisfied in the case of Warren-type lathe bed are i) the torsional rigidity must be greater than a specified quantity and ii) the natural frequencies of the structure are to be excluded from certain bands. In the case of milling machine, the design constraints are i) the maximum deflection of the centre of the cutter in any direction should not exceed a certain prescribed value ii) The natural frequencies of the structure are to be excluded from certain bands, and iii) The machine should not chatter under the stated cutting conditions. These constraints are stipulated so as to achieve a

high quality surface finish, to avoid mild harmonic forcing that might cause resonance and to increase the metal removal rate which may be affected due to the onset of chatter. In the design of metal cutting machine tools, the static and dynamic stiffness requirements are often more important than the load carrying capacity requirements since the induced stresses corresponding to the permissible deformations are generally far less in value than those permissible for the various materials. This characteristic has been observed in the present work also. Hence the strength was not considered as a design constraint in the present work.

2.4 DESIGN VARIABLES

Once the objective function and the design constraints are specified, the statement of the optimization problem will be complete as soon as the design variables are identified.

2.4.1 Lathe Bed

The details of a Warren-type lathe bed are shown in Fig. 2.1. The following parameters are taken as the design variables in the present work :

X_1 = thickness of the main members

X_2 = thickness of the lacing diagonals

X_3 = stiffener width on the main and lacing diagonals

X_4 = stiffener depth on the main and lacing diagonals

X_5 = width of the lathe bed

2.4.2 Milling Machine Structure

The structural details of a horizontal knee-type milling machine are shown in Fig. 2.2. In this case, the following quantities are considered as the design variables :

X_1 = column depth at the bottom

X_2 = thickness of the over-arm

X_3 = width of the machine

X_4 = thickness of the column and table

X_5 = column depth at the top

X_6 = square cross-sectional dimensions of the ribs on the over-arm and its joint with the column.

2.5 OPTIMIZATION PROBLEM

The complete optimization problem can now be stated as follows.

i) For lathe bed

Minimize

$$f(\vec{X}) = \sum_{j=1}^{N_P} V_j \rho_j + \sum_{j=1}^{N_F} V_{j+N_p} \rho_{j+N_p} \qquad (2.3)$$

subject to

$$d_L^{(u)} - d_L \geq 0 \qquad (2.4)$$

$$\omega_1 - \omega_1^{(\ell)} \geq 0 \qquad (2.5)$$

$$\omega_2 - (\omega_1 + 100) \geq 0 \qquad (2.6)$$

and

$$X_j^{(\ell)} \leq X_j \leq X_j^{(u)} \quad , \quad j = 1,2,\ldots,n \tag{2.7}$$

ii) For milling machine :

Minimize

$$f(\vec{X}) = \sum_{j=1}^{N_p} V_j \rho_j + \sum_{j=1}^{N_F} V_{j+N_p} \rho_{j+N_p} \tag{2.8}$$

subject to

$$d_c^{(u)} - d_c \geq 0 \tag{2.9}$$

$$\left|G_{MIN}^{(u)}\right| - \left|G_{MIN}\right| \geq 0 \tag{2.10}$$

$$\omega_1 - \omega_1^{(\ell)} \geq 0 \tag{2.11}$$

$$\omega_2 - (\omega_1 + 100) \geq 0 \tag{2.12}$$

and

$$X_j^{(\ell)} \leq X_j \leq X_j^{(u)} \quad , \quad j = 1,2,\ldots,n \tag{2.13}$$

where

$f(\vec{X})$ = weight of the structure (objective function)

V_j = volume of the j^{th} finite element (the area and the thickness of the plate are variables in case of plate elements, and the (square) cross-sectional area and the length are variables in case of frame elements).

ρ_j = density of j^{th} element

X_j = j^{th} design variable (superscript 'L' and 'U' indicate the lower and the upper limits on X_j)

N_p = number of plate elements

N_F = number of frame elements in which the design variables are involved.

d_L = angle of twist of one end of lathe bed when the other end is fixed

$d_L^{(u)}$ = upper bound on the angle of twist of one end of lathe bed when the other end is fixed

d_c = maximum deflection of the cutter centre (milling machine) in any direction

$d_c^{(u)}$ = upper bound on the maximum deflection of cutter centre (milling machine) in any direction

G_{MIN} = minimum negative in phase cross receptance of the cutter centre relative to the table (milling machine)

$G_{MIN}^{(u)}$ = upper bound on the minimum negative in phase cross receptance of the cutter centre relative to the table (milling machine)

$\omega^{(\ell)}$ = lower bound on the first natural frequency of vibration

ω_j = j^{th} natural frequency of vibration

Here the quantities d_L, d_c, G_{MIN} and ω_j are implicitly dependent on the design variables X_i and therefore the constraint equations (2.4) to (2.6) and (2.9) to (2.12) are called the behavior constraints. The method of evaluating the behavior quantities is discussed in chapters 4 and 5. Equations (2.7) and (2.13) represent the geometrical or side constraints, which

impose limitations on the size of the design variables. The geometrical constraint equations are linear where as the behavior constraints and the objective function are nonlinear and hence the problem formulated is a nonlinear mathematical programming problem.

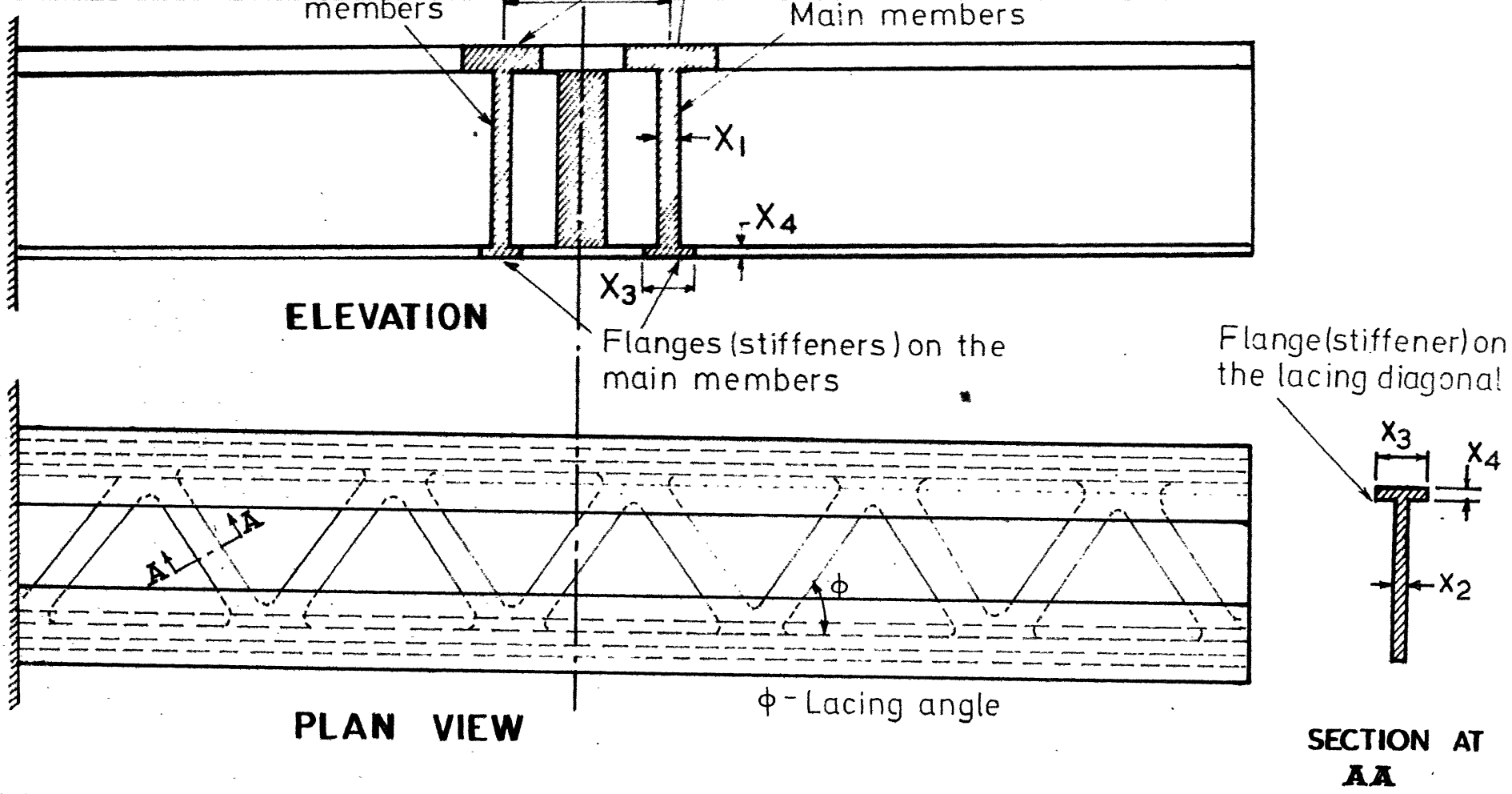

FIG. 2.1 WARREN-TYPE LATHE BED DETAILS

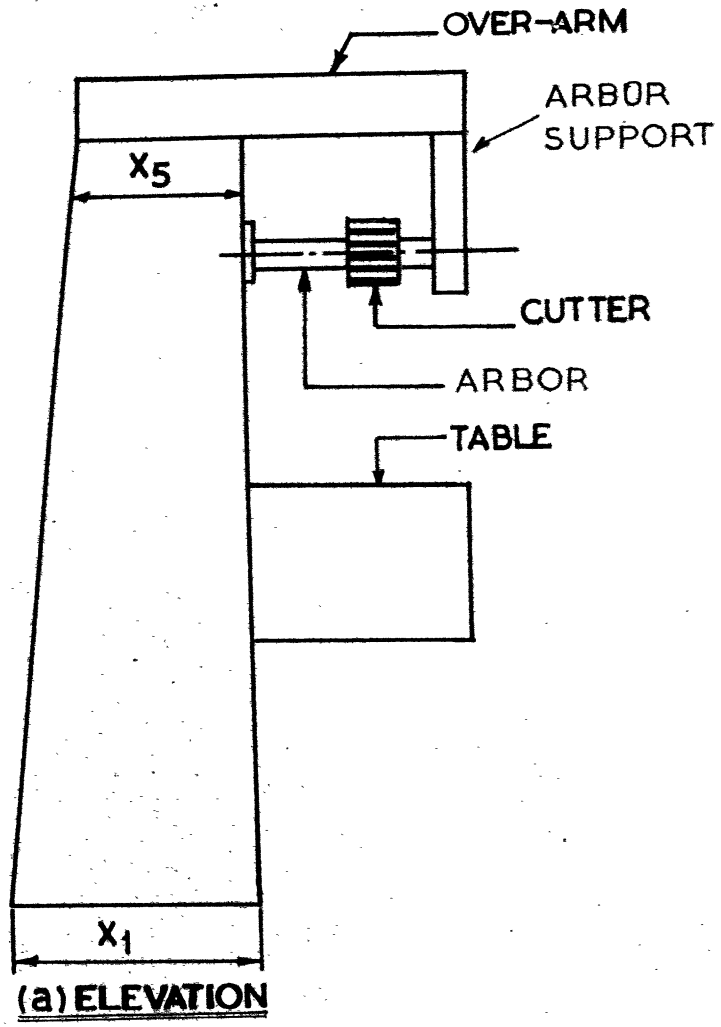

(a) ELEVATION

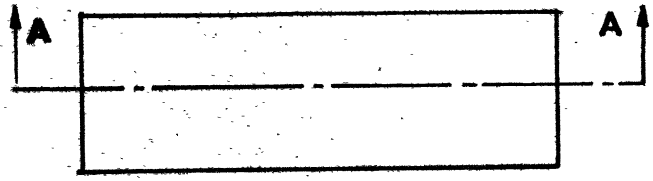

(C) PLAN VIEW

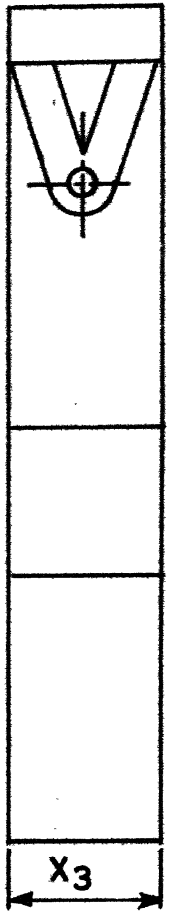

(b) SIDE VIEW

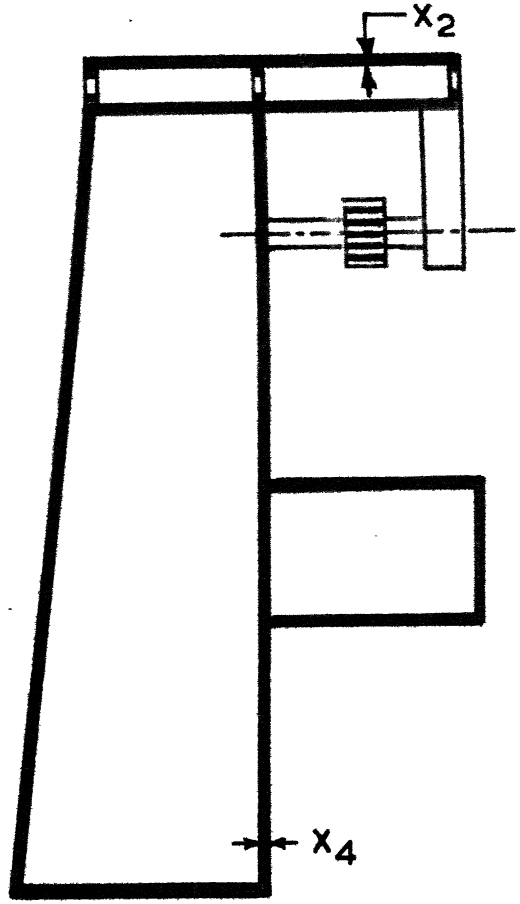

(d) SECTION AT 'A-A'

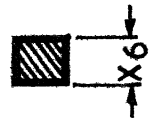

SQUARE CROSS SECTION OF RIBS ON THE OVER-ARM AND ITS JOINT WITH THE COLOUMN

CHAPTER 3

IDEALIZATION OF MACHINE TOOL STRUCTURES

Extensive efforts have been expended over the years for the development of techniques for the static and dynamic analysis of complex structures. With the advent of modern high-speed digital computers, the finite element displacement method has been developed as one of the most convenient tools for analyzing complex structures. There are several ways of modelling the structure by the finite element method. Therefore, in this work, a comparative study of the static and the eigen value solutions of Warren beam and milling machine structures is made by using two different triangular plate bending elements. For both the elements, the in-plane displacement components u and v are assumed to vary linearly as

$$u(x,y) = a_1 + a_2 x + a_3 y \tag{3.1}$$

$$v(x,y) = a_4 + a_5 x + a_6 y \tag{3.2}$$

where u and v indicate the components of displacement along the local x and y axes as shown in Fig. 3.1. For the first element, a 9-term transverse displacement model, valid for the whole triangular element, is used.[38, 39, 40] The displacement model is given by

$$w(x,y) = a_1 + a_2 x + a_3 y + a_4 x^2 + a_5 y^2 + a_6 xy + a_7 x^3 + a_8(x^2 y + x y^2) + a_9 y^3 \qquad (3.3)$$

where $w(x,y)$ represents the component of displacement along a direction transverse to the plane of the plate as shown in Fig.3.1. In the case of the second element, the triangular element is divided into three parts by joining its centroid to the three vertices as shown in Fig. 3.2. A six-term transverse displacement model is used for each of the sub-triangles as[42] :

$$w_m(x,y) = a_{1m} + a_{2m} x + a_{3m} y + a_{4m} x^2 + a_{5m} y^2 + a_{6m} xy, \qquad m = 1,2,3 \qquad (3.4)$$

where $w_m(x,y)$ is the component of displacement of the m^{th} sub-triangle along the local z-direction .

In three dimensional structural analysis, both the in-plane and the bending stiffnesses have to be considered. The in-plane and the bending stiffnesses are uncoupled for small displacements. These stiffnesses are combined to form the elemental stiffness matrix in local coordinate system as shown in Appendix A. Owing to the difficulty encountered during transformation, θ_z is not coming into the analysis.[43,44] As shown in Appendix A, θ_z and its conjugate force M_z are included in the analysis by inserting appropriate number of zeroes into the stiffness matrix. The following section gives the numerical results given by the two finite element idealizations.

in reference 5. Even in this structure it can be observed that the results obtained using the displacement model given in equation 3.3 are closer to the values reported in reference 5. The computer time required is also considerably smaller for this model as given in table 3.3. Hence this model was selected for this work. An important thing to be noted in the present study is that a lesser number of finite elements yielded results that are comparable with those obtained by using a larger number of elements in reference 5.

TABLE 3.1 DISPLACEMENT AND EIGEN VALUE RESULTS OF WARREN BEAM

	DISPLACEMENT MODELS USED AS GIVEN IN EQUATIONS 3.1, 3.2 and 3.3	DISPLACEMENT MODELS USED AS GIVEN IN EQUATIONS 3.1, 3.2 and 3.4	AS REPORTED IN REFERENCES 3 AND 4
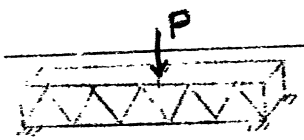 VERTICAL DISPLACEMENT UNDER THE LOAD IN INCHES P = 1000 lb	.0042	.0034	.0061
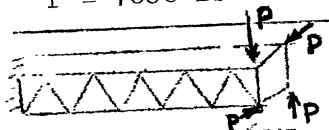 AVERAGE TORSIONAL DEFLECTION AT THE END IN RADIANS P = 250 lb.	.00795	.00082	.0013
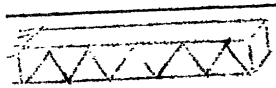 FIRST NATURAL FREQUENCY cycles/sec.	124	128	134

TABLE 3.2 DISPLACEMENT RESULTS OF MODEL MILLING MACHINE

		TEST 1		TEST 2		TEST 3	
		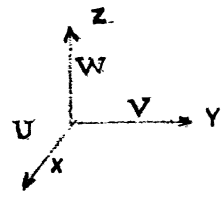	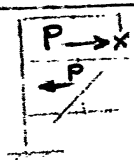	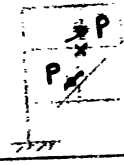		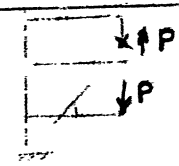	
		DEFLECTIONS OF POINT MARKED X IN μm					
P = 102 Kg.		V	W	U	V	V	W
DISPLACEMENT MODELS USED AS GIVEN IN EQUATIONS 3.1, 3.2 AND 3.3		9.76	2.60	-15.989	-	3.22	11.12
DISPLACEMENT MODELS USED AS GIVEN IN EQUATIONS 3.1, 3.2 AND 3.4		5.42	2.11	-13.348	-	2.82	9.20
AS REPORTED IN REFERENCES 5 AND 6	FINITE ELEMENT MESH 1	9.35	3.01	-15.42	-	3.48	14.5
	FINITE ELEMENT MESH 2	8.13	3.56	-16.4	-	10.8	23.0

TABLE 3.3 EIGEN VALUE RESULTS OF MODEL MILLING MACHINE

		FREQUENCIES IN RADIANS/SECOND				COMPUTER TIME ON IBM 370/155
		ω_1	ω_2	ω_3	ω_4	
NUMBER OF DEGREES OF FREEDOM = 348 BAND WIDTH OF THE STIFFNESS MATRIX = 102	DISPLACEMENT MODELS USED AS GIVEN IN EQUATIONS 3.1, 3.2 AND 3.3	1289	2183	2382	3236	5 MINUTES AND 5.84 SECONDS
	DISPLACEMENT MODELS USED AS GIVEN IN EQUATIONS 3.1, 3.2 AND 3.4	1301	2250	2363	2834	6 MINUTES AND 44.58 SECONDS
AS REPORTED IN REFERENCES 5 AND 6		1162-1190	2100/2390	2410-2567	2950-3140	

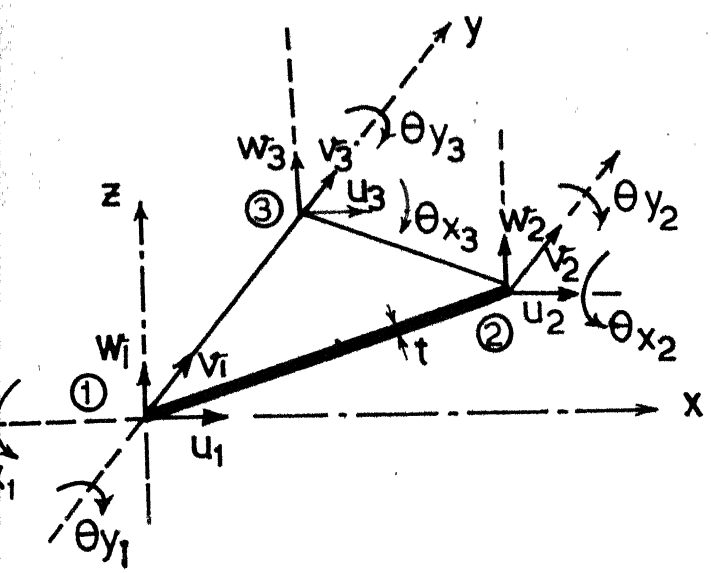

3·1 IN-PLANE AND BENDING DISPLACEMENT IN LOCAL CO-ORDINATE SYSTEM

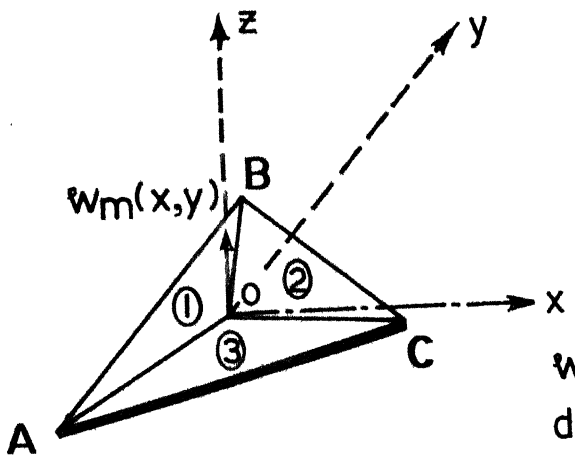

O = CENTROID OF THE TRIANGLE

ΔABO = SUB-TRIANGLE - 1

ΔBCO = SUB-TRIANGLE - 2

ΔCAO = SUB-TRIANGLE - 3

$w_m(x,y)$ is the component of displacement of the m^{th} sub-triangle

FINITE ELEMENT IS SUB-DEVIDED INTO THREE SUB-TRIANGLES

FIG 3·2 IDEALIZATION BY SUB-TRIANGLES

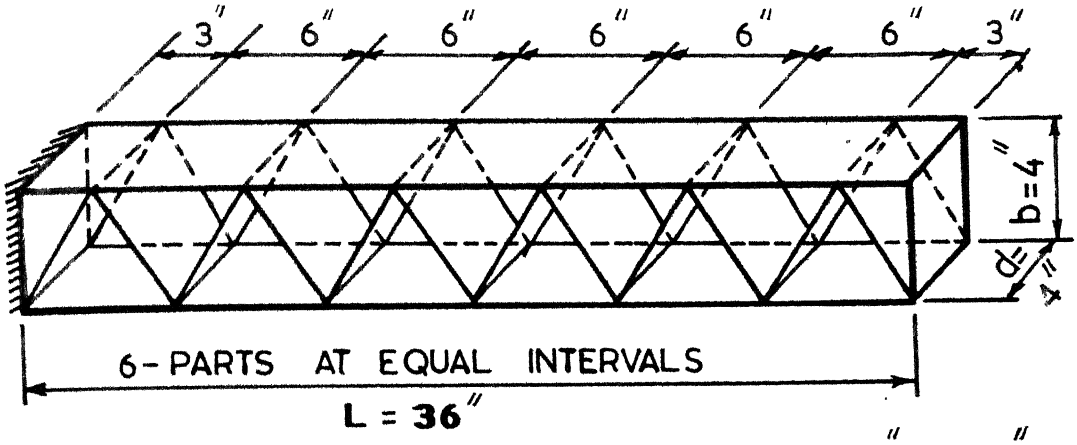

MATERIAL :- MILD STEEL FLAT STRIP 4" X 3/16"
IN A WELDED CONSTRUCTION

FIG. 3·3 **WARREN BEAM**

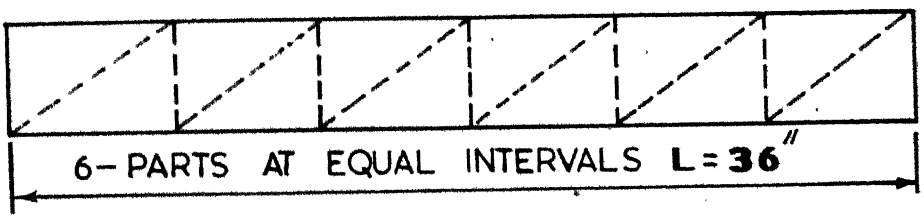

(a) FINITE ELEMENT GRID ON BOTTOM SURFACE

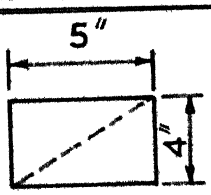

(b) LACING DIAGONAL

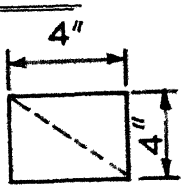

(c) SIDE PLATE

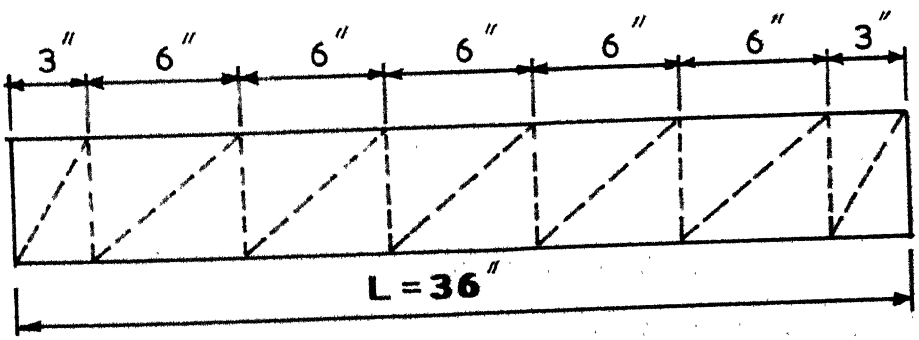

(d) FINITE ELEMENT GRID ON TOP SURFACE

dotted lines represent finite element grid

FIG. 3·4 **DETAILS OF IDEALIZATION OF WARREN BEAM (SHOWN IN FIG. 3·3)**

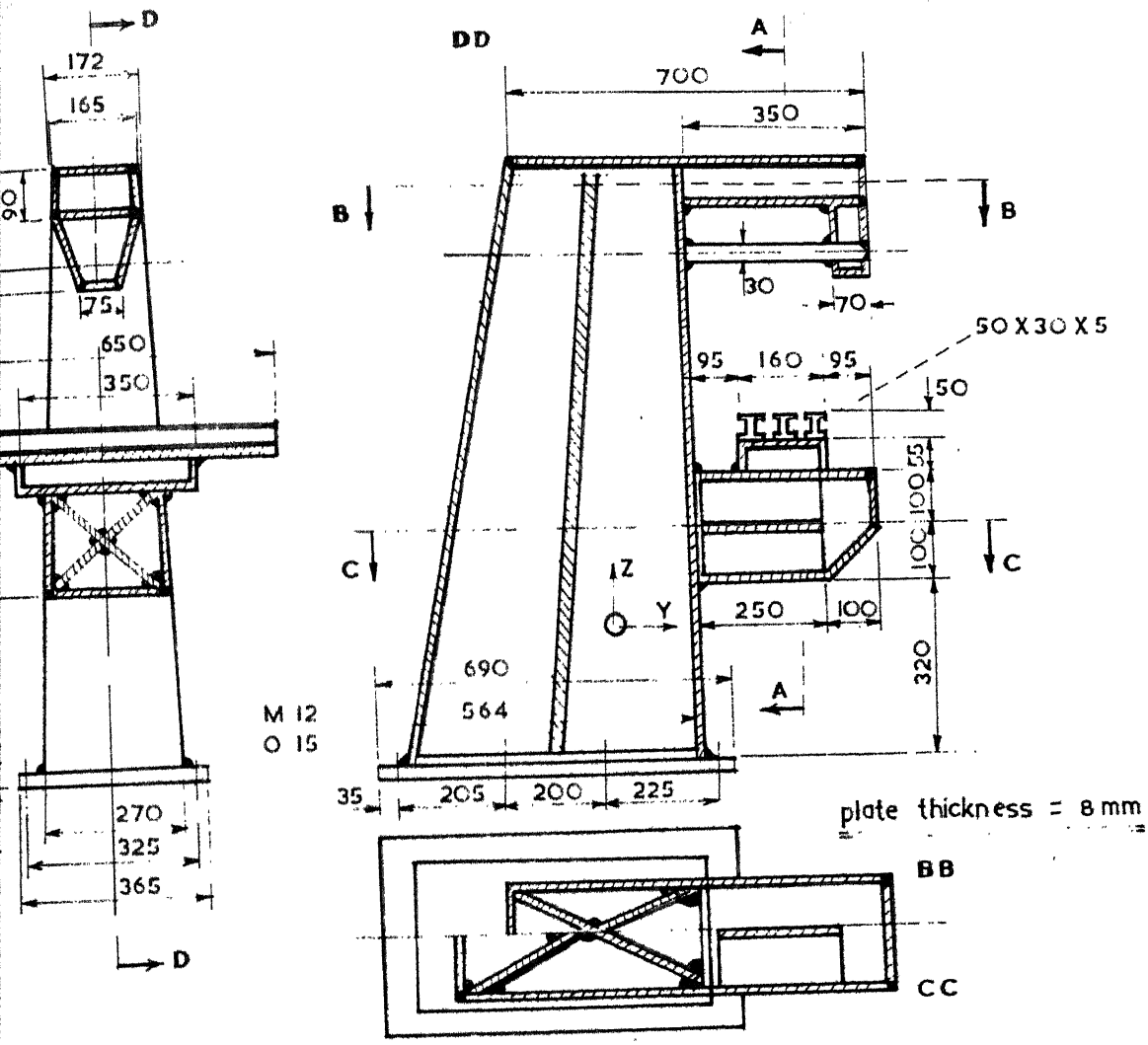

FIG.3·5 MODEL MILLING MACHINE

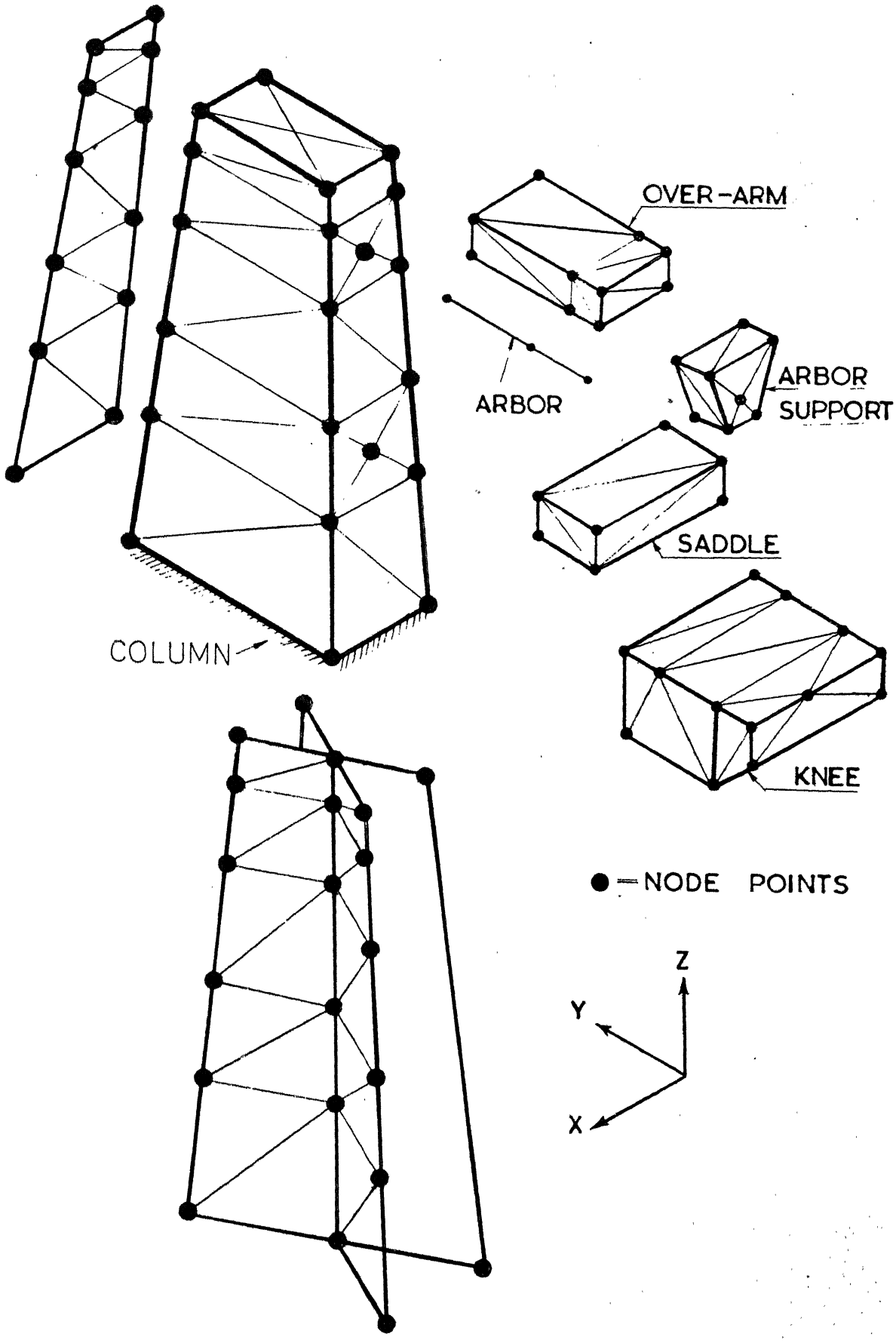

FIG. 3·6 FINITE ELEMENT DISTRIBUTION OF MODEL MILLING MACHINE

CHAPTER 4

ANALYSIS OF CUTTING FORCES AND CHATTER STABILITY

The static and dynamic rigidities of machine tool structures have an important influence upon both surface finish and metal removal rates. In this chapter, the force analysis in horizontal milling machines and lathe machines is made in order to evaluate static rigidity constraint. A method of including regenerative chatter stability constraint in the design of horizontal milling machines is also developed.

4.1 HORIZONTAL MILLING MACHINE

4.1.1 Chip Formation in Plain Milling Process

In plain milling operation, the milling cutter removes chips of varying thickness intermittently. The geometry of the plain milling process has been studied in a number of works[45-50]. A detailed analysis has been reported by Martelloti[48,49] who clearly showed that the path of a milling cutter tooth is trochoidal and therefore the milling chip cross sections are confined within the arcs of two trochoids. As shown in Fig. 4.1, the cutter rotates against the direction of the feed in 'up' or conventional milling, whereas, the cutter rotates along the direction of the feed in 'down milling'. Martelloti has developed the following equation for the maximum undeformed chip thickness (t_m) :

$$t_m = [\, s_t \sqrt{\{(\frac{D}{d} - 1)/\,(\frac{D}{2d})^2(1 \pm \frac{v}{V})^2 \mp \frac{v.D}{V.d}\}}\,] \cos\theta \qquad (4.1)$$

where,

D = cutter diameter, mm

d = depth of cut, mm

v = feed rate, mm/minute

V = cutting velocity, mm/minute

θ = helix angle, degrees

z = number of teeth in cutter

s_t = feed, mm/tooth

In equation 4.1, the upper sign refers to 'up' milling and the lower one refers to 'down' milling. If $V >> v$, the trochoidal arcs can be approximately taken as circular arcs[51]. The assumption of circular path for the tooth implies that the feed of the work piece is intermittent, so that the work piece is stationary during the engagement of a tooth and then moves suddenly by a distance of s_t before the next tooth starts cutting[57]. This assumption is necessary to arrive at simple approximate relations. Further, if $(\frac{d}{D}) << 1$, equation 4.1 can be written as:

$$t_m \approx s_t \, 2\sqrt{\frac{d}{D}} \cos\theta \qquad (4.2)$$

From Fig. 4.2,

$$\cos\psi = 1 - \frac{2d}{D} \qquad (4.3)$$

Hence,

$$\sin \psi \approx 2\sqrt{\frac{d}{D}} \tag{4.4}$$

Therefore equation 4.2 can be written as

$$t_m \approx s_t \cdot \sin \psi \cdot \cos \theta \tag{4.5}$$

Refering to Fig. 4.3, the uncut chip thickness at any instant is given by:

$$t_i = s_t \sin \psi_i$$

The average uncut area of cross-section traversed by one tooth for a straight teeth cutter is given by:

$$A_{avg} = B\, s_t \sin \left(\frac{\psi}{2}\right) \tag{4.6}$$

where B is the width of engagement

When more than one tooth is in contact as shown Fig. 4.4, the maximum uncut chip area is given by:

$$A_{max} = B\, s_t \sum_{i=1}^{z_i} \sin \psi_i \tag{4.7}$$

where z_i is the number of teeth in contact at any instant.

The average cross-section of the chip for helical and straight teeth cutters when several teeth are in engagement can be calculated as follows.

The material removed in one revolution of the cutter = $Bd\ s_t z = \pi D\ A_{avg}$

Hence,

$$A_{avg} = \frac{Bd\ s_t z}{\pi D} \tag{4.8}$$

where A_{avg} is the average cross-section of the chip due to a number of teeth in engagement.

4.1.2 Force System in a Plain Milling Process

Figure 4.5 illustrates the milling action of a straight teeth cutter simulated by a rotating single point cutting tool. The Merchant's[54] circle diagram for cutting forces is also indicated in this figure. Figure 4.5a gives, for 'up' milling,

$$F_T = R \cos(\lambda - \gamma), \tag{4.9a}$$

$$F_R = R \sin(\lambda - \gamma) \tag{4.9b}$$

and

$$R = \frac{F_s}{\cos(\phi + \lambda - \gamma)} \tag{4.9c}$$

where,

F_T = tangential force on the cutter

F_R = radial force on the cutter

R = resultant force on the cutter

F_s = shear force on the shear plane

λ = friction angle

γ = normal rake angle

ϕ = shear angle

Thus

$$F_T = \frac{F_s \cdot \cos(\lambda-\gamma)}{\cos(\phi+\lambda-\gamma)} \tag{4.10}$$

and

$$F_R = \frac{F_s \cdot \sin(\lambda-\gamma)}{\cos(\phi+\lambda-\gamma)} \tag{4.11}$$

The shear force F_s can be expressed as

$$F_s = B\,\tau_s\,s_t \sin(\psi_i) \tag{4.12}$$

The substituting of equation 4.12 into equations 4.10 and 4.11 gives

$$F_T = \frac{B\,\tau_s \cdot s_t \cdot \sin\psi_i \cos(\lambda-\gamma)}{\sin\phi \cdot \cos(\phi+\lambda-\gamma)} \tag{4.13}$$

and

$$F_R = \frac{B\,\tau_s \cdot s_t \cdot \sin\psi_i \cdot \sin(\lambda-\gamma)}{\sin\phi \cdot \cos(\phi+\lambda-\gamma)} \tag{4.14}$$

The horizontal and vertical force components acting on the cutter can be expressed as:

$$F_H = F_T \cos\psi_i + F_R \sin\psi_i$$

$$= \frac{B \cdot \tau_s \cdot s_t \cdot \sin\psi_i}{\sin\phi \cdot \cos(\phi+\lambda-\gamma)} [\cos\psi_i \cdot \cos(\lambda-\gamma) + \sin\psi_i \cdot \sin(\lambda-\gamma)]$$

$$= \frac{B \cdot \tau_s \cdot s_t \cdot \sin\psi_i}{\sin\phi \cdot \cos(\phi+\lambda-\gamma)} \cos(\lambda-\gamma-\psi_i) \tag{4.15}$$

and

$$F_V = F_R \sin \psi_i - F_T \sin \psi_i$$

$$= \frac{B.\tau_s.\ s_t.\ \sin \psi_i}{\sin \phi \cos (\phi+\lambda-\gamma)} [\cos \psi_i . \sin (\lambda-\gamma) - \sin \psi_i \cos (\lambda-\gamma)]$$

$$= \frac{B.\tau_s.s_t.\ \sin \psi_i}{\sin \phi . \cos (\phi+\lambda-\gamma)} . \sin (\lambda-\gamma-\psi_i) \qquad (4.16)$$

When more than one tooth is in contact, equations 4.13, 4.15 and 4.16 can be generalized as

$$F_T = \frac{B.\tau_s.s_t \cos (\lambda-\gamma)}{\sin \phi . \cos (\phi+\lambda-\gamma)} \sum_{1}^{z_i} \sin \psi_i \qquad (4.17)$$

$$F_H = \frac{B.\tau_s.\ s_t}{\sin \phi . \cos (\phi+\lambda-\gamma)} \sum_{1}^{z_i} \sin \psi_i \cos (\lambda-\gamma-\psi_i) \qquad (4.18a)$$

$$F_V = \frac{B.\tau_s.\ s_t}{\sin \phi . \cos (\phi+\lambda-\gamma)} \sum_{1}^{z_i} \sin \psi_i \sin (\lambda-\gamma-\psi_i) \qquad (4.18b)$$

where z_i is the number of teeth in contact at any instant and τ_s is the dynamic shear stress. Similarly, for down milling, it follows that (from Fig. 4.5b),

$$F_H = \frac{B.\tau_s.\ s_t}{\sin \phi . \cos (\phi+\lambda-\gamma)} \sum_{1}^{z_i} \sin \psi_i \cos (\lambda-\gamma+\psi_i) \qquad (4.19a)$$

and

$$F_V = \frac{B.\tau_s.\ s_t}{\sin\phi.\ \cos(\phi+\lambda-\gamma)} \sum_{1}^{z_i} \sin\psi_i \sin(\lambda-\gamma+\psi_i) \qquad (4.19b)$$

It is evident from equation 4.18 and also from experiment 1 results obtained by various authors[47,48,49 and 55] that the vertical component of the force is very small in 'up' milling and its intensity tends to decrease as the depth of cut is increased. A reversal of the direction of the vertical component of the force may occur when the depth of cut is large. In down milling, there will be no reversal of the vertical of the vertical component of force as the depth of cut is increased.

In 'up' milling for practical values of λ , γ and d the vertical force component will usually fluctuate between $-0.2F_T$ and $+ 0.2\ F_T$. The positive sign corresponds to the vertically upward direction and the negative sign corresponds to the vertically downward direction. In both the methods of milling, horizontal force components of considerable magnitude will occur as reported in references 47, 48, 49 and 55. This behavior is also evident from equations 4.18 and 4.19. In 'up' milling the usual range of F_H is given by $0.8\ F_T$ to $1.0\ F_T$.

The variation of the chip cross-sectional area and, hence, the cutting forces in plain milling operation with a helical cutter are dependent on the values of B,θ, d and ϕ_b, where ϕ_b is the angle by which the front and the back cutting edges of a helical

tooth differ. Opitz[52] has shown that the individual tooth pulse can be approximated by a saw-tooth shaped curve when $\phi_b < \psi$, and by trapezoidal curve when $\phi_b > \psi$. Singhet. al.[53] have experimentally observed such a periodicity in the cutting forces. When $\phi_b = m\psi_m$, where m is an integer and ψ_m is the pitch angle at the same cutting edge, the resultant tooth pulse would be a smooth curve. If m is an integer, the tooth pulse would be given by a constant superimposed by a pulse variation.

Boston et. al.[55] have experimentally measured the cutting forces in plain milling operation with helical cutters. With 25° helix angle, the axial force (F_A) was found to be approximately 20% of the tangential force for various take angles.

Vulf[56] has shown that the average F_T during plain milling can be estimated as:

$$P_T|_{avg} = \frac{c}{(t_{avg})^k} \cdot A_{avg} \qquad (4.20)$$

where,

t_{avg} = mean chip thickness in plain milling, in

$$= s_t \cdot \sin\frac{\psi}{2} \cdot \cos\theta$$

and c, k are the constants depending on the material of the work piece and the environment. By substituting the expressions of t_{avg}, $\sin\frac{\psi}{2}$ and A_{avg}, the equation 4.20 can be written as

$$P_T|_{avg} = \frac{c}{\pi} \cdot \frac{B}{(\cos\theta)^k} (s_t)^{1-k} \left(\frac{d}{D}\right)^{1-\frac{k}{2}} \cdot z \qquad (4.21)$$

In the present work, the static forces acting on horizontal milling machines are calculated using the following parameters:

D = 100mm

B = 90 mm

z = 12 teeth

s_t = 0.1 mm/tooth

ψ = 30°

θ = 25°

c = 140 (for mild steel)

k = 0.28 (for mild steel).

The orientation of the cutting forces in 'up' milling are generally more unfavourable from the point of view of the static ridity of cutter centre and also from chatter stability point of view. Hence, in the present work, only 'up' milling is considered in the design of horizontal milling machines with the following values of the cutting forces:

$F_H = F_T|_{avg}$ = 840 kg.

$F_V = 0.2\ F_T|_{avg}$ = 168 kg.

$F_A = 0.2\ F_T|_{avg}$ = 168 kg.

$R = \sqrt{F_H^2 + F_V^2 + F_A^2}$ = 875 kg.

4.2 FORCE SYSTEM IN LATHE DURING TURNING

The cutting forces in the general case of turning operation are shown in Fig. 4.6. The resultant force R is given by[51]

$$R = \sqrt{F_A^2 + F_N^2 + F_r^2}$$

where

F_A= feed force on the cutting tool in the direction of the tool travel

F_N= thrust force on the cutting tool in the direction perpendicular to the generated surface

F_r= cutting force on the cutting tool acting in the direction of the cutting velocity vector

In view of the fact that the twist of the lathe bed forms a large part of the total deformation, it will have a considerable influence upon the working accuracy[58]. Hence, torsional rigidity is included as one of the behavior constraints in the design of lathe beds. In lathe machine, the work piece and its support and the cutting tool and its support are much more flexible compared to the lathe bed. Hence the contribution of lathe bed for chatter in turning operation is not significant compared to the other machine members indicated. This is the reason why chatter stability is not included as a constraint in the design of lathe beds. - The maximum torque (T_{max}) on the work piece is calculated as:

$$2\pi N_{min} T_{max} = H.P._{max}$$

where N_{min} is the minimum spindle speed, and $H.P._{max}$ is the maximum horse power of the lathe.

The twisting moment acting on the lathe bed depends on the work piece diameter and the orientation of the cutting forces. In actual machine, it is very difficult to estimate the torque to which the bed is subjected. Hence, T_{max} is taken as the twisting moment acting at one end of the lathe bed (considering the other end is fixed) to compute the torsional deflection.

4.3 GENERAL FEATURES OF CHATTER IN MACHINE TOOLS

Severe vibrations in metal cutting machine tools are often encountered giving rise to undulations on the machined surface and excessive variations in the cutting forces. Such energetic vibrations belong to the class of self-excited vibrations, commonly known as 'chatter' in machine tools, and the source of self excited energy is derived from the cutting process itself. As presented in Fig. 4.7, the self excited vibrations are due to the interaction of cutting forces and the machine tool structural dynamics. Several researchers have proposed various models for the self excited vibrations in machine tools. Kasirin[59] and Arnold[60] have utilized 'velocity principle' for explaining chatter in machine tools. The velocity principle assumes that the characteristic of the cutting

force is that it has a negative slope with respect to the velocity of cutting. The regenerative chatter arises because of the variation of the cutting forces occuring due to the variation of the uncut chip thickness, and it is explained with respect to Fig. 4.8. For the sake of brevity, only a single degree of freedom system is illustrated in this figure. The cutting tool cuts a surface which it has already cut during the previous revolution in case of turning, during the previous stroke in case of plaining and by the preceding tooth in the case of milling[15]. Therefore, from Fig. 4.8, if there was a vibration between the tool and the work piece during the previous ith cut resulting in an undulated machined surface, the chip during the next $(i+1)^{th}$ cut is removed from the same undulated surface. Hence, the amplitude of variation in chip thickness, ΔY, is given by

$$\Delta Y = Y_{i+1} - Y_i \tag{4.22}$$

where

Y_i = vibration amplitude between tool and work piece normal to the cut surface in ith cut

Y_{i+1} = vibration amplitude between tool and work piece normal to the cut surface in (i+1)th cut

If Ψ is the phase difference between Y_i and Y_{i+1}, then ΔY can be written as

$$\Delta Y = q\, Y_i e^{-j\Psi} \tag{4.23}$$

where q is a constant.

The change in the cutting force (ΔP) due to the variation in the uncut chip thickness (ΔY) is given by

$$\Delta P = - B.r. \Delta Y \qquad (4.24)$$

where r is a coupling constant depending on the cutting conditions, and B is the width of chip. Thic change in the force component will again result in a vibration giving an undulated surface on the work piece and the regeneration of the undulation proceeds in subsequent cuts.

Tlusty and Polacek[61] proposed a model according to which different modes of vibration of the structure of a machine tool will be coupled with the 'cutting process dynamics' through cross-receptance and not by direct receptance. According to this model, chatter will occur when the energy delivered to the vibratory system by the cutting forces exceeds the energy dissipated by the vibratory system. This model is known as the 'mode coupling theory'.

In actual practice, all these three phenomena appear simultaneously and out of the three theories it is generally considered that the generated energy as given by the velocity component principle is low compared to those given by the regenerative chatter and mode coupling principles[15]. Tlusty and Polacek[61] have taken the simplest dynamic cutting-force relationship by assuming a direct proportionality between the force and the undeformed chip thickness. In the analysis

made by Tobias, et. al.[62,63], the cutting force relationship was related to the cutting speed and the feed rate apart from the undeformed chip thickness.

To derive the limits of stability for the machine tool and the cutting system, it is necessary to assume a force relationship for the cutting process and relate this to the machine dynamics. The governing equations of motion cannot be solved directly, but the analysis can be simplified very much by assuming the condition at the limit of stability.

4.4 MATHEMATICAL EXPRESSION FOR THE LIMIT OF STABILITY

In the present work, the basic theory of stability analysis as given by Tlusty and Polacek[15,61] is used in applying equation 4.24 for the design of milling machine structures. The simplifying assumptions made are:

a) The vibration system of the machine is linear

b) The variable component of the cutting force direction (Y) remains constant

c) The variable component of the cutting force depends only on vibrations in the direction of the normal to the cut surface

d) The value of the variable component of the cutting force (ΔP) varies proportionately and instantaneously with variable displacement, ΔY.

e) The frequency of vibration and the mutual phase shift of undulations are unaltered in subsequent overlapping cuts.

Equation 4.24 can be rewritten, in view of equation 4.22, as

$$\Delta P = Br\,(Y_{i+1} - Y_i) \qquad (4.25)$$

At the limit of stability, the variable component of cutting force ΔP will result in cross-receptance Y_{i+1} whose amplitude is same as Y_i. Hence

$$Y_{i+1} = \Delta P.\ \Phi\ (\omega) \qquad (4.26)$$

and

$$\left| \frac{Y_i}{Y_{i+1}} \right| = 1 \qquad (4.27)$$

where $\Phi(\omega)$ is the absolute cross-receptance of the vibratory system

$$\Phi\,(\omega) = G(\omega) + jH(\omega)$$

where, $G(\omega)$ and $H(\omega)$ are the real and imaginary components of $\Phi\,(\omega)$ respectively.

Here Φ is taken as a particular case of cross-receptance in which the variable cutting force (ΔP) is along the direction of the cutting force and the resulting relative vibration (ΔY) between the

tool and the work piece is along the normal to the cut surface. Combining the equations 4.25, 4.26 and 4.27, the following equation is obtained:

$$\left| \frac{1/(Br) + G + jH}{G + jH} \right| = 1 \qquad (4.28)$$

Since the imaginary parts of the numerator and the denominator of equation 4.28 are equal, it follows that,

$$\left| \frac{1/(Br) + G}{G} \right| = 1 \qquad (4.29)$$

Equation 4.29 is satisfied only if,

$$\frac{1}{Br} + G = -G$$

or

$$\frac{1}{2Br} = - G \qquad (4.30)$$

For certain specified cutting conditions, the value of the coupling coefficient (r) is fixed. Therefore, the limiting value of chip width B_{LIM} at the limit of stability, for these specified cutting conditions, is governed by the minimum negative real cross-receptance ($-G_{LIM}$) of the structural system. Therefore, the lowest limit of stability is determined from the following equation

$$\frac{1}{2B_{LIM}r} = - G_{LIM} \qquad (4.31)$$

The meaning of equation 4.31 can also be explained with reference to Fig. 4.9.

4.5 DETERMINATION OF COUPLING CONSTANT IN PLAIN MILLING

Equation 4.31 is used, for the design of horizontal milling machines for regenerative chatter stability, in the present work. The value of coupling coefficient (r) depends on the cutting conditions. If the critical or the maximum value of coupling coefficient ($r_{critical}$) can be estimated from all the commonly used cutting conditions, structure can be designed for chatter stability by putting a limit on the negative inphase cross receptance ($G_{LIM} = -\frac{1}{2B_{LIM}\, r_{critical}}$). Therefore it becomes essential to analyze the various cutting conditions inorder to estimate $r_{critical}$ so that the value of G_{LIM} can be determined.

4.5.1 Coupling Coefficient for Straight Teeth Cutter from Basic Theory of Metal Cutting.

In Fig. 4.10, ΔY and ΔP are shown for a straight teeth cutter in horizontal milling machine. Refering to Fig. 4.4, equations 4.18a and 4.18b for 'up' milling can be written as

$$F_H = \frac{B\ \tau_s}{\sin\phi \cos(\phi+\lambda-\gamma)} \sum_{1}^{z_i} (s_t \sin\psi_i).\ \cos(\lambda-\gamma-\psi_i) \qquad (4.32a)$$

and

$$F_V = \frac{B\ \tau_s}{\sin\phi\cos(\phi+\lambda-\gamma)} \sum_{1}^{z_i} (s_t \sin\psi_i).\ \sin(\lambda-\gamma-\psi_i) \qquad (4.32b)$$

where $s_t \sin\psi_i$ indicates the uncut chip thickness at ith tooth. Refering to Fig. 4.10a, for a relative displacement (ΔY) of the cutter centre with respect to the work piece, the change in uncut chip thickness at i^{th} tooth is given by $\Delta Y.\cos\psi_{yi}$, where ψ_{yi} is the angle between i^{th} tooth and the normal direction to the cut surface as shown in Fig. 4.11.

The corresponding new horizontal force F_H^* and the vertical force F_V^* become

$$F_H^* = \frac{B.\tau_s}{\sin\phi\cos(\phi+\lambda-\gamma)} \sum_{1}^{z_i} (s_t.\sin\psi_i - \Delta Y.\cos\psi_{yi}).\ \cos(\lambda-\gamma-\psi_i) \qquad (4.33a)$$

and

$$F_V^* = \frac{B.\tau_s}{\sin\phi\cos(\phi+\lambda-\gamma)} \sum_{1}^{z_i} (s_t.\sin\psi_i - \Delta Y.\cos\psi_{yi}).\sin(\lambda-\gamma-\psi_i) \qquad (4.33b)$$

The changes in the forces are given by

$$\Delta F_H = F_H - F_H^* = \frac{B.\tau_s}{\sin\phi\cos(\phi+\lambda-\gamma)} \sum_{1}^{z_i} \Delta Y.\cos\psi_{yi}.\cos(\lambda-\gamma-\psi_i) \qquad (4.34a)$$

$$\Delta F_V = F_V - F_V^* = \frac{B.\tau_s}{\sin\phi\cos(\phi+\lambda-\gamma)} \sum_{1}^{z_i} \Delta Y.\cos\psi_{yi}.\sin(\lambda-\gamma-\psi_i) \qquad (4.34b)$$

Using equation 4.24, the coupling constants can be expressed as:

$$r_H = \frac{\Delta F_H}{B.\Delta Y} = \frac{\tau_s}{\sin\phi\cos(\phi+\lambda-\gamma)} \sum_{1}^{z_i} \cos\psi_{yi} \cos(\lambda-\gamma-\psi_i) \tag{4.35a}$$

and

$$r_V = \frac{\Delta F_V}{B.\Delta Y} = \frac{\tau_s}{\sin\phi\cos(\phi+\lambda-\gamma)} \sum_{1}^{z_i} \cos\psi_{yi} \sin(\lambda-\gamma-\psi_i) \tag{4.35b}$$

where r_H and r_V are the coupling constants in horizontal and vertical directions respectively.

Therefore

$$r = \sqrt{r_H^2 + r_V^2} \tag{4.36}$$

Similarly for down milling,

$$r_H = \frac{\tau_s}{\sin\phi\cos(\phi+\lambda-\gamma)} \sum_{1}^{z_i} \cos\psi_{yi} \cos(\lambda-\gamma+\psi_i) \tag{4.37a}$$

and

$$r_V = \frac{\tau_s}{\sin\phi\cos(\phi+\lambda-\gamma)} \sum_{1}^{z_i} \cos\psi_{yi} \sin(\lambda-\gamma+\psi_i) \tag{4.37b}$$

In the present work, the relationship due to Lee and Shaffer[64] is used for computing the shear angle:

$$\phi = \frac{\pi}{4} + \gamma - \lambda$$

For $\lambda = 18°$ and $\gamma = 10°$, this equation gives $\phi = 37°$.

The dynamic shear stress, τ_s, is computed from the Abuladze's[65] shear stress relationship for ductile materials:

$$\tau_s = 0.74 \quad \sigma_u \, (6)^{-6e} \qquad (4.38)$$

where σ_u is the ultimate tensile strength of the material and e is the percentage elongation.

For $\sigma_u = 40$ kg/mm^2, e = .2 the value of τ_s obtained is 36 kg/mm^2.

The values of coupling coefficients (r) obtained by using equations 4.35 to 4.37 for various values of ψ are given in Table 5.1. The cutter teeth are taken to be symmetrically disposed to the mean direction Y(normal to the cut surface).

4.5.2 Coupling Coefficient from Vulf's Formula

Refering equation 4.20,

$$P_T|_{avg} = \frac{c}{(t_{avg})^k} \cdot A_{avg}$$

Since $F_H = P_T|_{avg}$, $F_V = 0.2\ P_T|_{avg}$, $F_A = 0.2\ P_T|_{avg}$,

$$R = \sqrt{F_H^2 + F_V^2 + F_A^2} = 1.04\ P_T|_{avg}$$

$$\approx P_T|_{avg}$$

Hence,

$$R = \frac{c}{(t_{avg})^k} \cdot A_{avg} \tag{4.39}$$

If the displacement of the cutter along the normal direction to the cut surface is Δt_{avg} and the corresponding change in the cutting force is ΔR,

$$\frac{\Delta R}{\Delta t_{avg}} = - Br \tag{4.40}$$

As $\Delta R \to 0$, one obtains from equation 4.39,

$$\frac{\Delta R}{\Delta t_{avg}} \approx \frac{dR}{dt_{avg}} = - Br = c. A_{avg}. (-K) (t_{avg})^{-k-1} \tag{4.41}$$

Substituting the value of A_{avg} from equation 4.8, equation 4.41 can be written as

$$r = c \left(\frac{d}{D}\right) \cdot \left(\frac{s_t}{\pi}\right) z.k \, (t_{avg})^{-k-1} \tag{4.42}$$

since $t_{avg} = s_t \cdot \sin\frac{\psi}{2} \cdot \cos\theta$,

$$r = \frac{c.z.k}{\pi(\cos\theta)^{k+1}} \frac{\left(\frac{d}{D}\right)^{\frac{1-k}{2}}}{(s_t)^k} \tag{4.43}$$

By substituting the values of c, z, k, θ and s_t given in section 4.1.2, in equation 4.43,

$$r = (331) \, (d/D)^{.36} \tag{4.44}$$

The value of r for various values of $(\frac{d}{D})$ are given in Table 5.2 along with the corresponding values of ψ.

It can be observed, from the tables 5.1 and 5.2, that the values of r obtained by using equation 4.44 agree very well with those obtained by using the basic theory of metal cutting. In the present work the critical value of (r_{LIM}) is taken as 165 kg/mm^2. The width of cut (B) is taken as 9 cm.

In the chatter stability constraint, the upper limit on $|G_{MIN}^{(u)}|$ is taken as

$$|G_{MIN}^{(u)}| = \frac{1}{2\ B\ r_{LIM}} = .000003 \text{ cm./kg.}$$

TABLE 4.1

VALUES OF COUPLING CONSTANTS FROM BASIC THEORY OF METAL CUTTING

	Coupling constants r (kg/mm^2)	
ψ	'up' milling	'down' milling
35°	179	158
40°	159	157
45°	159	156

TABLE 4.2

VALUES OF COUPLING CONSTANTS FROM EMPIRICAL FORMULA

ψ	d/D	r(kg/mm^2)
35°	.09	139
40°	.116	152
45°	.146	165

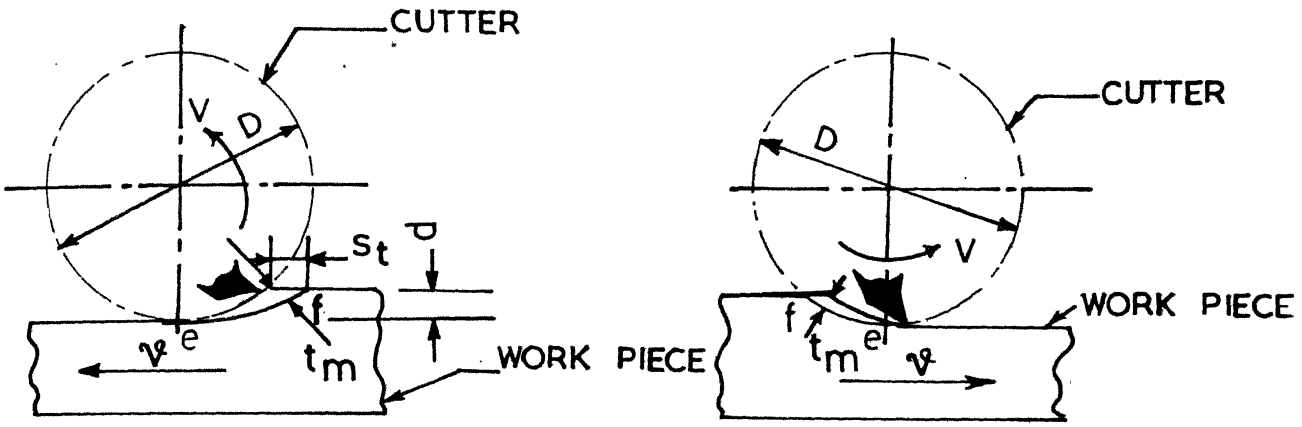

FIG.4·1 THE PLAIN MILLING PROCESS WITH STRAIGHT TEETH CUTTER

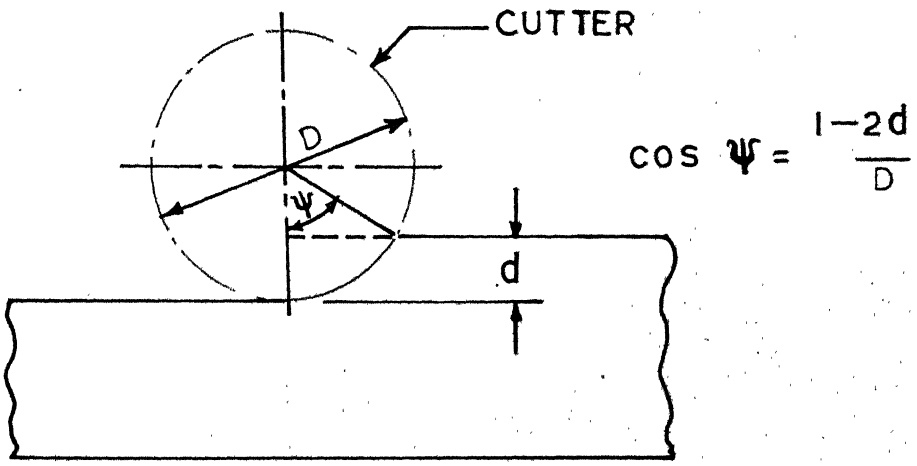

FIG.4·2 GEOMETRY OF THE PLAIN MILLING PROCESS

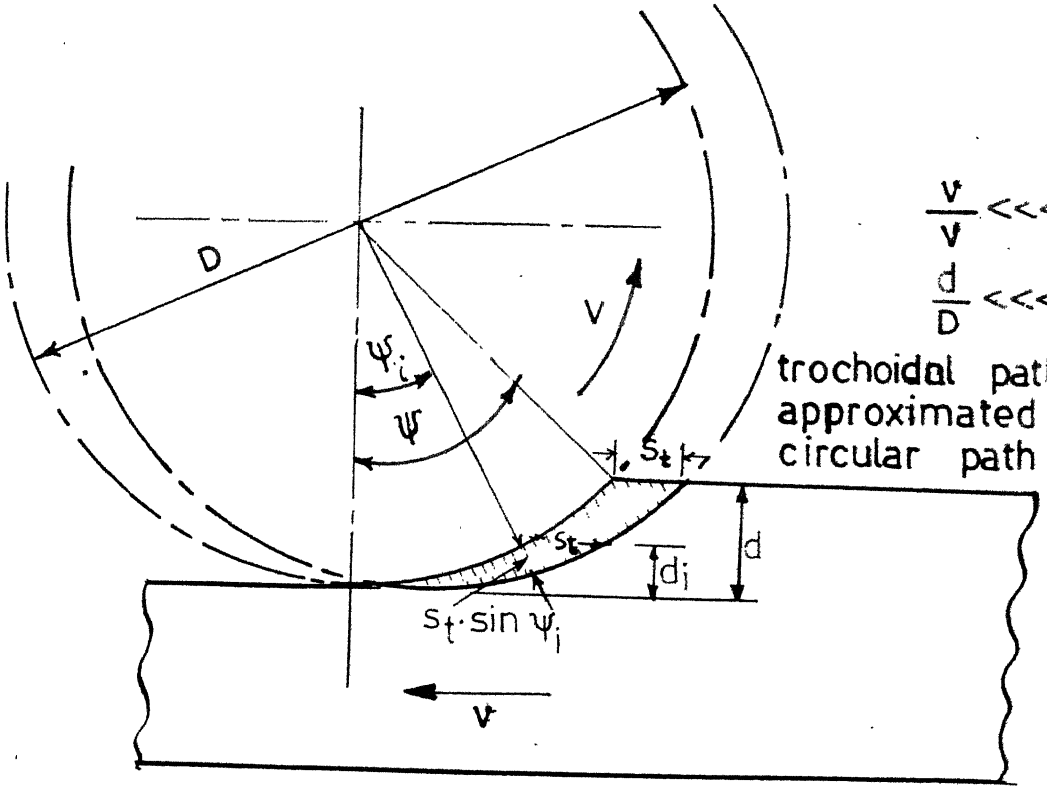

$\frac{v}{V} <<< 1$

$\frac{d}{D} <<< 1$

trochoidal path is approximated as circular path

FIG.4.3 THE UNCUT AREA OF CHIP-CROSS SECTION (CONFINED WITHIN TWO CIRCULAR ARCS) TRAVERSED BY ONE TOOTH

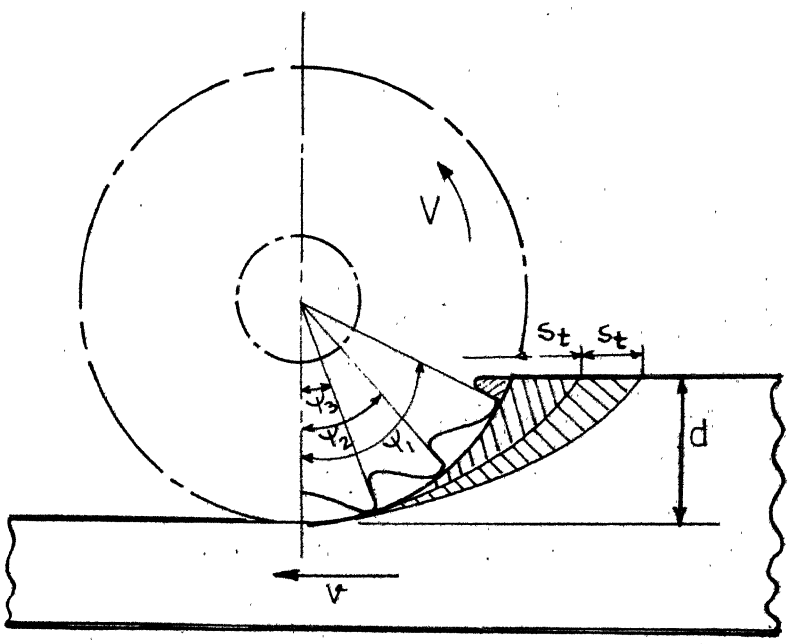

4.4 MULTI TOOTH CUTTING IN PLAIN MILLING WITH

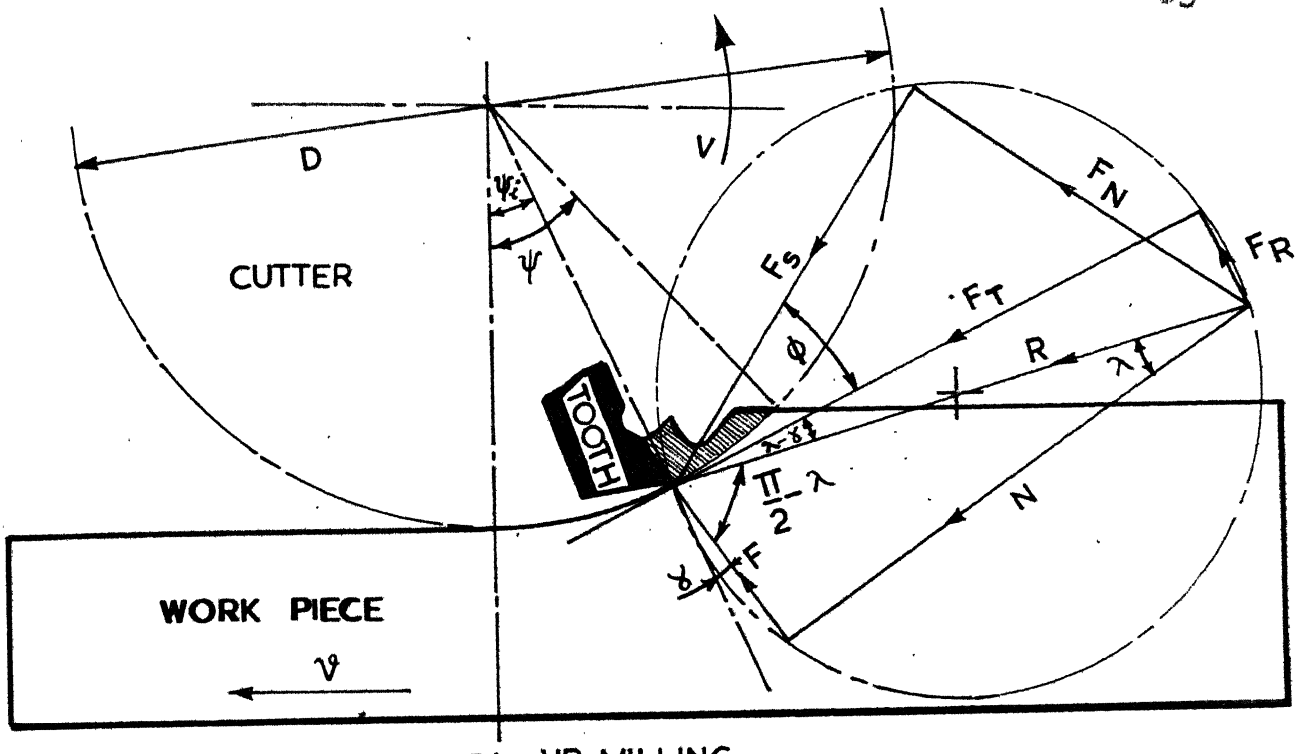

(a) UP MILLING

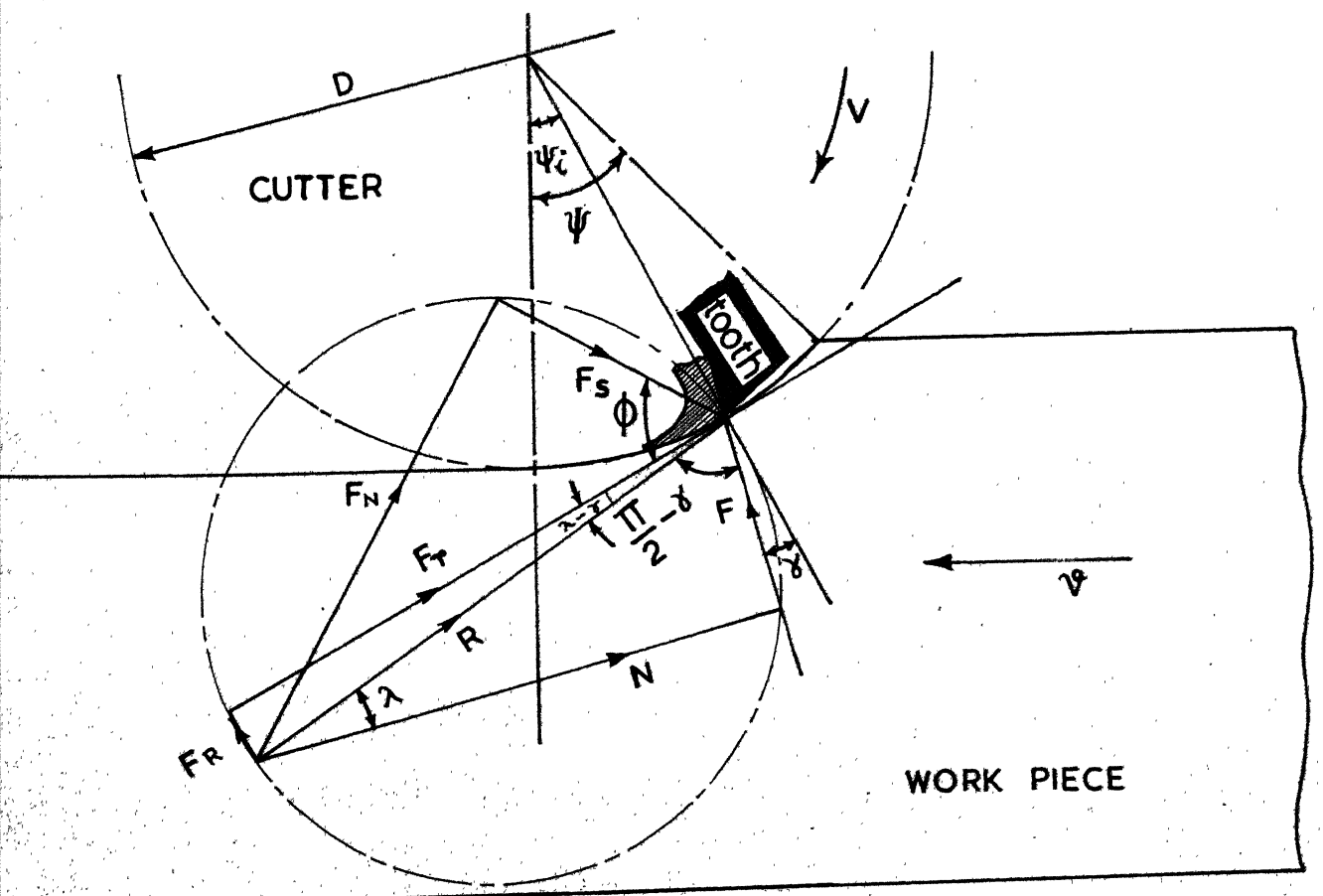

(b) DOWN MILLING

6.4.5 MERCHANT'S CIRCLE DIAGRAM FOR CUTTING FORCES IN A PLAIN MILLING SIMULATED BY A ROTATING SINGLE POINT CUTTING TOOL

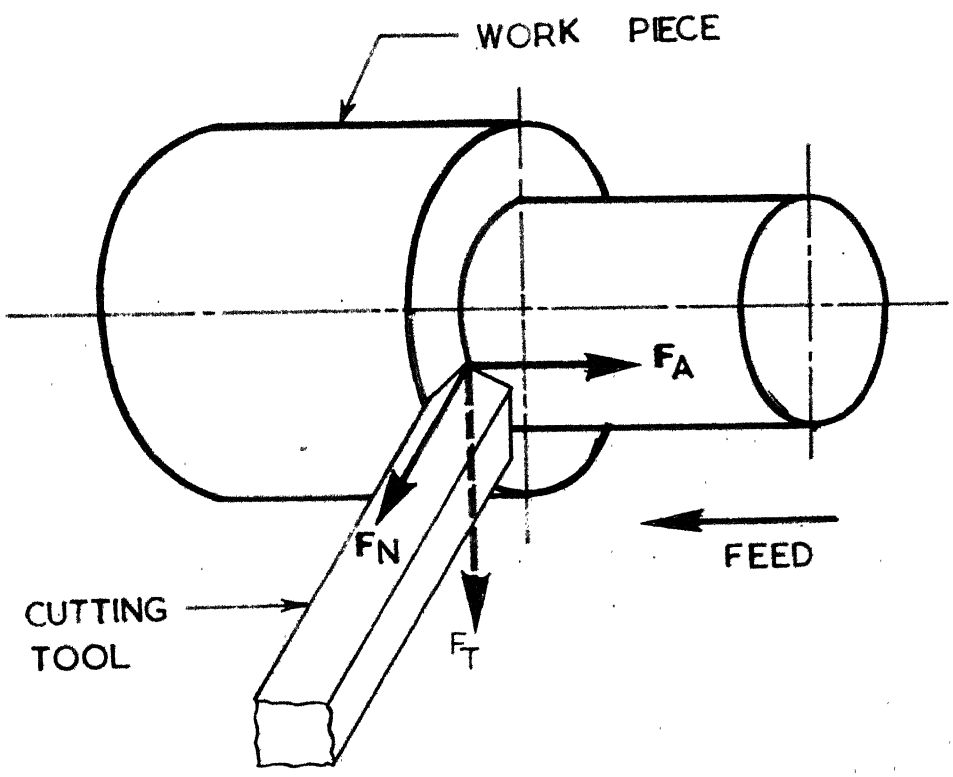

FIG. 4.6 CUTTING FORCES IN CONVENTIONAL TURNING

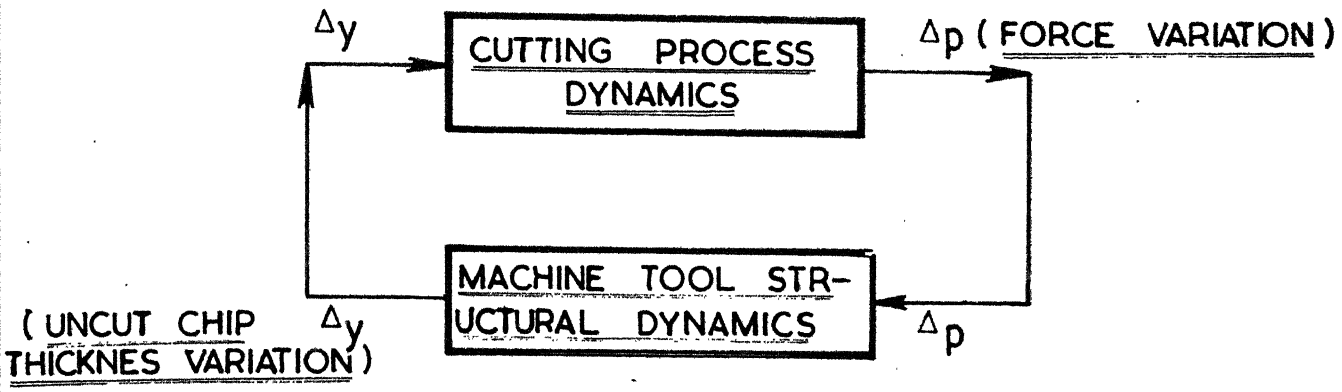

FIG-4.7 BASIC DIAGRAM OF CHATTER IN MACHINE TOOLS

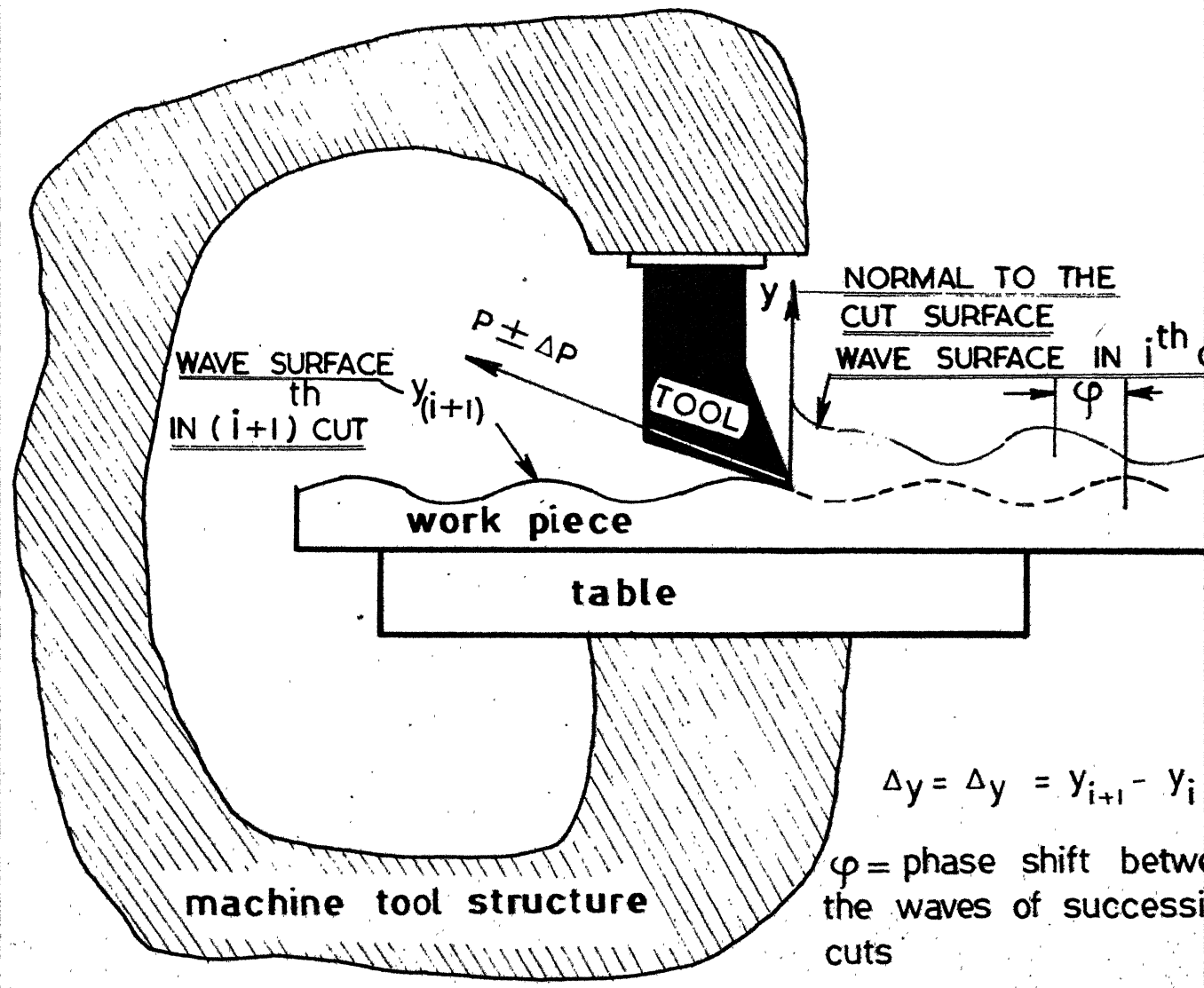

FIG 4.8 BASIC DIAGRAM REPRESENTATION FOR THE PROCESS OF SELF EXCITED VIBRATIONS IN MACHINE TOOLS

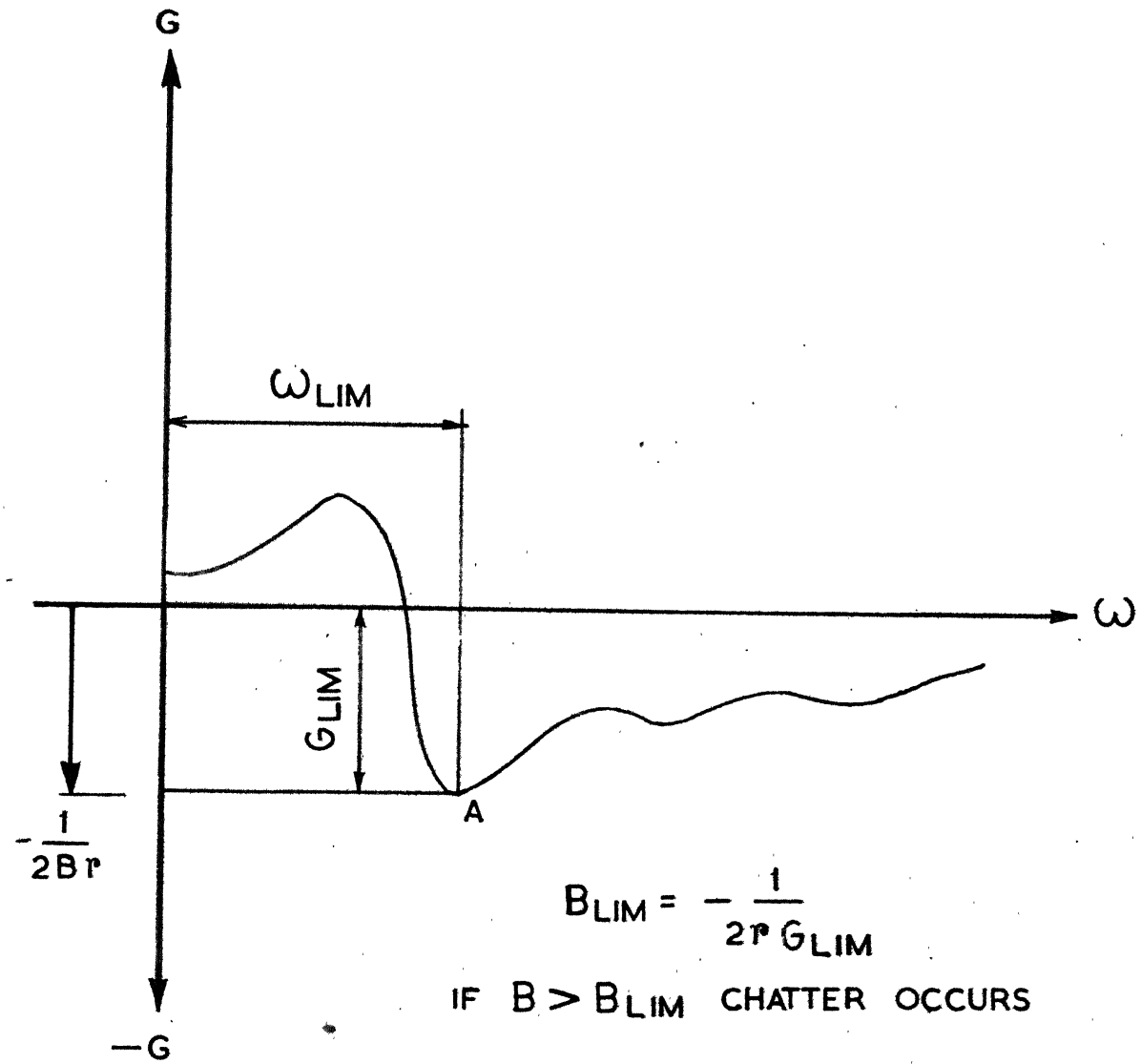

FIG.4.9 REAL CROSS-RECEPTANCE CURVE WITH RESPECT TO FREQUENCY

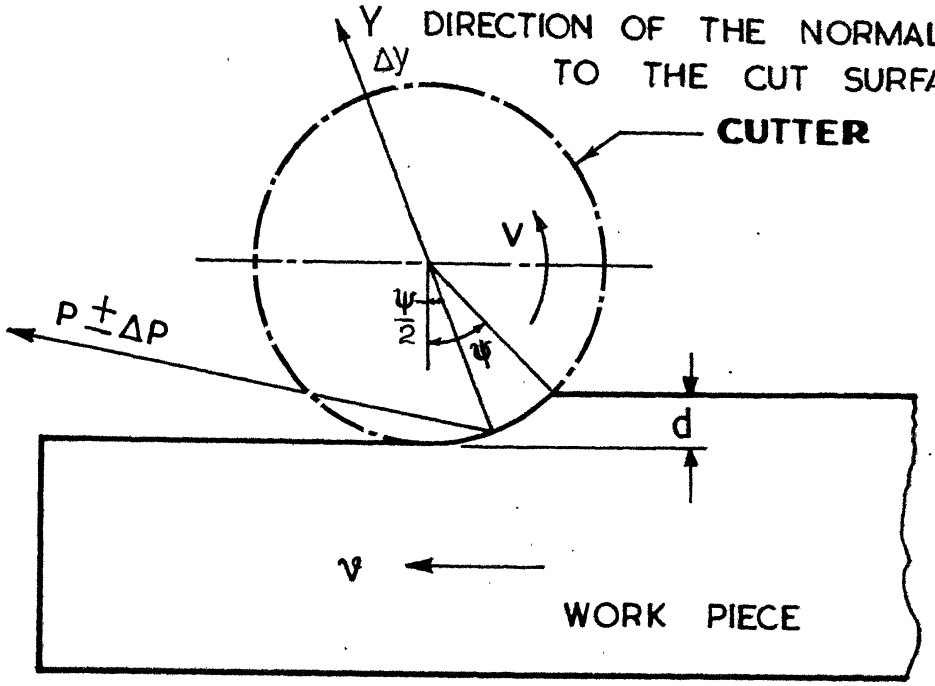

(a) **UP MILLING**

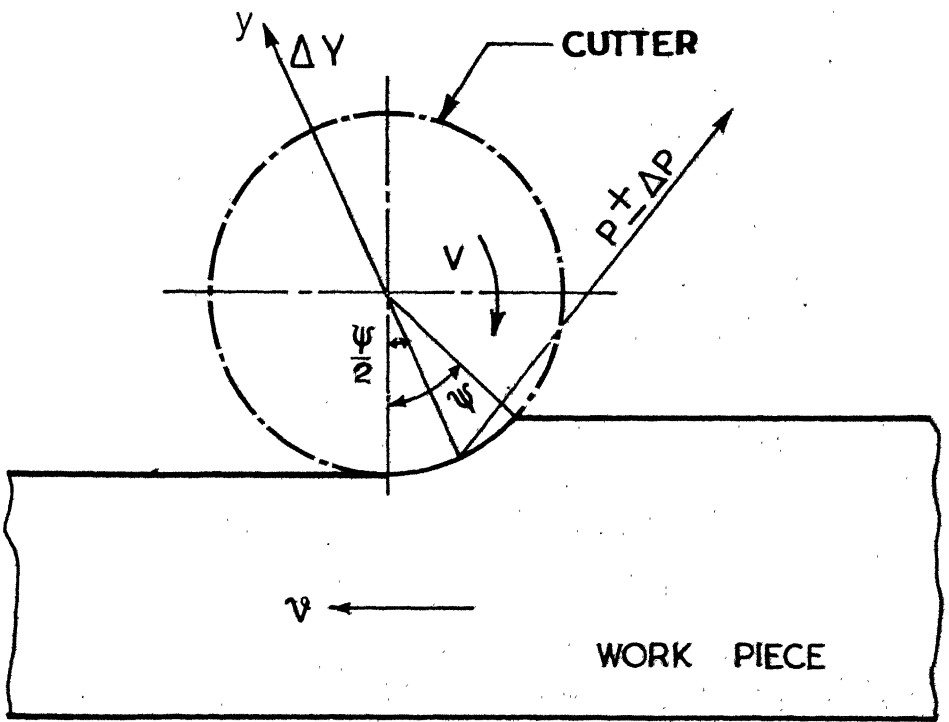

(b) **DOWN MILLING**

FIG. 4·10 ORIENTATION OF CUTTING FORCES AND THE DIRECTION OF THE NORMAL TO THE CUT SURFACE IN HORIZONTAL MILLING

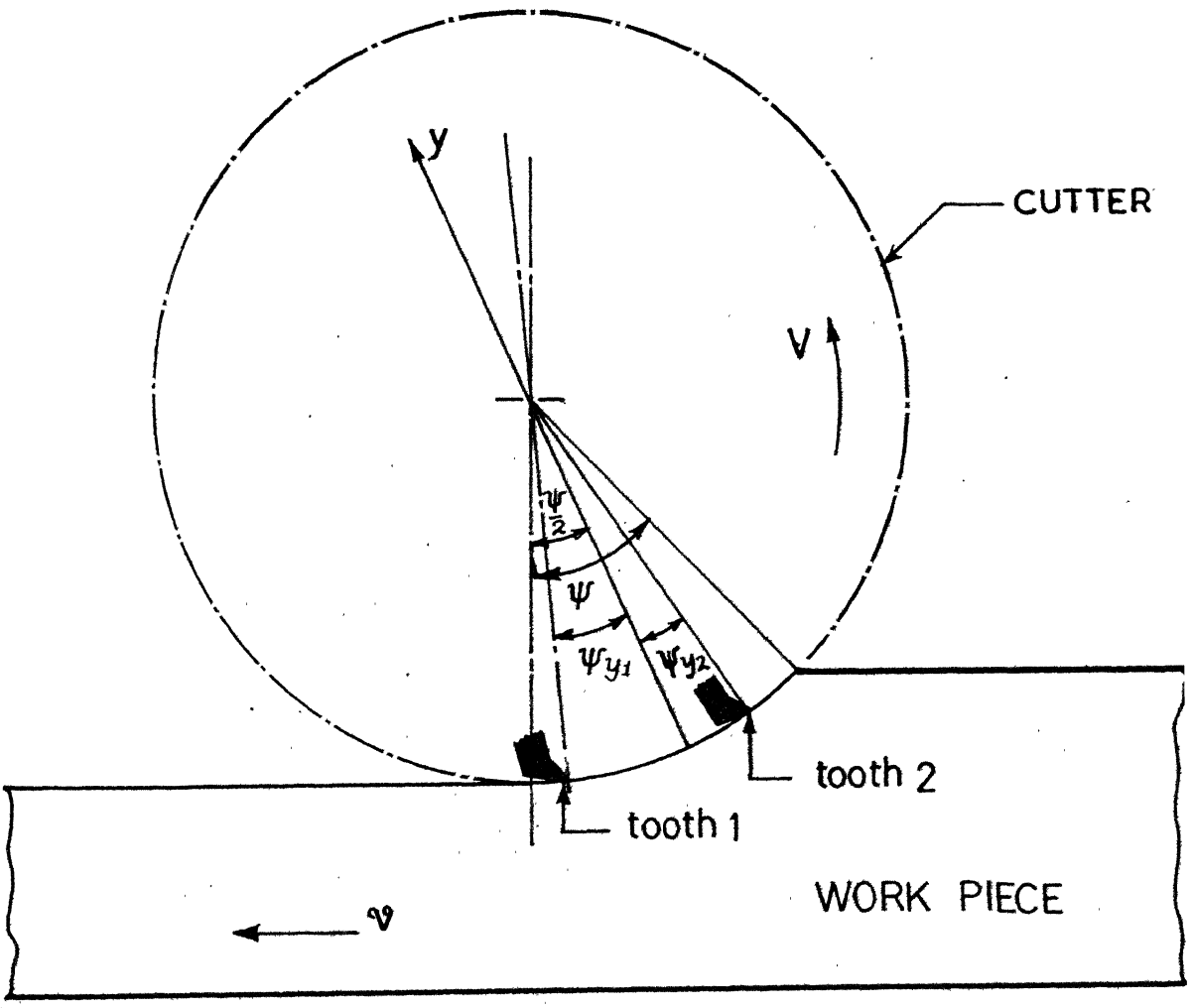

FIG.4.11 ORIENTATION OF CUTTING TEETH IN ACTION WITH RESPECT TO THE NORMAL TO THE CUT SURFACE

CHAPTER 5

STATIC AND DYNAMIC ANALYSIS OF MACHINE TOOL STRUCTURES

5.1 DEFLECTION AND STRESS ANALYSIS

Once the load vector $\vec{P}$, for which the machine tool structure is to be designed, is determined as explained in the previous chapter, the displacement vector $\vec{Y}$ can be computed by solving the following equations :

$$[\vec{K}]\,\vec{Y} = \vec{P} \qquad (5.1)$$

where $[\vec{K}]$ is the master stiffness matrix of the structure. In the present work, the solution of equation 5.1 is obtained by the cholesky decomposition of the symmetric banded matrix, storing only the upper triangular matrix, followed by forward and backward elimination technique. The horizontal milling machine structure shown in Fig. 5.1 is analysed for static deflections and stresses. The idealisation of the structure is shown in Fig. 5.2. The dove-tail (vertical guide for the knee) thickness on the front face of the column is taken as 3.5 cm. The dove-tail thickness on the over-arm is taken as 2.5 cm. These thicknesses are added to the thickness of the front face of the column and the bottom side of the over-arm respectiv The arbor support is idealised as two frame elements. The rectangular cross-section of these frame elements are taken as 7 x 10 cm. The arbor diameter is taken as 4 cm.

The maximum deflection of the cutter centre in any direction is .0066cm.In metal cutting machine tools, the induce stresses, corresponding to the permissible deformations, are generally far less in value than the allowable stresses for various materials. For the structure shown in Fig. 5.1, the maximum principal stress developed in the structure is 11.97 Kg and the maximum shear stress induced is 6.63 Kg/cm^2. It is obv that these values are far below the allowable ones. Hence in t design of machine tool structures strength was not taken as a design constraint. The stresses are computed from the known no displacements by using the stress-strain and the strain-displac relations of linear elasticity.

In the design of horizontal milling machines, the maximum cutter centre deflection should not exceed the upper bo $d_c^{(u)}$ and this requirement can be stated in the optimum design problem as

$$d_c^{(u)} - d_c \geq 0 \qquad (5.2$$

5.2 EIGEN VALUE PROBLEM

In the finite element method, the eigenvalue problem solved by choosing the nodal displacements as generalized coord nates. Thus, the linear eigenvalue problem given by the follow equation

$$[\bar{K}] \vec{Y} = \lambda [\bar{M}] \vec{Y} \qquad (5.3$$

Fig. 5.3. Since the eigen vectors are required to be ortho-norma the reduction of the generalized mass matrix $[\tilde{M}]$ to an identity matrix is used as a convergence criterian in sub-space iteration. For the milling machine structure (Fig. 5.1), the natural freque and the mode shapes are shown in Fig. 5.4. For the lathe bed (Fi the natural frequencies and the mode shapes are shown in Fig. 5.6

5.3 DYNAMIC RESPONSE OF THE STRUCTURE

The dynamic response of the structure has been obtained by using modal coordinate system. The damping matrix [C] is taken proportional to a linear combination of the stiffness and mass matrices. Since it is not possible to estimate the modal damping factors from the blue prints of a given structure, the values of damping factors have to be obtained from experimental results on similar structures. In the present work, in the design of horizo milling machines, the damping factors are assumed to have a value 0.06 for the first few modes. By choosing the nodal displacement as generalized coordinates, the differential equations of motion structure can be written in the following form :

$$[\bar{M}]\ \ddot{\vec{Y}} + [C]\ \dot{\vec{Y}} + [\bar{K}]\ \vec{Y} = \vec{F}\ \sin \omega t \qquad (5.4$$

where, $\vec{F}$ is the vector of force amplitudes acting at the various nodes of the structure and ω is the forcing frequency.

By using coordinate transformation

$$\vec{Y} = [U]\ \vec{\eta} \qquad (5.5$$

in which $[U]$ is the $[\bar{M}]$-orthonormal modal matrix, and $\vec{\eta}$ represents the vector of modal or normal coordinates.

From equation 5.5,

$$\dot{\vec{Y}} = [U]\ \dot{\vec{\eta}} \tag{5.6}$$

$$\ddot{\vec{Y}} = [U]\ \ddot{\vec{\eta}} \tag{5.7}$$

Substituting equations 5.5, 5.6 and 5.7 in equation 5.4, and by premultiplying throughout by $[U]^T$,

$$[U]^T [\bar{M}] [U]\ \ddot{\vec{\eta}} + [U]^T [\bar{C}] [U]\ \dot{\vec{\eta}} + [U]^T [\bar{K}] [U]\ \vec{\eta} = [U]^T \vec{F} \sin \omega t \tag{5.8}$$

where $[U]^T$ is the transpose of $[U]$. Since the modal matrix is orthonormal with respect to the mass matrix $[\bar{M}]$, and the damping matrix is proportional to a linear combination of $[\bar{K}]$ and $[\bar{M}]$, equation 5.8 results in a set of decoupled differential equations :

$$[\ddots]\ \ddot{\vec{\eta}} + [\ddots]\ \dot{\vec{\eta}} + [\ddots]\ \vec{\eta} = \vec{Q} \sin \omega t \tag{5.9}$$

where, $\vec{Q}$ is equal to $[U]^T \vec{F}$ and ζ represents damping factors. If only p natural modes out of N are used in $[U]$, equations 5.9 represent p uncoupled second order ordinary differential equations. The equations 5.9 can also be written as

$$\ddot{\eta}_i + 2\zeta_i \omega_i \dot{\eta}_i + \omega_i^2 \eta_i = \vec{Q}_i \sin \omega t \tag{5.10}$$

Equation 5.10 can be solved to find the normal displacement $\eta_i(t)$.

These displacements, $\eta_i(t)$, can be used to obtain the dynamic displacement amplitude vector, $\vec{Y}$ with the help of equation 5.5.

The inphase component $G(\omega)$ of the absolute cross-receptance $\Phi(\omega)$ of the horizontal milling machine, shown in Fig. 5.1, are plotted in Fig. 5.7. In Fig. 5.7, the values of $G(\omega)$ are shown in X, Y and Z directions for the cutter centre and the table centre separately. The harmonic response loci for the same structure are shown in Fig. 5.8.

In the design of horizontal milling machine structures for chatter stability, the negative inphase cross-receptances of the cutter centre relative to the table have been computed at an interval of 10 radians/second beginning from the first natural frequency to the fourth natural frequency of vibration and from these, the minimum value (G_{MIN}) has been found. The values of G_{MIN} have been evaluated for different inclinations of unit amplitude of harmonic forcing with respect to the horizontal direction (θ). The values of G_{MIN} for various inclinations are given in Table 5.1. From these results, it can be observed that there is no significant difference in the value of G_{MIN} for various values of θ encountered in practical 'up' milling.

The chatter stability constraint in the optimum design of horizontal milling machine structures can be stated as follows :

$$\left|G_{MIN}^{(u)}\right| - \left|G_{MIN}\right| \geq 0 \qquad (5.11)$$

where $$G_{MIN}^{(u)} = - \frac{1}{2\, B_{LIM}\, r_{LIM}}$$

Although the receptances of the milling machine structure have been computed taking the modal damping factors as 0.06, a study has been made to find the effect of damping factors on the receptances. For a 10% change in the damping factors, the response loci of the structure are compared in Fig. 5.9. From the figure it can be observed that G_{MIN} values have changed approximately by 8%.

TABLE 5.1 VALUES OF G_{MIN} FOR DIFFERENT INCLINATIONS OF UNIT AMPLITUDE OF HARMONIC FORCING

θ (degrees)	-20	-10	0	+10	+20
G_{MIN} cm./kg x 10^5	0.6721	0.6769	0.6818	0.6721	0.6657

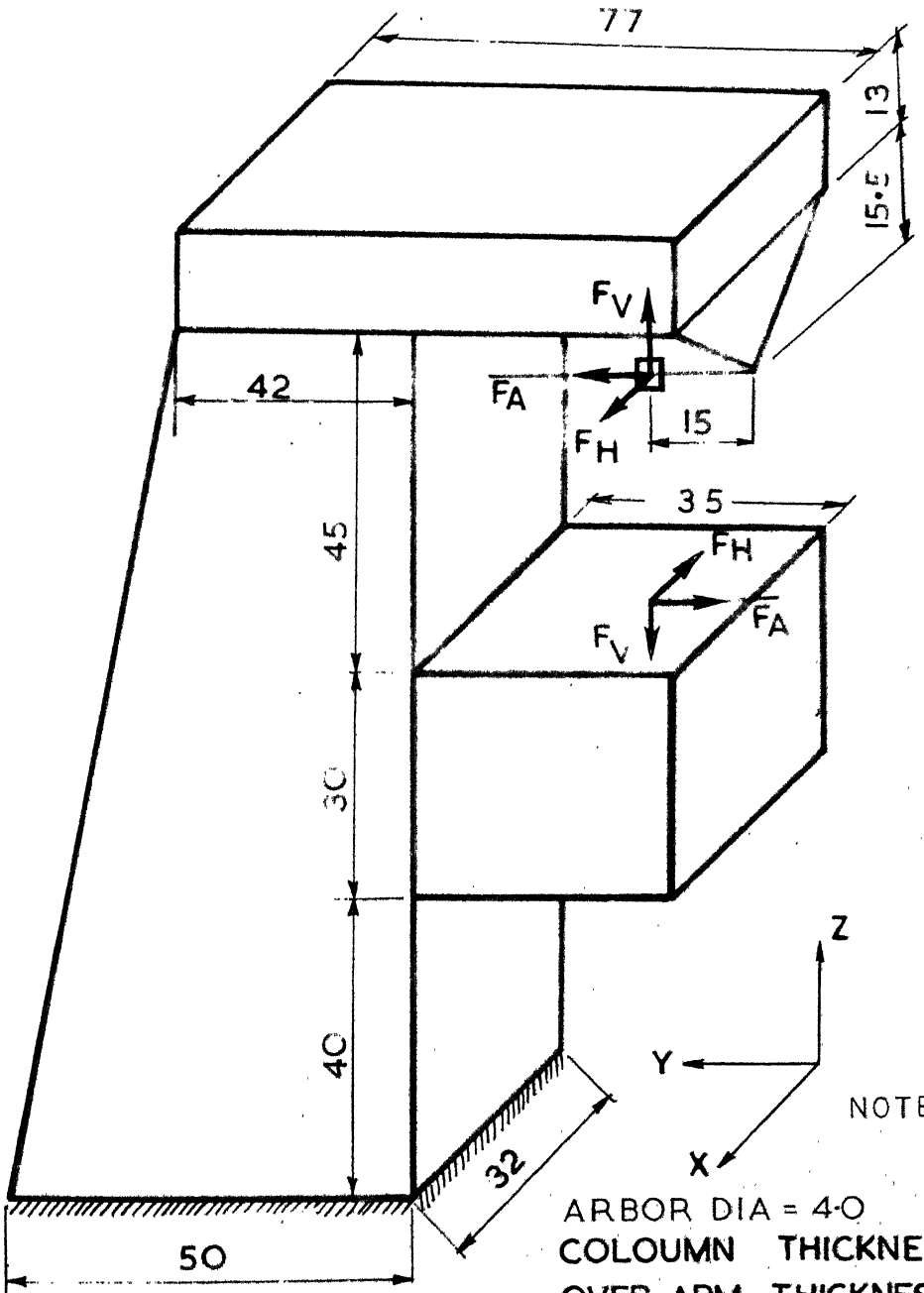

NOTE:— All dimensions in cm.

ARBOR DIA = 4·0
COLOUMN THICKNESS= 2.8
OVER-ARM THICKNESS = 2.8
TABLE THICKNESS = 2.8
SQUARE RIB SECTION = 3 X 3

FIG.5·1 HORIZONTAL KNEE TYPE MILLING MACHINE

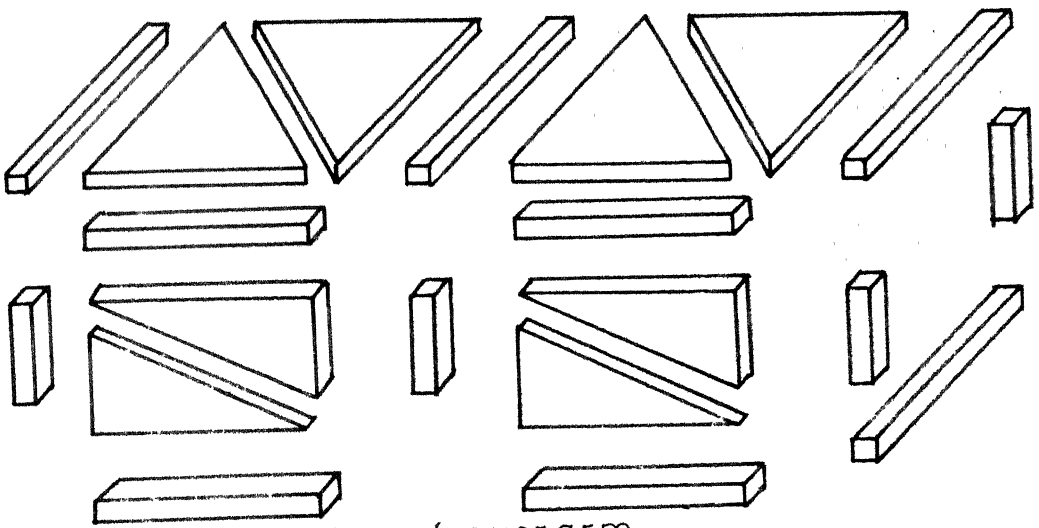

Idealization of overarm

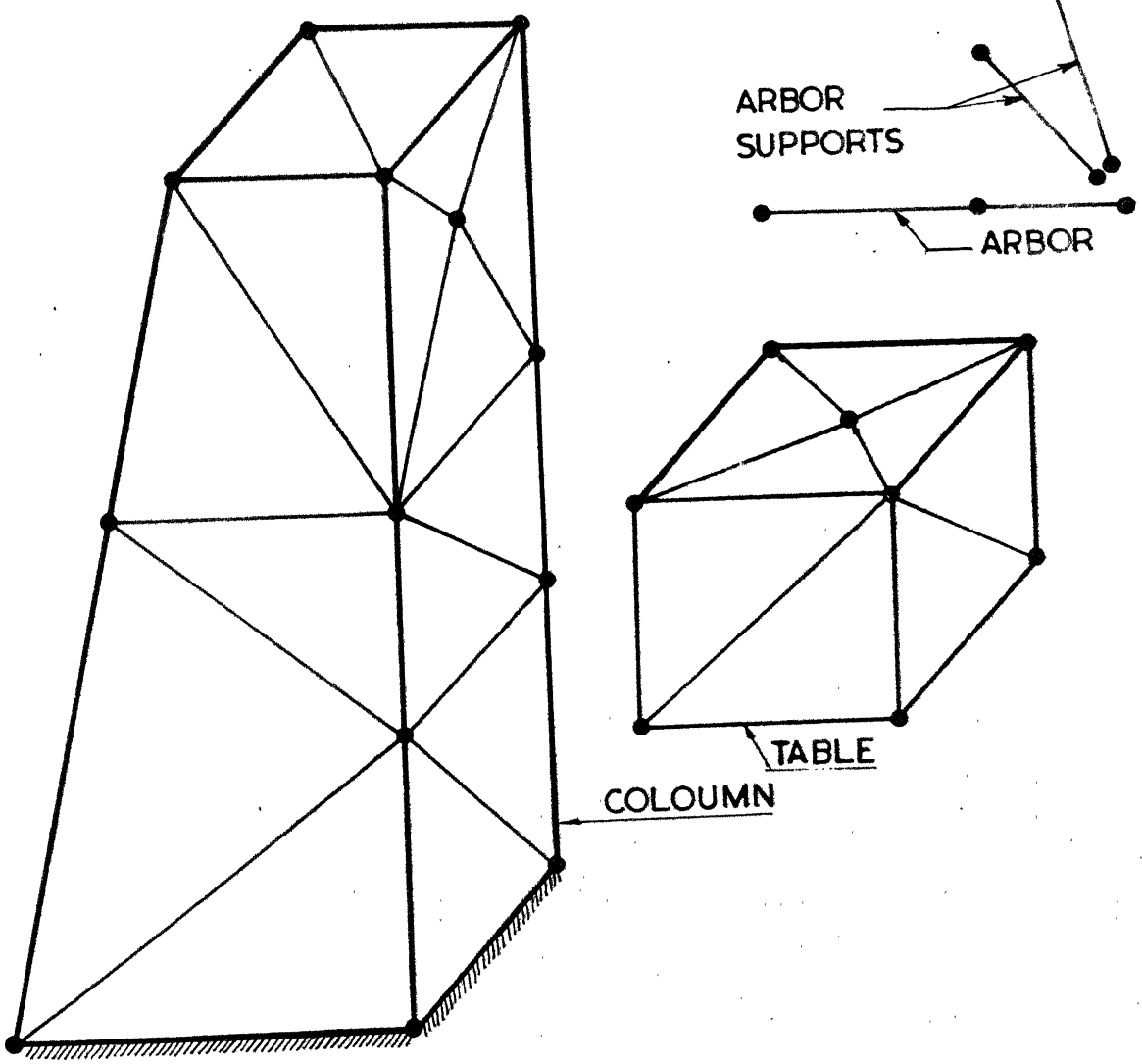

G.5.2 FINITE ELEMENT IDEALISATION OF MILLIING MACHINE

(SHOWN IN FIG.5-1)

$\tilde{[K]}$ = generalised stiffness matrix

$\tilde{[M]}$ = generalised mass matrix

$[X]$ = initial approximate vectors

N = degrees of freedom

p = number of required first few modes.

$ITER_{max}$ = maximum number of subspace iterations allowed

$[Q]$ = Eigen vectors of the projected operators

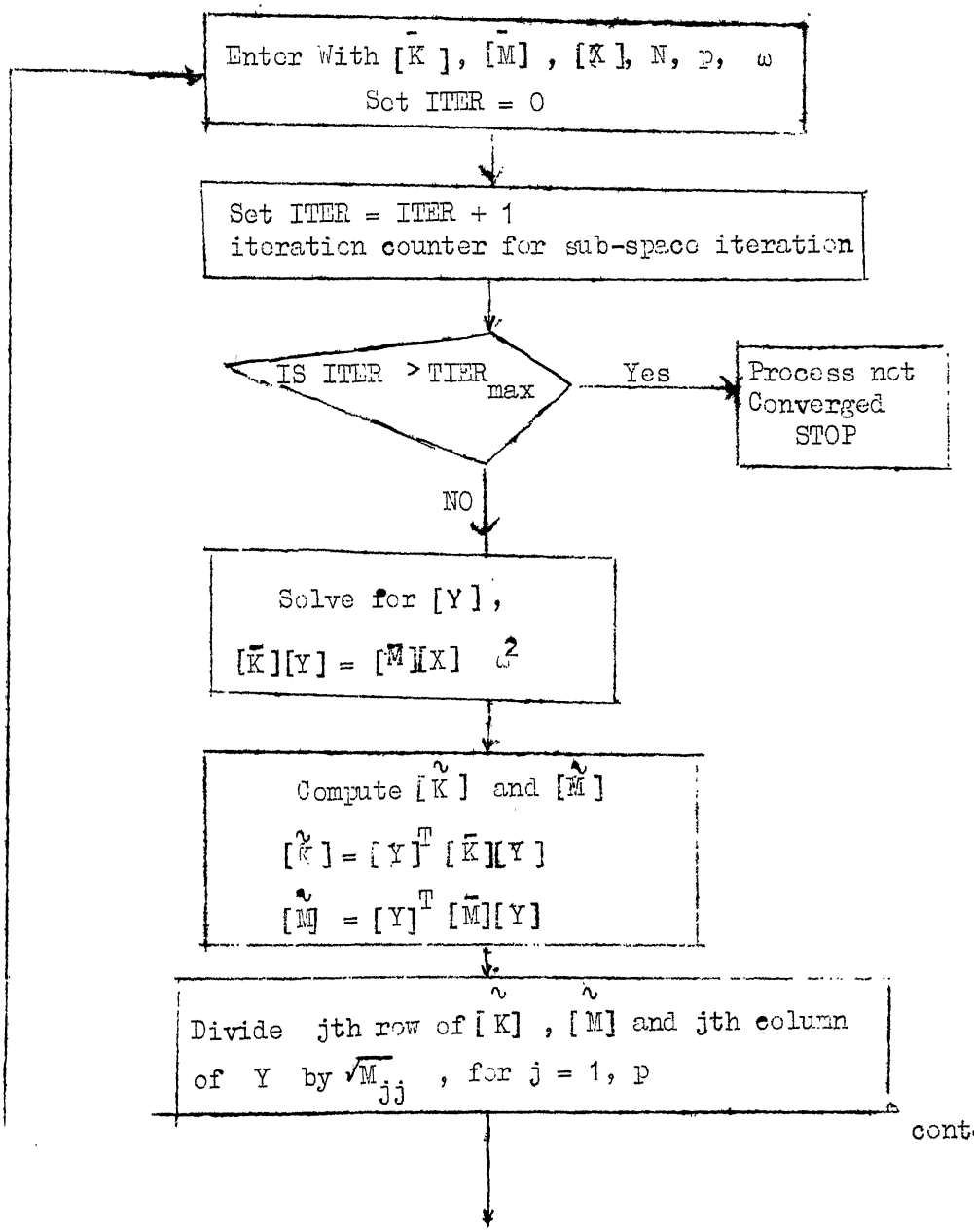

contd...

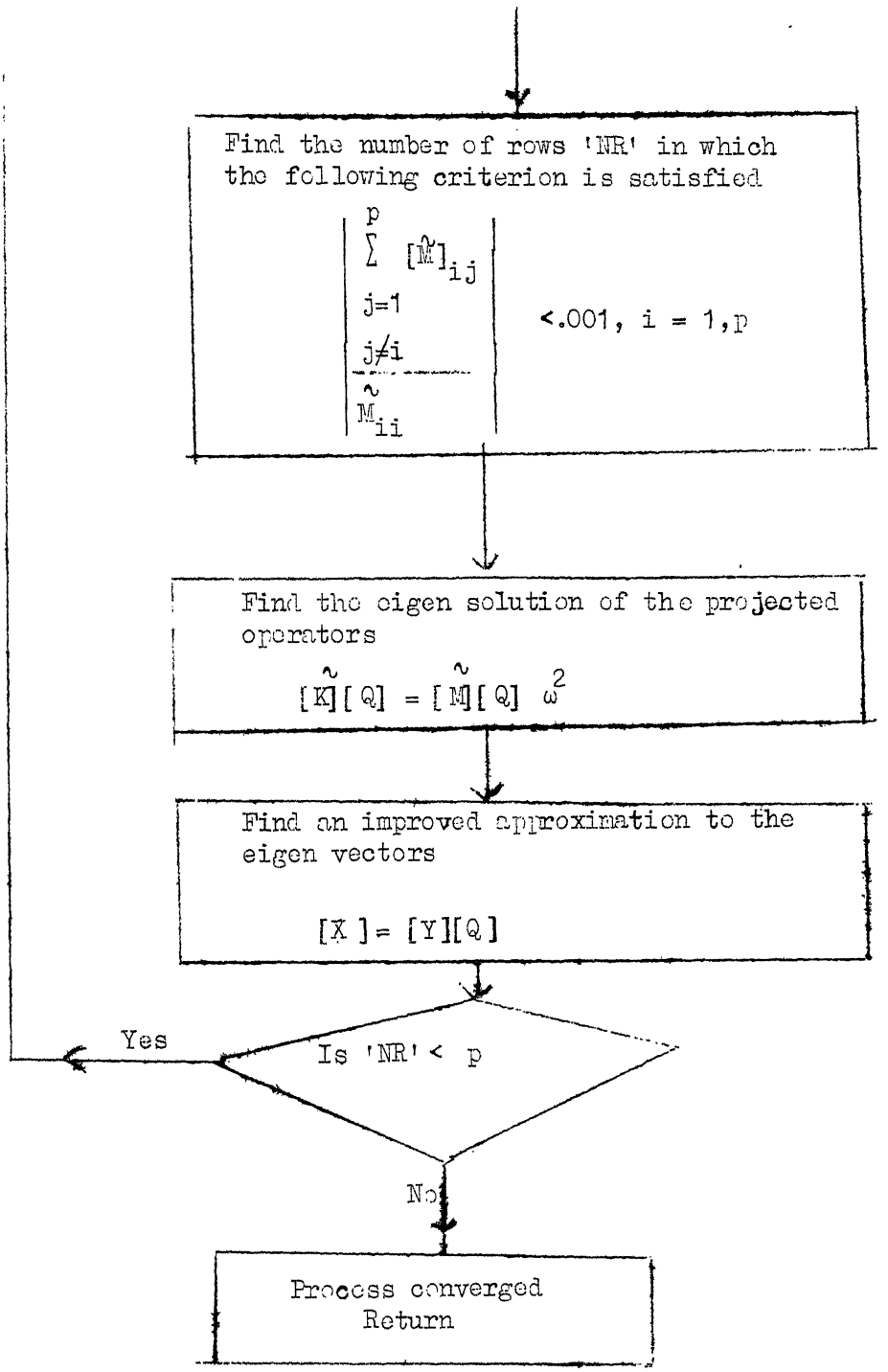

Fig. 5.3 Rayleigh-Ritz Sub Space Iteration Algorithm for Determining Eigensolutions

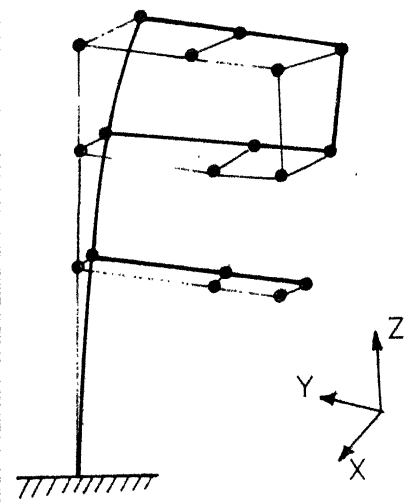

ST MODE
URAL FREQUENCY 1003

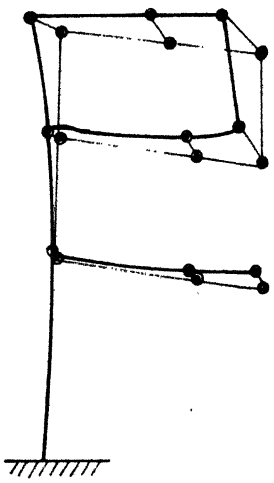

b). SECOND MODE
NATURAL
FREQUENCY 1150

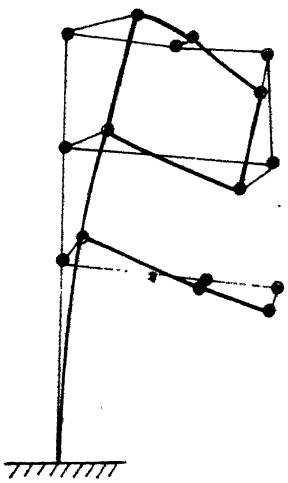

C). THIRD MODE
NATURAL
FREQUENCY 1521

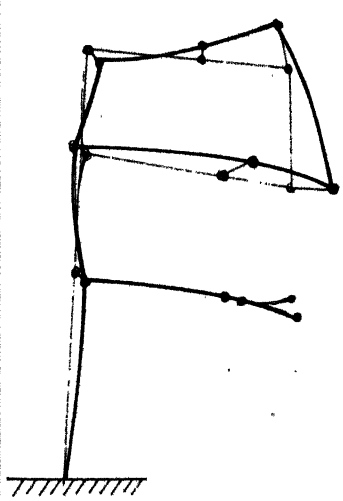

URTH MODE
TURAL
REQUENCY 2296

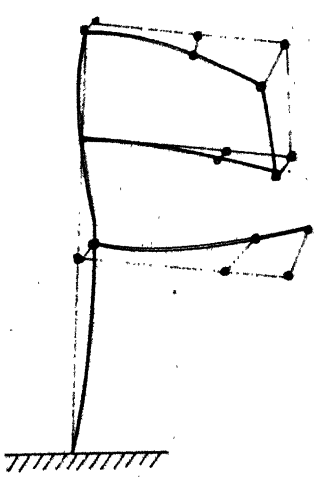

e). FITH MODE
NATURAL
FREQUENCY 3009

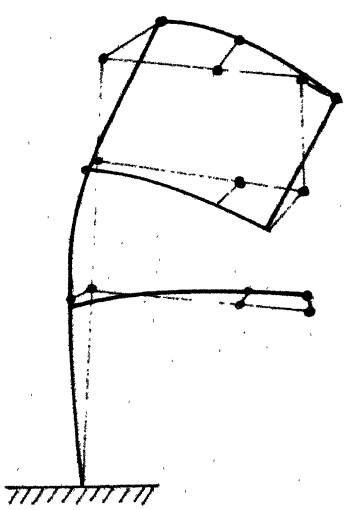

f). SIXTH MODE
NATURAL
FREQUENCY 3581

FREQUENCIES IN RADIANS / SEC.

FIG.5.4 MODE SHAPES OF HORIZONTAL MILLING MACHINE.

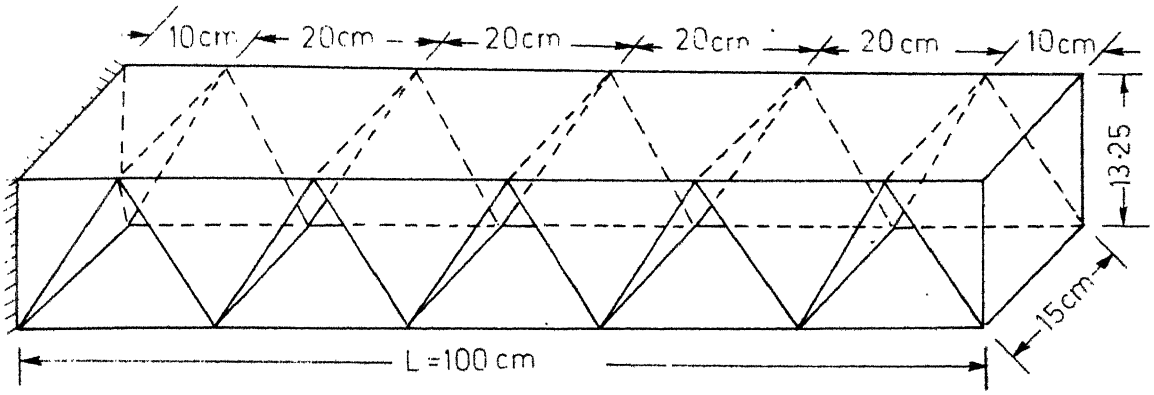

(a) WARREN TYPE LATHE BED

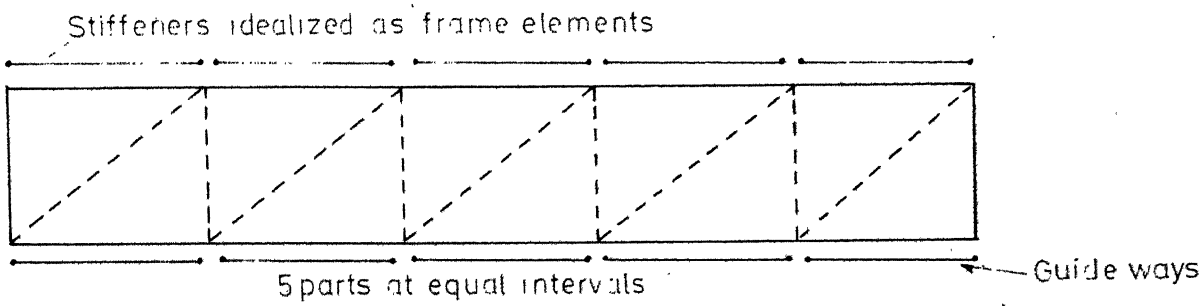

(b) FINITE ELEMENT GRID ON BOTTOM SURFACE

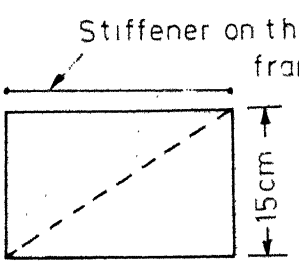

(c) LACING DIAGONAL

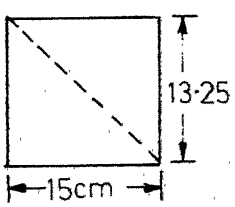

(d) SIDE PLATE

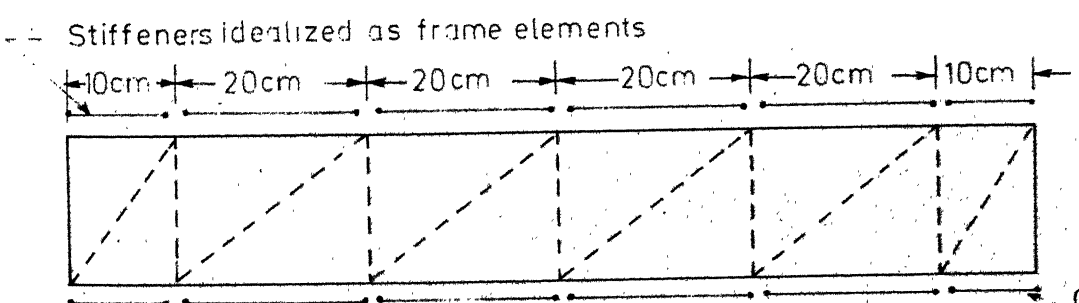

(e) FINITE ELEMENT GRID ON TOP SURFACE

Dotted lines represent finite element grid

5·5 DETAILS OF IDEALIZATION OF WARREN TYPE

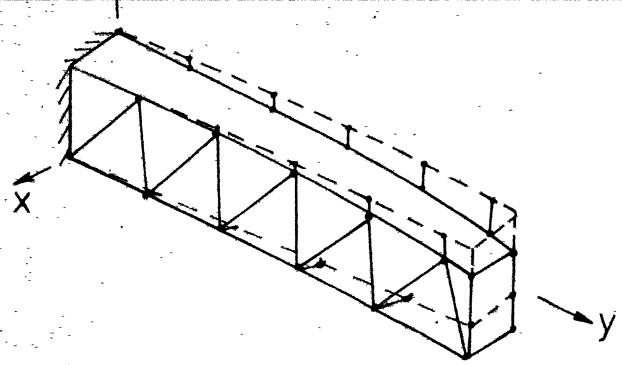

(a) First mode ($\omega_1 = 734$)

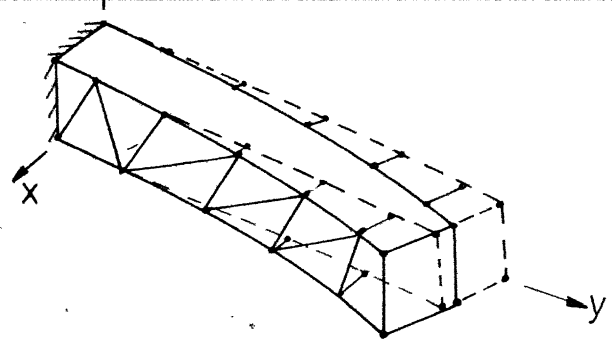

(b) Second mode ($\omega_2 = 970$)

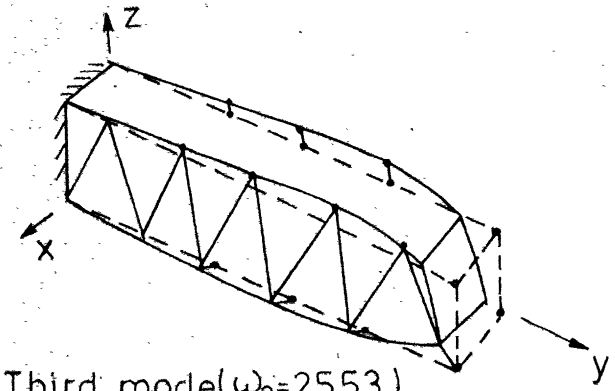

(c) Third mode($\omega_3 = 2553$)

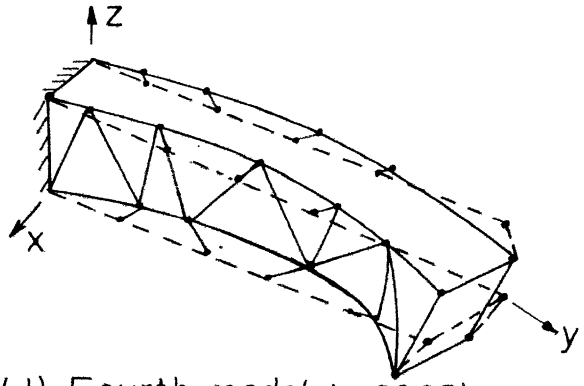

(d) Fourth mode($\omega_4 = 3325$)

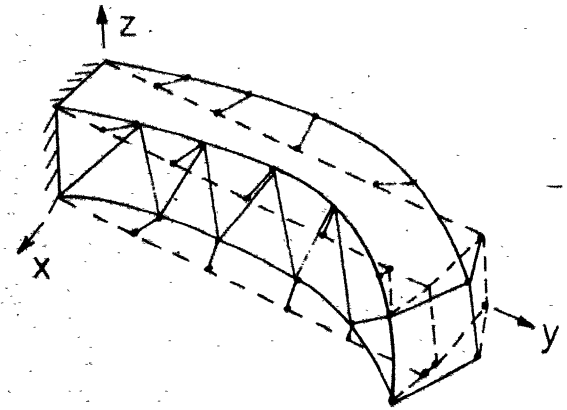

(e) Fifth mode($\omega_5 = 4632$)

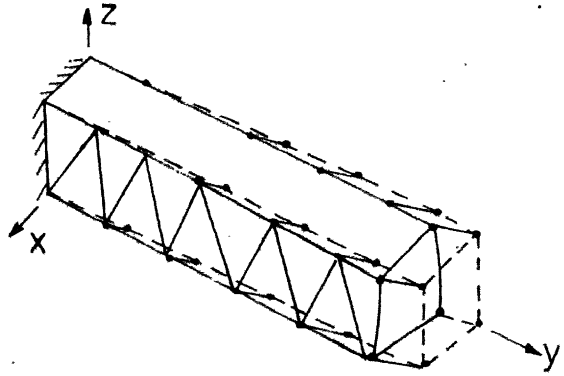

(e) Sixth mode ($\omega_4 = 5405$)

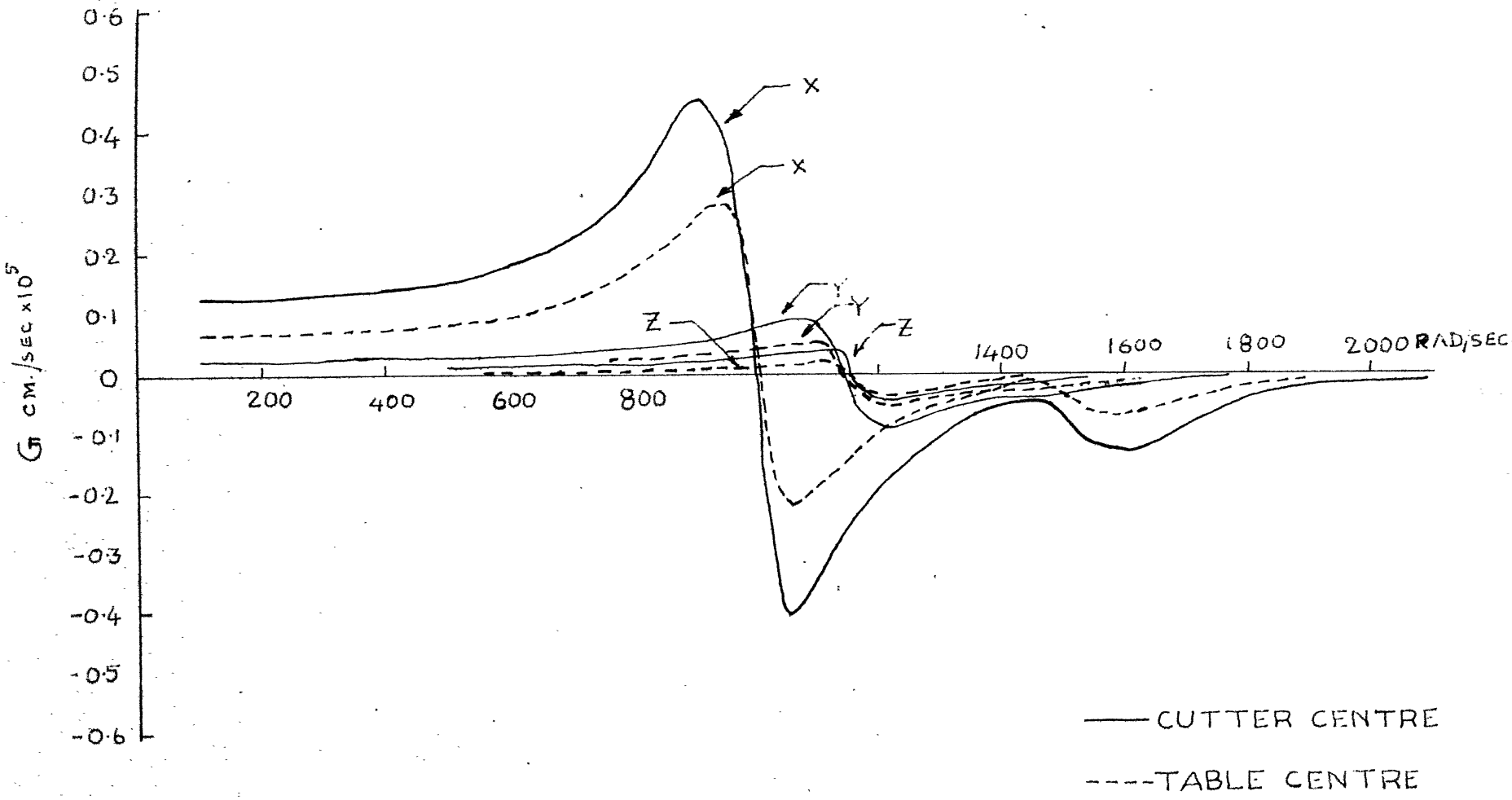

FIG.5·7 INPHASE CROSS RECEPTANCES OF CUTTER CENTRE AND TABLE (ALONG X, Y, Z DIRECTIONS) OF MILLING MACHINE.

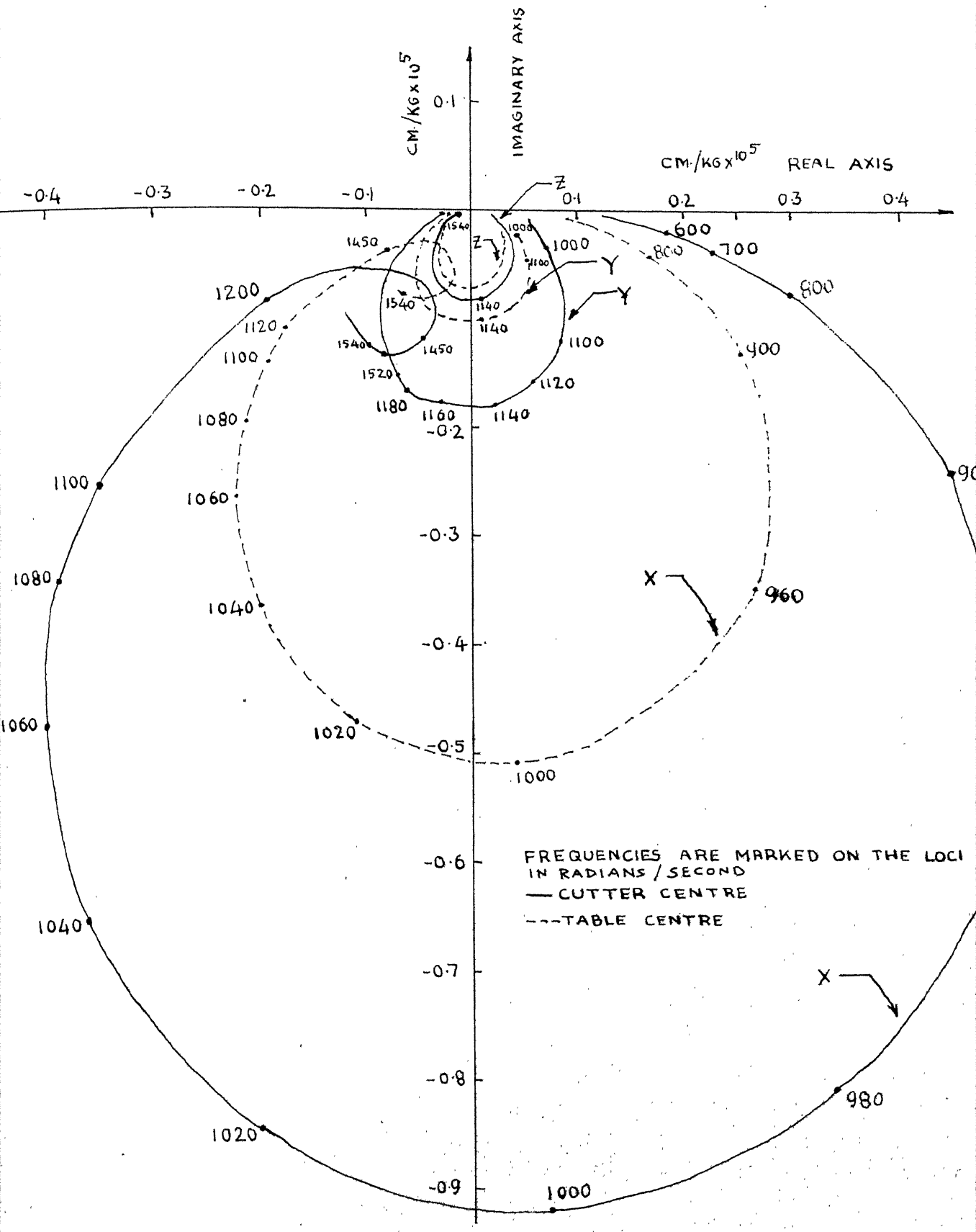

FIG.5.8 HARMONIC RESPONSE LOCI OF CUTTER CENTRE AND TABLE (X,Y,Z DIRECTIONS) OF MILLING MACHINE.

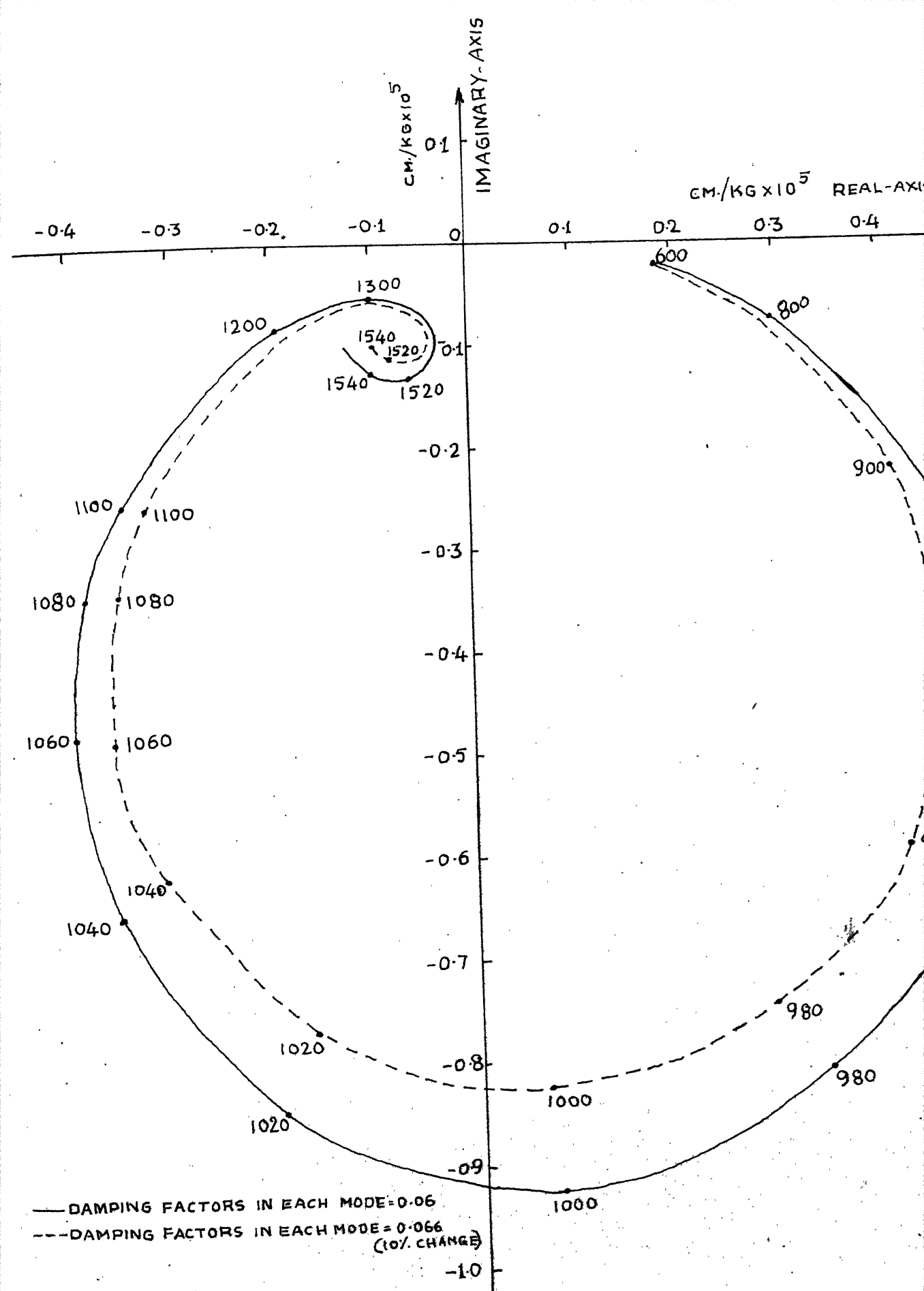

FIG.5.9 EFFECT OF DAMPING FACTORS ON HARMONIC RESPONSE LOCUS (X-DIRECTION) OF MILLING MACHINE

CHAPTER 6

OPTIMIZATION METHOD

In chapter 2, the problem of optimum design of machine tool structures has been formulated as a nonlinear mathematical programming problem. The methods of computing static deflections, natural frequencies and the receptances, on which restrictions are to be imposed, have been developed in chapter 3, 4 and 5. The choice of the method of optimization procedure and its description is the topic of this chapter.

6.1 CHOICE OF THE METHOD

The three general classes of widely used nonlinear programming methods are as follows:[67] a) Gradient projection method of Rosen[68] subsequently modified by Goldfarb[69]: Though this method works well with linear constraints, its efficiency is considerably reduced in the case of nonlinear constraints. b) Feasible directio method of Zoutendijk[70]: This method would also present difficulti similar to the gradient projection method. c) Penalty function method : In these methods, the constrained formulation is transformed into a sequence of unconstrained optimizations which can be solved without much difficulty. These methods are quite reliable and the sequential nature of these methods allows a gradual approac to criticality of constraints. These methods allow course

approximations to be used during early stages of the optimization procedure and close approximations during the final stages. The computational time, however, is more in these methods because the minimization problem has to be solved a number of times. To reduce the computer time, the penalty function methods allow the use of approximate analysis without effecting the accuracy and stability of the procedure. In the present work, the penalty function method of Fiacco and McCormick[71] is used as it has been found to be quite reliable.

6.2 FIACCO- McCORMICK INTERIOR PENALTY FUNCTION METHOD

In this method, the objective function is augumented with a penalty term consisting of the constraints as shown below:

$$\phi(\vec{X}, r_k) = f(\vec{X}) - r_k \sum_{j=1}^{m} \frac{1}{g_j(\vec{X})} \qquad (6.1)$$

where $\phi(\vec{X}, r_k)$ is called the penalty function, and r_k is called penalty parameter in k^{th} minimization step. The minimization of ϕ-function is performed for a decreasing sequence of r_k so that

$$r_{k+1} < r_k \qquad (6.2)$$

The equation 6.1 requires a feasible starting point and, in the present work, it is found by trial and error. Since each of the designs generated during the optimization process lies inside the acceptible design space, the method is classified as interior penalty function formulation.

6.3 DAVIDON - FLETCHER - POWELL VARIABLE METRIC UNCONSTRAINED MINIMIZATION METHOD

In the penalty function formulations, since a sequence of unconstrained minimizations has to be performed, the selection of an efficient method of unconstrained minimization becomes very important. All the methods of unconstrained minimization find a sequence of improved approximations to the optimum according to the iteration :

$$\vec{X}_{i+1} = \vec{X}_i + \tau^* \vec{S}_i \qquad (6.3)$$

where,

$\vec{X}_{i+1}$ = the design vector corresponding to the minimum of ϕ-function along the current direction $\vec{S}_i$

$\vec{X}_i$ = the starting design vector

τ^* = the minimizing step length in the direction $\vec{S}_i$.

There are several methods available for finding the search direction $\vec{S}_i$ in equation 6.3.

In the present work, the Davidon-Fletcher-Powell Variable Metric method[72] is used. This method can be considered as a quasi-Newton algorithm, and is a very powerful general procedure for finding a local unconstrained minimum of a function of many variable In this method, the i^{th} search vector $\vec{S}_i$ in equation 6.3 is computed according to the following relation

$$\vec{S}_i = -[H_i] \nabla\phi (\vec{X}_i) \qquad (6.4)$$

where $\nabla\phi\ (\vec{X}_i)$ denotes the gradient of the ϕ-function at $\vec{X}_i$ and $[H_i]$ is a positive definite symmetric matrix. The matrix $[H_i]$ is updated according to the following procedure

$$[H_{i+1}] = [H_i] + [A_i] + [B_i] \tag{6.5}$$

where,

$$[A_i] = \frac{\tau^* \vec{S}_i \vec{S}_i^T}{\vec{S}_i^T \vec{V}_i} \tag{6.6}$$

$$[B_i] = \frac{[H_i] \vec{V}_i \vec{V}_i^T [H_i]^T}{\vec{V}_i^T [H_i] \vec{V}_i} \tag{6.7}$$

and

$$\vec{V}_i = \nabla\phi\ (\vec{X}_{i+1}) - \nabla\phi(\vec{X}_i) \tag{6.8}$$

The updating of $[H_i]$ preserves the symmetric positive definiteness of $[H_{i+1}]$ which ensures the stability of the procedure. The positive definiteness of $[H_{i+1}]$ is influenced only by the accuracy with which τ^* is determined. To start with $[H_0]$ is taken as the identity matrix.

6.4 ONE DIMENSIONAL MINIMIZATION METHOD

In the present work, the one dimensional minimization is accomplished by cubic interpolation method. In this method, the algorithm used to compute τ^* is reapplied until $\vec{S}_i^T \cdot \nabla\phi_{i+1}$

becomes moderately small. If the cosine of the angle between the vectors $\vec{S}$ and $\nabla\phi$ at the minimizing step length τ^* is sufficiently small quantity (ε), i.e.

$$\cos\theta = \frac{\vec{S}^{T} \cdot \nabla\phi}{|\vec{S}| \cdot |\nabla\phi|} < \varepsilon \quad , \tag{6.9}$$

the one dimensional minimization is considered to have converged to τ^*. In the present work, the value of ε is taken as 0.05. However to reduce the computer time, the number of cubic interpolations is limited to three.

6.5 ADDITIONAL CONSIDERATIONS AND CONVERGENCE CRITERIA

6.5.1 Initial and Subsequent Values of r_k

The initial value of r is taken such that[74]

$$1.5 \quad f(\vec{X}_o) \leq f(\vec{X}_o, r_1) \leq 2f(\vec{X}_o) \tag{6.10}$$

and the subsequent values of r_k are found by using the following relation

$$\frac{r_{k+1}}{r_k} = 0.1 \tag{6.11}$$

6.5.2 Restarting the [H] Matrix

If a function that is to be minimized is highly distorted, it might occur that $\vec{S}_i \cdot \nabla\phi_i$ is positive after a few iterations, indicating that $\vec{S}_i$ is not a direction of descent. In such cases the remedy is to set $[H_i]$ as $[H_o]$ and start all over again.

In the present work, however, such a situation never occurred in all the examples studied.

6.5.3 Termination of Minimization for Each r_k

The minimization of ϕ- function for each value of r_k is terminated when the predicted percentage difference between the current and the optimal ϕ -values is smaller than a small quantity, ε[74] :

$$\frac{\nabla\phi_i^T [H_i] \nabla\phi_i}{2\phi_i} = \frac{S_i^T \cdot \nabla\phi_i}{2\phi_i} < \varepsilon \qquad (6.12)$$

The value of ε used in the present work varied from 0.05 for r_1 to 0.005 for subsequent r_k .

6.5.4 Relative and Global Minima

In the design of horizontal milling machine structures, two completely different starting design vectors are used for the sequence of minimizations to see whether any relative minima exist in the design space. Two different starting design vectors led to the same optimum design. Although, merely on the basis of two trial starting designs, it is hard to say that the minimum obtained is the absolute minimum over the design space; finding the similar least weight design by starting from two different initial designs is at least a pointer in that direction.

6.6 COMPUTATION OF THE GRADIENT OF ϕ - FUNCTION ($\nabla\phi$)

The variable metric method, used in the present work, requires the gradient of the ϕ-function for computing every new search direction and the one dimensional minimization method might require the evaluation of $\vec{S}^{T}\nabla\phi$ more than once in every search direction. The gradient of the ϕ-function is obtained by differentiating the ϕ-function with respect to the design variables as,

$$\nabla\phi = \begin{bmatrix} \partial\phi/\partial X_1 \\ \partial\phi/\partial X_2 \\ \vdots \\ \partial\phi/\partial X_n \end{bmatrix} \qquad (6.13)$$

In the present work, the forward finite difference scheme is used for computing the gradient $\nabla\phi$. This scheme requires (n+1) evaluations of the ϕ-function where n is the number of design variables to compute $\nabla\phi$. Apart from this a few more ϕ-function evaluations are required for each one dimensional minimization. Since the evaluation of one ϕ-function itself requires a lot of computer time, any alternative procedure, which computes the gradient faster, would substantially improve the efficiency of the optimization program.

In computing the ϕ-function at any design vector, a major portion of computer time is spent in the evaluation of the stiffness

and mass matrices and the response quantities i.e., static deflections, natural frequencies of vibration and the dynamic displacements of the structure. In the present work, an alternate procedure, which is more efficient than the finite difference scheme, is developed for the evaluation of the gradient of ϕ . This method is based on the reanalysis technique of modified structures. The reanalysis procedure deals with the best way of obtaining the response quantities at a modified design vector given the stiffness and mass matrices and the response quantities at a certain design vector.

6.6.1 Derivatives of Static Displacements[75]

Consider again the matrix equations

$$[\bar{K}]\,\vec{Y} = \vec{P} \tag{6.14}$$

where $[\bar{K}]$ and $\vec{P}$ depend on the design vector $\vec{X}$. By taking the derivatives of equation 6.14 with respect to the design variable X_i ,

$$[\bar{K}]\,\frac{\partial \vec{Y}}{\partial X_i} + \frac{\partial [\bar{K}]}{\partial X_i}\,\vec{Y} = \frac{\partial \vec{P}}{\partial X_i} \tag{6.15}$$

i.e.

$$[\bar{K}]\,\frac{\partial \vec{Y}}{\partial X_i} = \frac{\partial \vec{P}}{\partial X_i} - \frac{\partial [\bar{K}]}{\partial X_i}\,\vec{Y} \tag{6.16}$$

The terms $\frac{\partial \vec{P}}{\partial X_i}$ and $\frac{\partial [\bar{K}]}{\partial X_i}$ on the right side of equation 6.16 are computed by finite difference method. Let the design $\vec{X}$ be

perturbed to $\vec{X}^*$ by changing X_i to $X_i + \Delta X_i$. At this new design $\vec{X}^*$, the stiffness matrix $[\bar{K}^*]$ can be generated by the regular procedure.

Thus

$$[\frac{\partial \vec{K}}{\partial X_i}] = \frac{[\bar{K}^*] - [\bar{K}]}{\Delta X_i} \tag{6.17}$$

similarly,

$$\frac{\partial \vec{P}}{\partial X_i} = \frac{\vec{P}^* - \vec{P}}{\Delta X_i} \tag{6.18}$$

where $\vec{P}^*$ is the load vector at $\vec{X}_i^*$.

Therefore equation 6.16 can be written as

$$[\bar{K}]\frac{\partial \vec{Y}}{\partial X_i} = \frac{\vec{P}^* - \vec{P}}{\Delta X_i} + [\frac{[\bar{K}^*] - [\bar{K}]}{\Delta X_i}]\vec{Y} \tag{6.19}$$

On the right hand side of equation 6.19, there will be as many vectors as the number of design variables. Therefore this problem reduces to solving an equilibrium equation with 'n' vectors on the right hand side. Equation 6.19 has been solved to get $\frac{\partial \vec{Y}}{\partial X}$ by the cholesky decomposition of symmetric banded matrices as discussed in the previous chapter. The displacements at $\vec{X}^*$ computed by using equation 6.19 are compared with those obtained by the exact method in Table 6.1. It can be observed from this table, that the values given by the present approximate method are almost same as those obtained by the exact method.

6.6.2 Derivatives of the Natural Frequencies

Since the first few natural frequencies of vibration of a general eigenvalue problem

$$[\bar{K}]\,\vec{Y} = \omega^2 [\bar{M}]\,\vec{Y} \tag{6.20}$$

are only involved in the constraints, the values of $\frac{\partial \omega}{\partial X_k}$, $k = 1,2,\ldots,n$, required for use in the reanalysis cycle of optimization. By differentiating equation 6.20, the exact expression for the rates of changes of eigenvalues is given by

$$\frac{\partial \omega}{\partial X_k} = \frac{1}{2\omega_i\, Y_i^T [\bar{M}_{ij}]\, \vec{Y}_i} \left[\vec{Y}_i^T \left[\frac{\partial [\bar{K}]}{\partial X_k} \right] \vec{Y}_i - \omega_i^2\, Y_i^T \frac{\partial [M_{ij}]}{\partial X_k} \vec{Y}_i \right] \tag{6.21}$$

This equation has been used for the eigenvalue analysis at modified designs by Fox and Kapoor[21]. The partial derivatives of $[\bar{K}]$ are found by using equation 6.17 and those of $[\bar{M}]$ using a similar equation:

$$\left[\frac{\partial \bar{M}}{\partial X_i} \right] = \frac{[\bar{M}^*] - [\bar{M}]}{\Delta X_i} \tag{6.22}$$

Thus equation 6.21 becomes

$$\frac{\partial \omega_i}{\partial X_k} = \frac{1}{2\omega_i\, \Delta X_k\, \vec{Y}_i^T [\bar{M}]\, \vec{Y}_i} \left[\vec{Y}_i^T [\bar{K}^*] \vec{Y}_i - \vec{Y}_i^T [\bar{K}]\, \vec{Y}_i - \omega_i^2\, \vec{Y}_i^T [\bar{M}^*] \vec{Y}_i + \omega_i^2\, \vec{Y}_i^T [\bar{M}]\, \vec{Y}_i \right] \tag{6.23}$$

The values of ω_i at $\vec{X}^*$ calculated by using equation 6.23 are compared with those obtained by the exact method in Table 6.1. It can be seen that the values obtained by equation 6.23 are in excellent agreement with those obtained by the exact method. The values of ω_i as predicted by the approximate method (equation 6.23) and by the exact method for various percentage changes in the design variable are shown in Table 6.2 and in the Fig. 6.1. These results indicate that the frequency values do not differ by more than 2.5% even for a change of 20% in the value of the design variable.

6.6.3 Derivatives of the Eigen Vector

In the present work, a partial solution to the general eigenvalue problem

$$[\bar{K}]\ \vec{Y} = \lambda[\bar{M}]\ \vec{Y} \tag{6.24}$$

is solved for computing the receptances of the structures. Since the eigen vectors form a complete set of vectors, any N-component vector can be represented as a linear combination of the N-eigen vectors as[74]:

$$\frac{\partial \vec{Y}_i}{\partial X_j} = \sum_{k=1}^{N} a_{ijk}\ \vec{Y}_k \tag{6.25}$$

where,

$$a_{ij\ell} = \frac{\vec{Y}_i^T \left[\frac{\partial[\bar{K}]}{\partial X_j} - \lambda_i \frac{\partial[\bar{M}]}{\partial X_j} \right] \vec{Y}_i}{(\lambda_i - \lambda_\ell)}, \quad i \neq \ell \qquad (6.26)$$

$$a_{iji} = \frac{\vec{Y}_i^T [\bar{M}] \vec{Y}_i}{2}, \quad i = \ell, \qquad (6.27)$$

and Y_i are $[\bar{M}]$ - orthonormal vectors. When a partial eigen solution is available, the derivatives of an eigen vector can be approximated as

$$\frac{\partial \vec{Y}_i}{\partial X_j} \approx \sum_{k=1}^{p} a_{ijk} \vec{Y}_k \qquad (6.28)$$

where $p < N$.

This approach has been used by Kapoor to find the eigen vectors and dynamic displacements at modified designs[76]. Recently, Imam, Sandor and Kramor[77] used this approach in the deflection and stress analysis of high speed planar mechanisms with elastic links.

The quantities $\frac{\partial[\bar{K}]}{\partial X_j}$ and $\frac{\partial[\bar{M}]}{\partial X_j}$ are obtained in the same way as explained in the previous sections. In the present work, using the equation 6.28, the approximate eigen vectors are computed at $\vec{X}^*$ and then the corresponding values of G_{MIN} are computed. The values thus computed are compared with those obtained by an exact eigen solution in Table 6.1. Here again, it can be observed that the two sets of values agree well with each other.

TABLE 6.1 COMPARISION OF RESPONSE QUANTITIES BY EXACT AND APPROXIMATE METHOD

	for 1% change in X_1		for 1% change in X_2		for 1% change in X_3		for 1% change in X_4		for 1% change in X_5		for 1% change in X_6	
	correct method	approx. method	correct method	approx. method	correct method	approx. method	correct method	approx. method	correct method	approx. method	correct method	approx. method
d_o cm. x 10^5	660.48	660.47	660.43	660.46	658.4	658.41	660.0	659.38	660.52	660.59	660.72	660.74
G_{MIN} cm./kg x 10^9	644	645	643	645	660	644	638	641	645	646	645	646
ω_1 rad./sec.	1003.73	1003.723	1001.39	1001.38	1008.11	1007.96	1005.24	1005.23	1001.97	1002.3	1002.61	1002.57
ω_2 rad./sec.	1158.21	1158.27	1148.25	1148.22	1148.09	1148.27	1153.78	1153.66	1149.48	1149.56	1149.63	1149.62

TABLE 6.2 THE VALUES OF ω_1 BY EXACT AND APPROXIMATE METHODS

	PERCENTAGE CHANGES IN DESIGN VARIABLE X_1			
	5%	10%	15%	20%
EXACT METHOD	1005.57 rad./sec.	1008.42 rad./sec.	1010.70 rad./sec.	1012.78 rad./sec.
APPROXIMATE METHOD	1005.18 rad./sec.	1010.06 rad./sec.	1023.20 rad./sec.	1036.27 rad./sec.

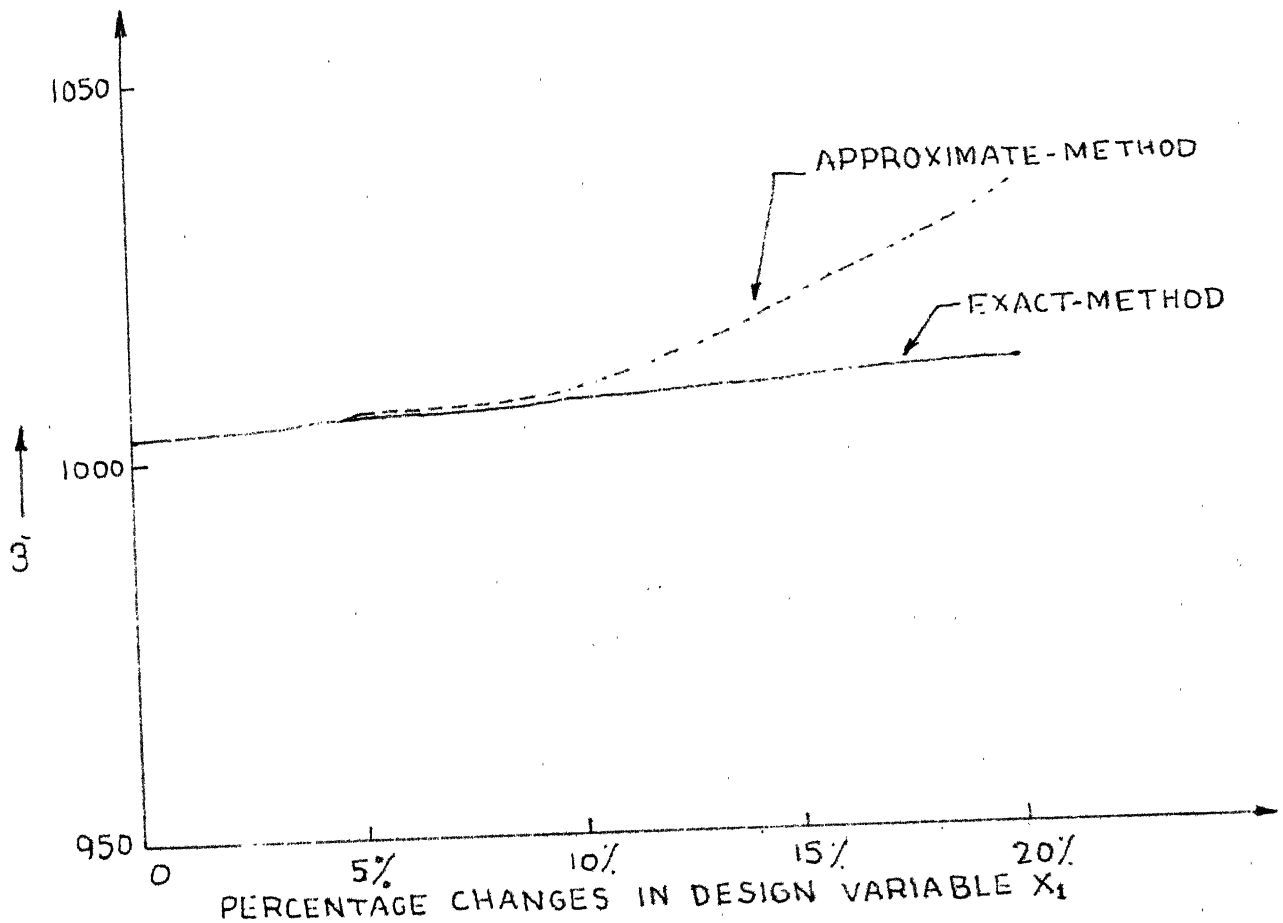

FIG·6·1 COMPARISION OF FUNDAMENTAL NATURAL-FREQUENCY BY EXACT AND APPROXIMATE METHOD.

CHAPTER 7

ILLUSTRATIVE EXAMPLES

The optimization problem formulated in the previous chapters has been applied to the minimum weight design of two different types of machine tool structures, namely, the lathe bed and a horizontal knee-type of milling machine structure . These machine tool structures were optimized in order to demonstrate the feasibility and effectiveness of designing complex structures with multiple behavior constraints. A computer program has been developed to optimize machine tool structures using finite element idealization. As stated earlier, the analysis routine incorporates the frame elements, triangle bending elements and triangular plane stress elements. These elements are sufficiently general to idealize several types of machine tool structures. The static and dynamic analysis programs as well as the optimization program are also written as general subroutines. Hence, the optimum design of any other type of machine tool structure can be accomplished by using the present computer program by making little modifications. The computer program developed is described in Appendix B.

The results of the present optimization study are presented in this chapter.

7.1 LATHE BED DESIGN

Example 1 :

The first example considered is a Warren-type lathe bed shown in Fig. 7.1. The over-all diamensions of this bed are taken

from the bed of lathe machine model No. MB02, year 1967, manufactured by Mysore Kirloskar Ltd., Harihar, India. This bed is optimized with a lower limit of 630 radians/second on the fundamental frequency and an upper limit of 0.00174 radians on the torsional deflection when a torque of 13,000 kg.cm. is applied at one end of the structure by keeping the other end fixed. This torque corresponds to a horse power of 4 if the turning is done at the lowest spindle speed of 22 rpm. In this design, 4 design variables and 10 design constraints are considered. The finite element modelling for this structure is shown in Fig. 7.2. The idealization of the structure consists of 26 node points, 46 triangular plate bending elements and 32 frame elements. The number of degrees of freedom considered in the static and eigenvalue analysis is 132. The band width of the stiffness matrix is 36. The guides on the main members are taken to be rectangular in cross section (6.5 cm x 2.0 cm.).

In the generation of the global stiffness and mass matrices, identically disposed finite elements of the same size and shape are grouped together so as to reduce the computational effort involved. This resulted in the saving of computer time upto about 80% in the generation of global stiffness and mass matrices. The design variables are :

X_1 = thickness of the main members

X_2 = thickness of the lacing diagonals

X_3 = stiffener width on the main and lacing diagonals

X_4 = stiffener depth on the main and lacing diagonals.

The material of the structure is taken as grey cast iron with the following material properties :

density (ρ) = 7.2 gms./cm^3.

Young's modulus (E) = 1.12 x 10^6 kg/cm^2.

Poisson's ratio (ν) = 0.25

The geometrical and behavior constraints are as follows :

Geometrical constraints :

g_1 = 1.0 cm. - X_1

g_2 = X_1 - 2.0 cm.

g_3 = 1.0 cm. - X_2

g_4 = X_2 - 2.0 cm.

g_5 = 1.75 cm. - X_3

g_6 = X_3 - 3.2 cm.

g_7 = 1.0 cm. - X_4

g_8 = X_4 - 2.2 cm.

Behavior constraints :

g_9 = d_L - 0.00174 radians

g_{10} = 630 radians/second - ω_1

where d_L is the average torsional deflection of one end of the bed in radians. The optimization results are shown in Table 7.1. The progress of the optimization path, showing the cumulative number of one-dimensional minimizations verses the weight of the structure, for this example is given in Fig. 7.3. The least weight design has a weight of 47.93 kg. with a reduction of 45.5% compared to the starting design.

Among the side constraints, X_1 and X_2 are at their lower bounds. None of the behavior constraints are active in this example. The natural frequency ω_1 gradually increased from 718 radians/second at initial design to 735 radians/second at optimum design, whereas, ω_2 gradually decreased from 978 radians/second at initial design to 949 radians/second at optimum design. The average computer time taken for one one-dimensional minimization is 3.5 minutes on IBM 370/155 computer. The number of one-dimensional minimizations is 10 and the computer time taken is 35 minutes.

Example 2 :

In this example, the same lathe bed shown in Fig. 7.1 is optimized by taking 5 design variables and 14 design constraints. The design variables X_1, X_2, X_3 and X_4 are same as before. The width of the lathe bed is included as the fifth design variable X_5 in this example. A limitation is also placed on the second natural frequency in this example. The initial design vector is chosen such that the behavior constraints are nearly satisfied at $\vec{X}_o$. This was done to see whether any weight could be reduced from this starting design vector. The starting design corresponds to a weight of 87.49 kg. The geometrical and the behavior constraints in this example are as follows :

Geometrical constraints :

$g_1 = 1.0 \text{ cm.} - X_1$

$g_2 = X_1 - 2.0 \text{ cm.}$

$$g_3 = 1.0 \text{ cm.} - X_2$$

$$g_4 = X_2 - 2.0 \text{ cm.}$$

$$g_5 = 1.75 \text{ cm.} - X_3$$

$$g_6 = X_3 - 3.2 \text{ cm.}$$

$$g_7 = 1.0 \text{ cm.} - X_4$$

$$g_8 = X_4 - 2.2 \text{ cm.}$$

$$g_9 = X_2 - X_3$$

$$g_{10} = 10.0 \text{ cm.} - X_5$$

$$g_{11} = X_5 - 18.0 \text{ cm.}$$

Behavior constraints :

$$g_{12} = d_L - .0005 \text{ radians}$$

$$g_{13} = 700 \text{ radians/second} - \omega_1$$

$$g_{14} = \omega_1 + 100 - \omega_2$$

The optimization results are shown in Table 7.2. The torsional deflection constraint is active in this example. The width of lathe bed (X_5) at optimum design is 13.50 cm. and it corresponds to a lacing angle of 53.5°. The proposed least weight design has a weight of 77.42 kg. with a reduction of 11.45% compared to the starting design. The progress of the optimization path is shown in Fig. 7.4. The number of one-dimensional minimizations is 14 and the computer time taken is 55 minutes.

7.2 HORIZONTAL KNEE-TYPE MILLING MACHINE STRUCTURAL DESIGN

Example 3(a) :

The horizontal knee-type milling machine structure, shown in Fig. 7.5, is considered for optimization in this example.

The finite element modelling for this structure is shown in Fig.7.6. In this example, 6 design variables and 16 design constraints are considered. The idealization of the structure consists of 30 node points, 50 triangular plate bending elements and 18 frame elements. The number of elastic degrees of freedom is 5[illegible] and the band width of the stiffness matrix is 42. In this problem, about 20% of the computer time was saved in generating the global stiffness and mass matrices by grouping finite elements of the same size and shape having the same transformation matrix from local to global coordinate system.

The arbor diameter is taken as 4 cm. The arbor support is idealized as two frame elements of rectangular cross-section (10 cm. x 7 cm.). The thickness of the dove-tail on front face of the column is taken as 3.5 cm. and it is added to the thickness of the column (X_4) on the front face. The thickness of the dove-tail on the bottom side of the over-arm is taken as 2.5 cm. This thickness is added to the thickness of the over-arm (X_2) on the bottom side.

The design variables are :

X_1 = column depth at the bottom

X_2 = thickness of the over-arm

X_3 = width of the machine

X_4 = thickness of the column and table

X_5 = column depth at the top

X_6 = square cross-sectional diamensions of the ribs on the over-arm and its joint with the column.

The geometrical and the behavior constraints are as follows :

Geometrical constraints :

$$g_1 = X_1 - 54.0 \text{ cm.}$$

$$g_2 = 35.0 \text{ cm.} - X_1$$

$$g_3 = 0.8 \text{ cm.} - X_2$$

$$g_4 = X_2 - 4.0 \text{ cm.}$$

$$g_5 = 24.0 \text{ cm.} - X_3$$

$$g_6 = X_3 - 35.0 \text{ cm.}$$

$$g_7 = 0.8 \text{ cm.} - X_4$$

$$g_8 = X_4 - 4.0 \text{ cm.}$$

$$g_9 = X_5 - X_1$$

$$g_{10} = 30.0 \text{ cm.} - X_5$$

$$g_{11} = -X_6$$

$$g_{12} = X_6 - 6.0 \text{ cm.}$$

Behavior constraints :

$$g_{13} = d_c - 0.009 \text{ cm.}$$

$$g_{14} = |G_{MIN}| - 0.000003 \text{ cm./kg.}$$

$$g_{15} = 850.0 \text{ radians/second} - \omega_1$$

$$g_{16} = \omega_1 + 100 - \omega_2$$

where,

d_c = maximum cutter centre deflection, and

G_{MIN} = minimum negative inphase cross receptance of cutter centre relative to table.

The material of the column, table, over-arm and arbor support is taken as grey cast iron with the same material properties given in the case of Warren type lathe bed. The material for arbor is assumed as wrought steel with the following material properties :

density (ρ) = 0.78 gms./cm^3.

Young's modulus (E) = 2.1 x 10^6 kg./cm^2.

Poisson's ratio (ν) = 0.3

The optimization results are tabulated in Table 7.3. The starting design corresponds to a weight of 740 kg. The proposed optimum design corresponds to a weight of 300.78 kg. with a reduction of 45.5% weight compared to the initial design. The active behavior constraints are static deflection (d_c = 0.008932 cm.) and the difference of ω_1 and ω_2 ($\omega_1 - \omega_2$ = 113 radians/second). The constraints on ω_1 and G_{MIN} approached criticality as the optimization process progressed. Among the geometrical constraints, X_2 = .987 cm. and X_4 = 0.905 cm. are near to their respective lower bounds. The average computer time required for one one-dimensional minimization is 8 minutes on IBM 370/155 system. The progress of the optimization path as a plot of 'f' and 'ϕ' functions verses the cumulative number of one-dimensional minimizations is shown in Fig. 7.7.

Example 3(b) :

In order to see whether the optimum design obtained in example 3(a) corresponds to a local minimum or the absolute minimum

in the design space, the same example has been rerun with a different starting design vector. The plot of 'f' and ϕ-function as the optimization progressed is shown in Fig. 7.8. It can be observed that the plot is similar to the one shown in Fig. 7.7. The optimization results for the example are shown in Table 7.4. The optimum design variables in the two cases agree well with each other except for small differences that might have occurred due to some round of errors and numerical instabilities in the optimization process. Although, merely on the basis of two trial starting designs, it is hard to say that the minimum obtained is the absolute minimum over the design space; finding the similar least weight design by starting from two different initial designs is atleast a pointer in that direction.

7.3 SENSITIVITY ANALYSIS

In practice , a designer would be interested in knowing how the response quantities vary with a change in the design parameters. This type of sensitivity analysis will help the designer in manipulating the design variables to suit some specific requirements. Further, in some cases, the results obtained from the optimization procedure may have to be rounded off to the nearest practical values of the design variables. Hence a sensitivity analysis of the response quantities d_c , ω_1 and G_{MIN} with respect to the various design variables is conducted. In this analysis, the reference design is taken same as the starting design point of example 3.

The results of the sensitivity analysis are shown in Figs. 7.9 to 7.11. From these figures, it can be seen that all the response quantities are most sensitive with respect to the width of the machine. The responses d_c, and G_{MIN} can be observed to be least affected by a change in the cross-section of the ribs on the over-arm . The natural frequency (ω_1) has been found to be least affected by a change in the depth of the column at the base. It can also be seen that the fundamental frequency varies nearly linearly with respect to each of the design variables.

TABLE 7.1 OPTIMIZATION RESULTS OF WARREN TYPE LATHE BED (EXAMPLE 1)

DESIGN VARIABLE	INITIAL DESIGN	BOUNDS		OPTIMUM DESIGN
		LOWER	UPPER	
X_1	1.80 cm.	1.00 cm.	2.00 cm.	1.029 cm.*
X_2	1.80 cm.	1.00 cm.	2.00 cm.	1.029 cm.*
X_3	2.90 cm.	1.75 cm.	3.20 cm.	1.970 cm.
X_4	1.90 cm.	1.00 cm.	2.20 cm.	1.110 cm.
TORSIONAL DEFLECTION (radians x 10^3)	0.44	--	1.74	0.826
FIRST NATURAL FREQUENCY (radians/second)	718	630	--	735
OBJECTIVE FUNCTION (weight of lathe bed)	88.25 kg.	--	--	47.92 kg.

REDUCTION IN WEIGHT OBTAINED BY OPTIMIZATION = 40.33 kg. (45.5%)
NUMBER OF ONE-DIMENSIONAL MINIMIZATIONS = 10
COMPUTER TIME REQUIRED = 35 minutes on IBM 370/155 system

*ACTIVE CONSTRAINTS

TABLE 7.2 OPTIMIZATION RESULTS OF WARREN TYPE LATHE BED (EXAMPLE 2)

DESIGN VARIABLE	INITIAL DESIGN	BOUNDS LOWER	BOUNDS UPPER	OPTIMUM DESIGN
X_1	1.75 cm.	1.00 cm.	2.00 cm.	1.605 cm.
X_2	1.75 cm.	1.00 cm.	2.00 cm.	1.553 cm.
X_3	3.00 cm.	1.75 cm.	3.20 cm.	2.764 cm.
X_4	2.00 cm.	1.00 cm.	2.20 cm.	1.676 cm.
X_5	13.25 cm.	10.00	18.00 cm.	13.504 cm.
TORSIONAL DEFLECTION (radians) x 10^3	0.453	0.50	0.5	0.499*
FIRST NATURAL FREQUENCY (radians/second)	718	700	--	734*
SECOND NATURAL FREQUENCY (radians/second)	1272	ω_1 + 100	--	979
OBJECTIVE FUNCTION (weight of lathe bed)	87.49 kg.	--	--	77.42 kg.

REDUCTION IN WEIGHT OBTAINED BY OPTIMIZATION = 10.07 kg. (11.45%)
NUMBER OF ONE-DIMENSIONAL MINIMIZATIONS = 14
COMPUTER TIME REQUIRED = 55 minutes on IBM 370/155 system.

*ACTIVE CONSTRAINTS

TABLE 7.3 OPTIMIZATION RESULTS OF HORIZONTAL MILLING MACHINE (EXAMPLE 3a)

DESIGN VARIABLE	INITIAL DESIGN	BOUNDS LOWER	BOUNDS UPPER	OPTIMUM DESIGN
X_1	50.00 cm.	35.00 cm.	54.00 cm.	50.120 cm.*
X_2	2.80 cm.	0.80 cm.	4.00 cm.	0.987 cm.*
X_3	32.00 cm.	24.00 cm.	35.00 cm.	28.826 cm.
X_4	2.80 cm.	0.80 cm.	4.00 cm.	0.906 cm.*
X_5	42.00 cm.	40.00 cm.	X_1	41.494 cm.
X_6	3.00 cm.	0.00 cm.	6.00 cm.	0.896 cm.
MAXIMUM DEFLECTION OF CENTRE OF THE CUTTER IN ANY DIRECTION cm. x 10^5	661	--	900	893*
FIRST NATURAL FREQUENCY (ω_1) (radians/second)	1003	850	--	913*
SECOND NATURAL FREQUENCY(ω_2) (radians/second)	1150	ω_1+100	--	1024
MINIMUM NEGATIVE INPHASE CROSS RECEPTANCE OF CUTTER CENTRE RELATIVE TO TABLE cm/kg x 10^8	65	300	--	200
OBJECTIVE FUNCTION (Wt. of the Milling Machine including column, table and over-arm)	740 kg.	--	--	300.78 kg.

REDUCTION OF WEIGHT OBTAINED BY OPTIMIZATION = 439.22 kg.(62.6%)
COMPUTER TIME REQUIRED = 105 minutes on IBM 370/155 system
CUMULATIVE NUMBER OF ONE-DIMENSIONAL MINIMIZATIONS = 13

*ACTIVE CONSTRAINTS

TABLE 7.4 OPTIMIZATION RESULTS OF HORIZONTAL MILLING MACHINE (EXAMPLE 3b)

DESIGN VARIABLE	INITIAL DESIGN	BOUNDS LOWER	BOUNDS UPPER	OPTIMUM DESIGN
X_1	52.00 cm.	35.00 cm.	54.00 cm.	50.314 cm.
X_2	3.20 cm.	0.80 cm.	4.00 cm.	1.069 cm.*
X_3	30.00 cm.	24.00 cm.	35.00 cm.	28.978 cm.
X_4	3.00 cm.	0.80 cm.	4.00 cm.	0.9102 cm.*
X_5	45.00 cm.	40.00 cm.	X_1	42.434 cm.
X_6	2.80 cm.	0.00 cm.	6.00 cm.	0.866 cm.
MIXIMUM DEFLECTION OF THE CENTRE OF THE CUTTER IN ANY DIRECTION cm. x 10^5	662	--	900	884*
FIRST NATURAL FREQUENCY (ω_1) (radians/second)	961	850	--	914*
SECOND NATURAL FREQUENCY(ω_2) (radians/second)	1187	ω_1+100	--	1016*
MINIMUM NEGATIVE INPHASE CROSS RECEPTANCE OF CUTTER CENTRE RELATIVE TO TABLE cm/kg. x 10^8	68	300	--	206
OBJECTIVE FUNCTION	780.5 kg.	--	--	308.8 kg.

REDUCTION OF WEIGHT OBTAINED BY OPTIMIZATION = 471.7 kg. (60.4%)
COMPUTER TIME REQUIRED = 101 minutes on IBM 370/155 system
COMULATIVE NUMBER OF ONE-DIMENSIONAL MINIMIZATIONS = 12

*ACTIVE CONSTRAINTS

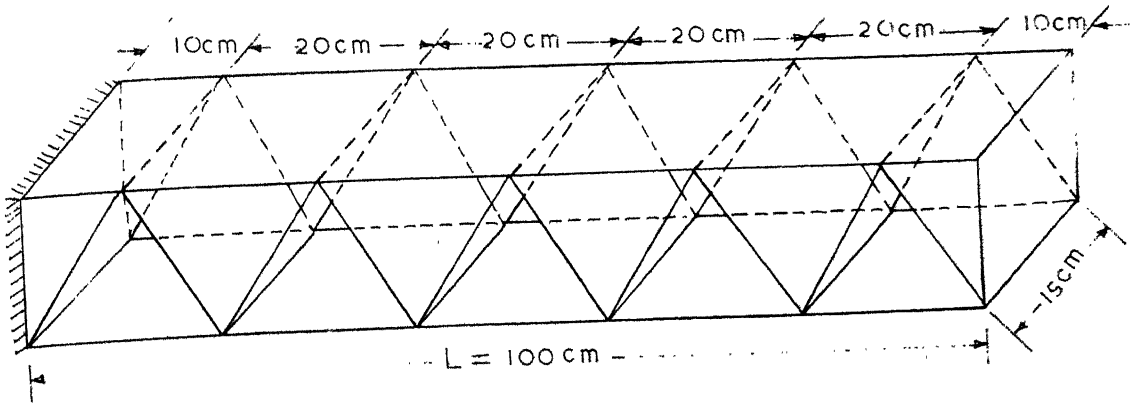

FIG.7.1 WARREN TYPE LATHE-BED

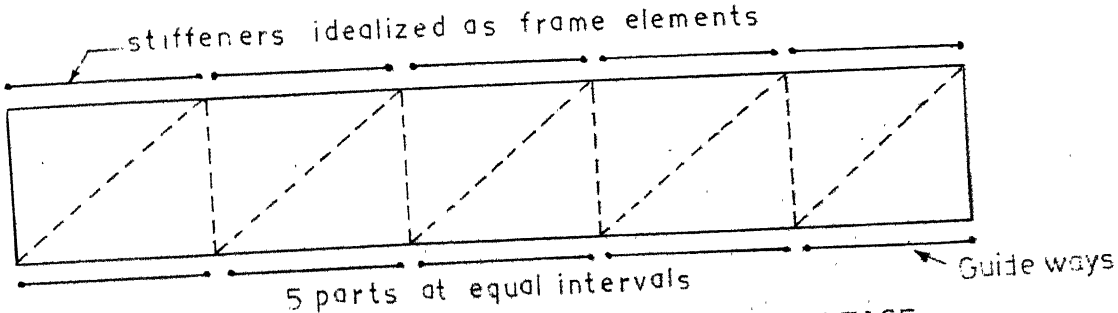

a). FINITE ELEMENT GRID ON BOTTOM SURFACE

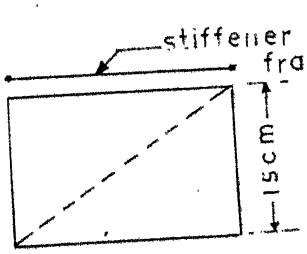

b). LACING DIAGONAL

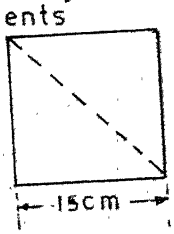

C). SIDE PLATE

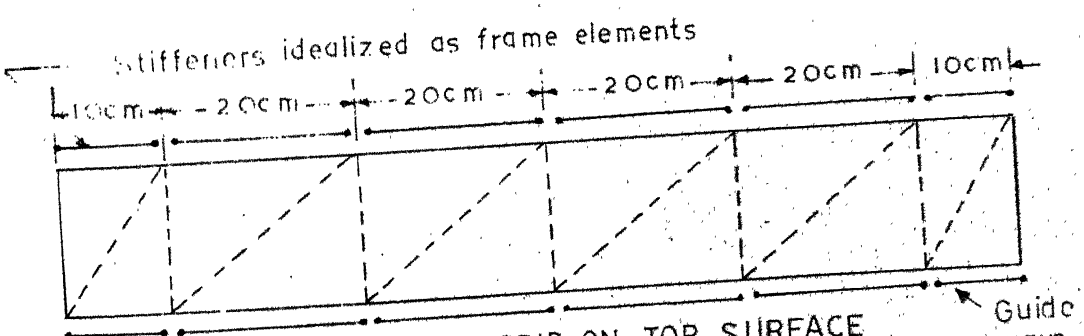

d). FINITE ELEMENT GRID ON TOP SURFACE
Dotted lines represent finite element grid

FIG.7.2 DETAILS OF IDEALIZATION OF WARREN TYPE LATHE-BED

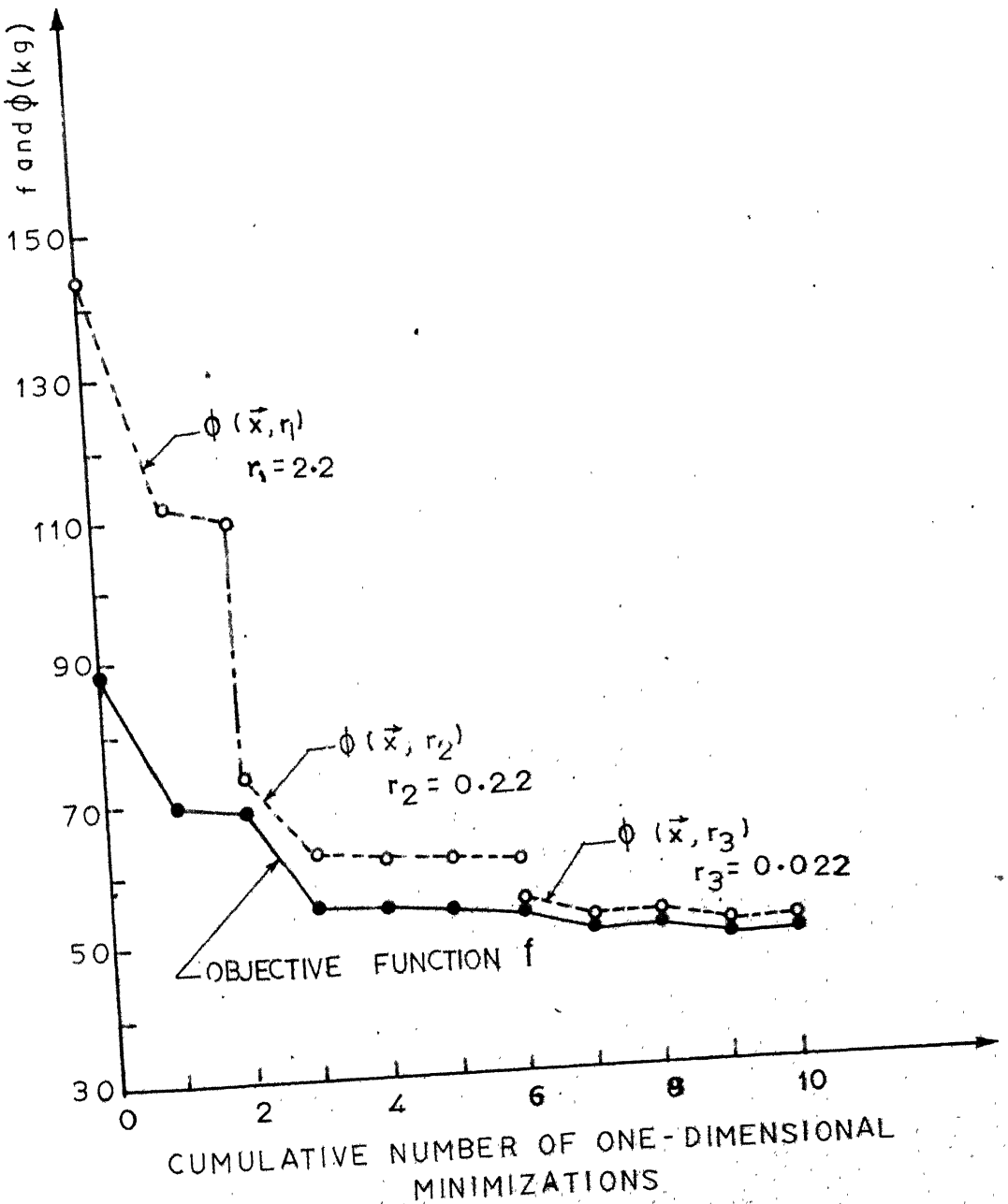

FIG·7·3 PROGRESS OF OPTIMIZATION PATH FOR EXAMPLE I

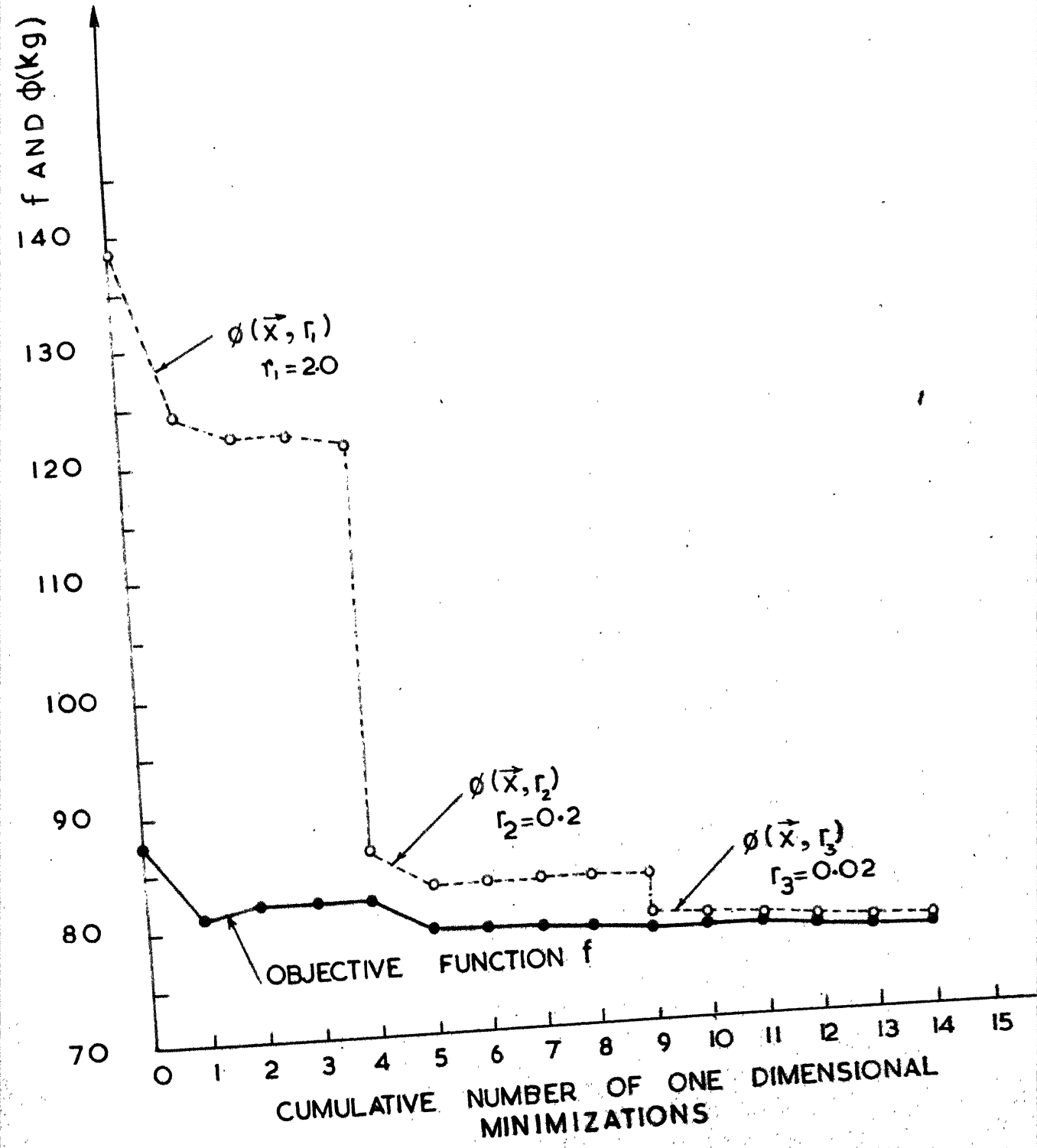

FIG.7.4 PROGRESS OF OPTIMIZATION PATH FOR EXAMPLE 2

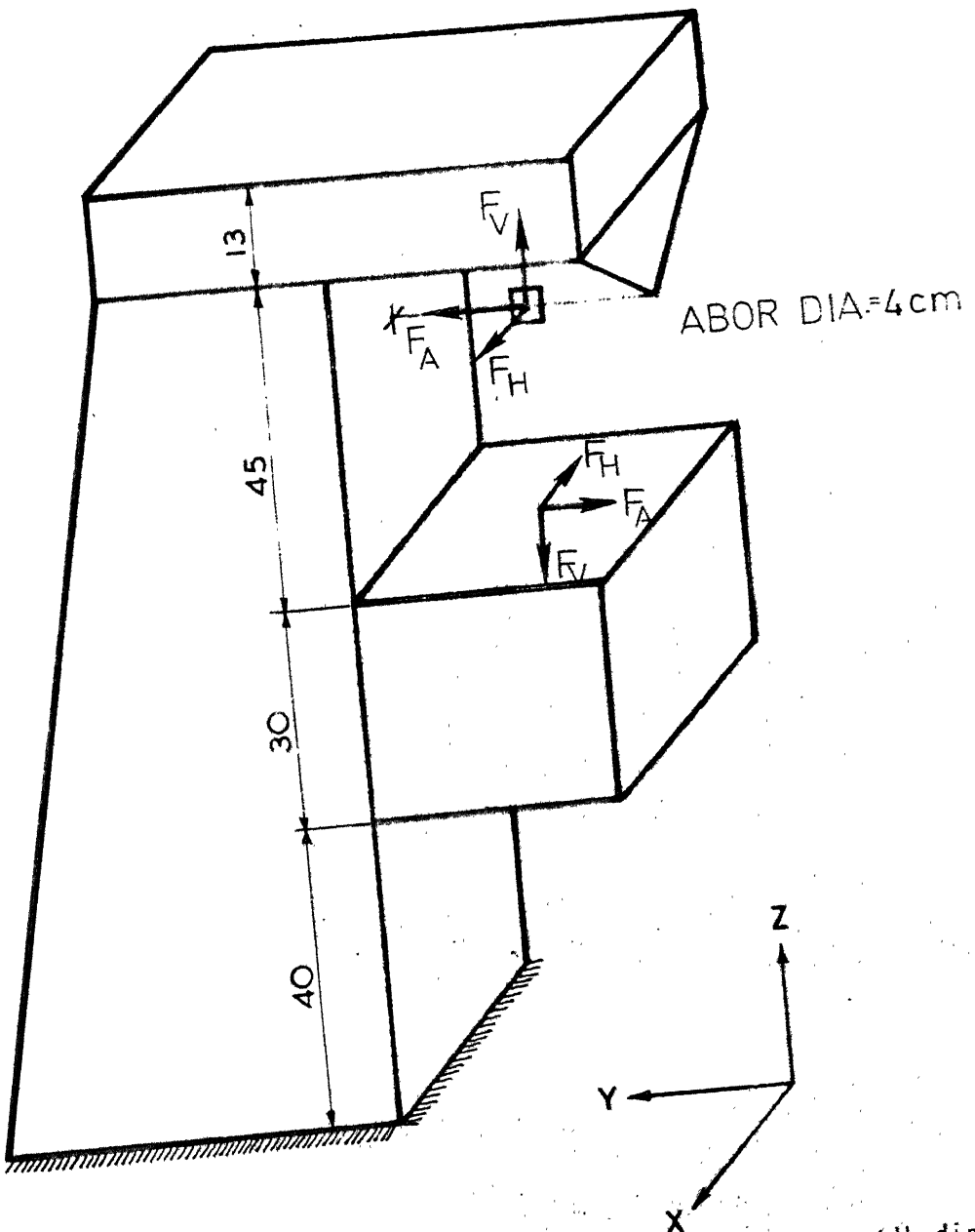

FIG.75 HORIZONTAL MILLING MACHINE STRUCTURE
(EXAMPLES 3.a and 3b)

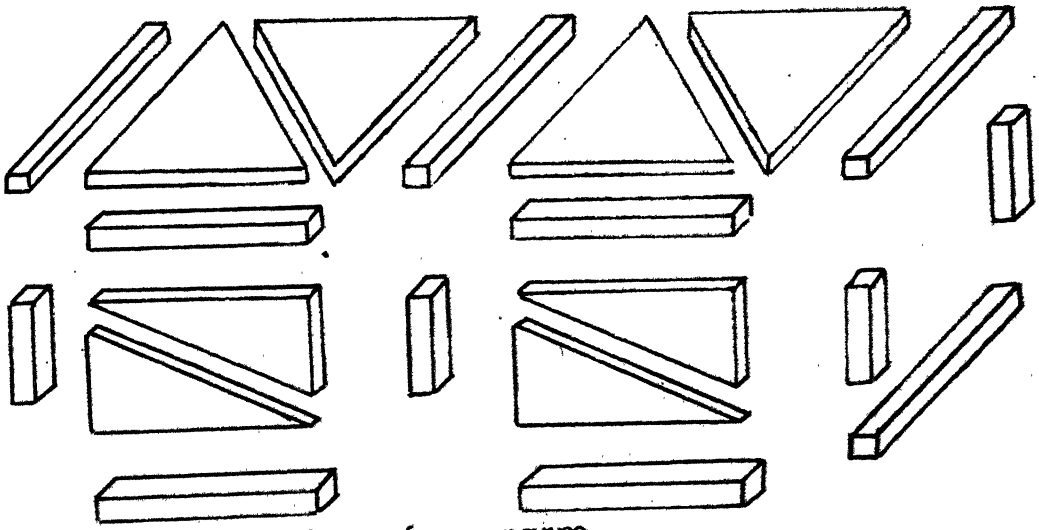

Idealization of overarm

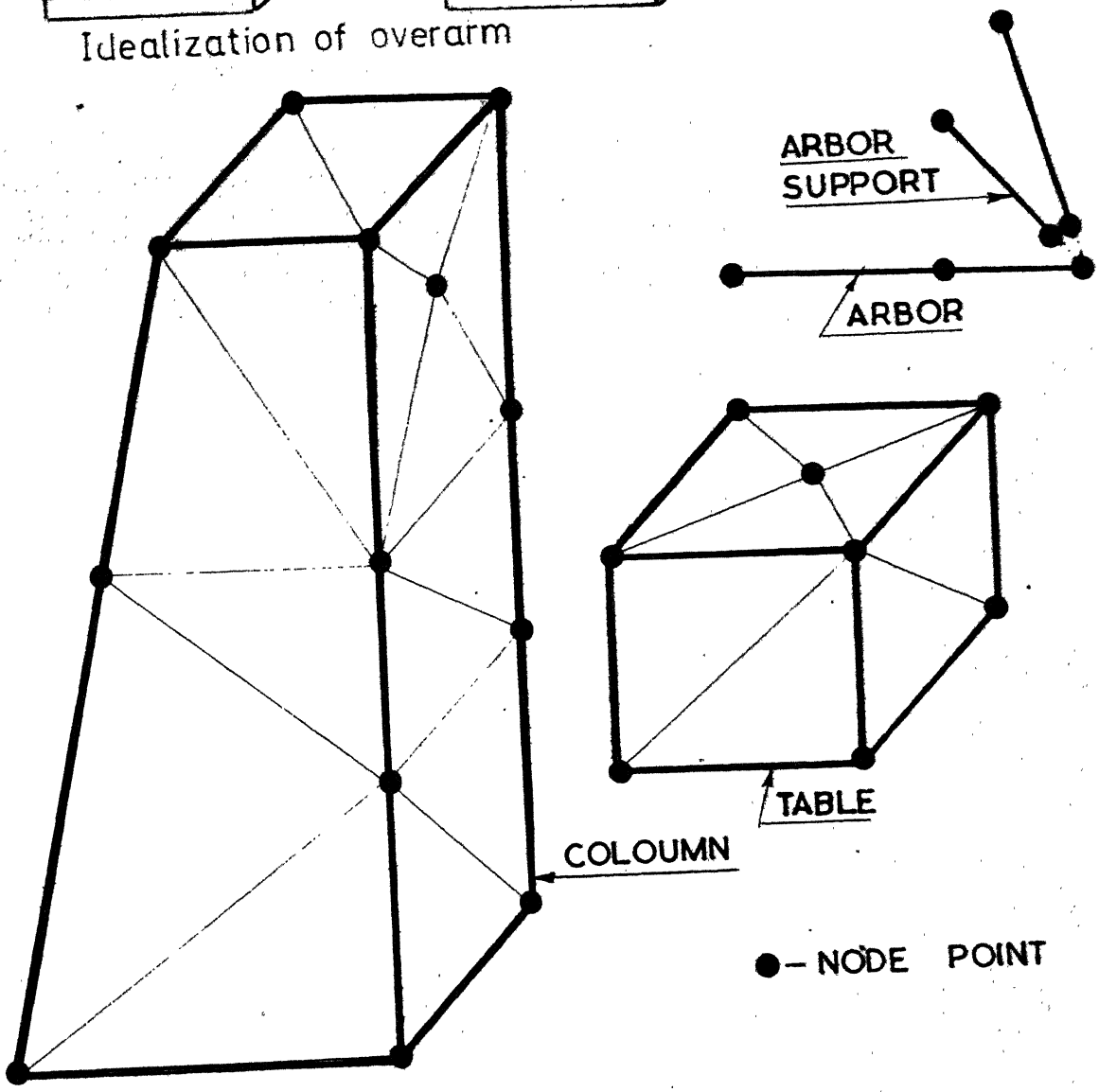

FIG.7.6 FINITE ELEMENT MODELLING OF HORIZONTAL MILLING MACHINE (EXAMPLES 3a and 3b)

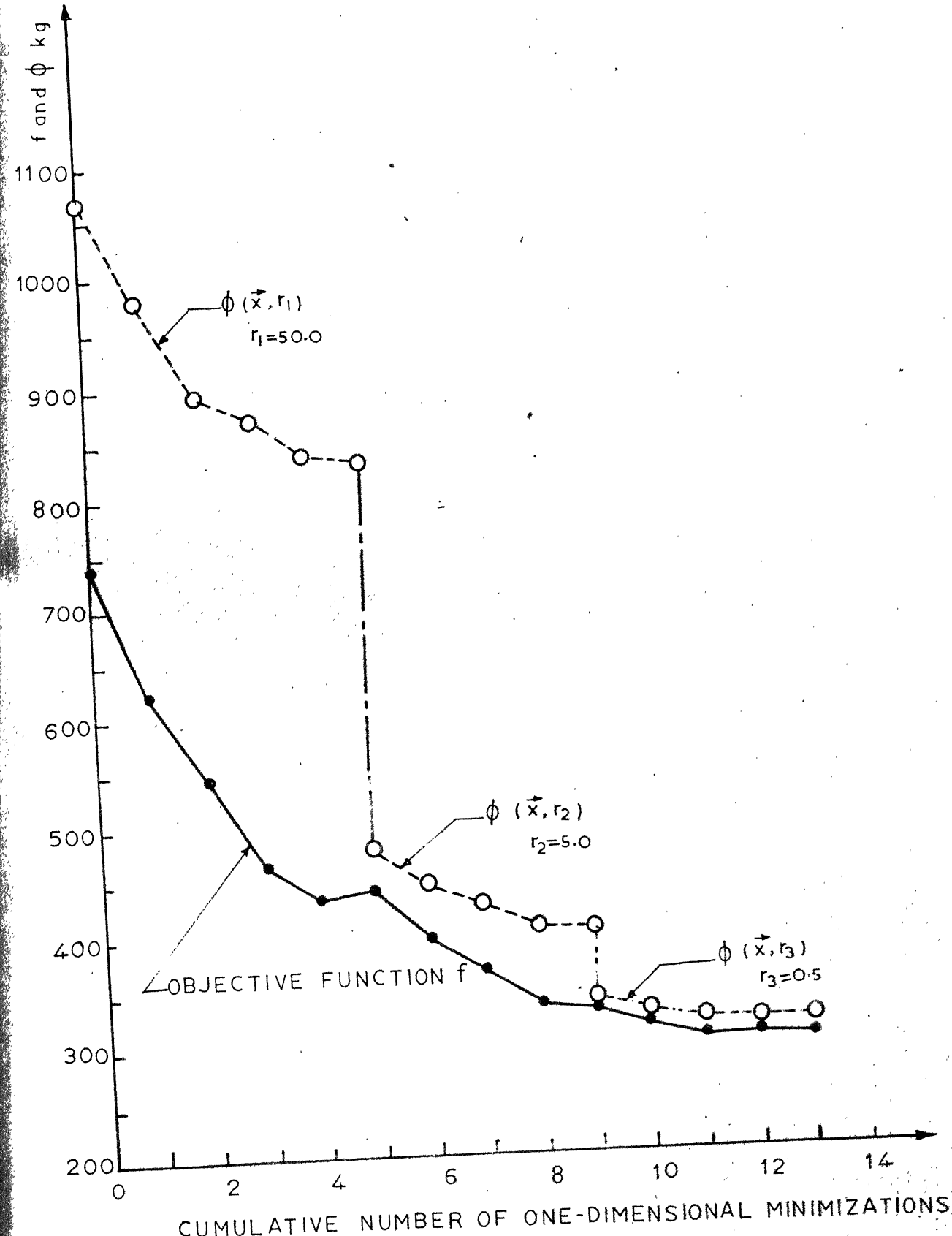

FIG. 7.7 PROGRESS OF OPTIMIZATION PATH FOR EXAMPLE 3(a)

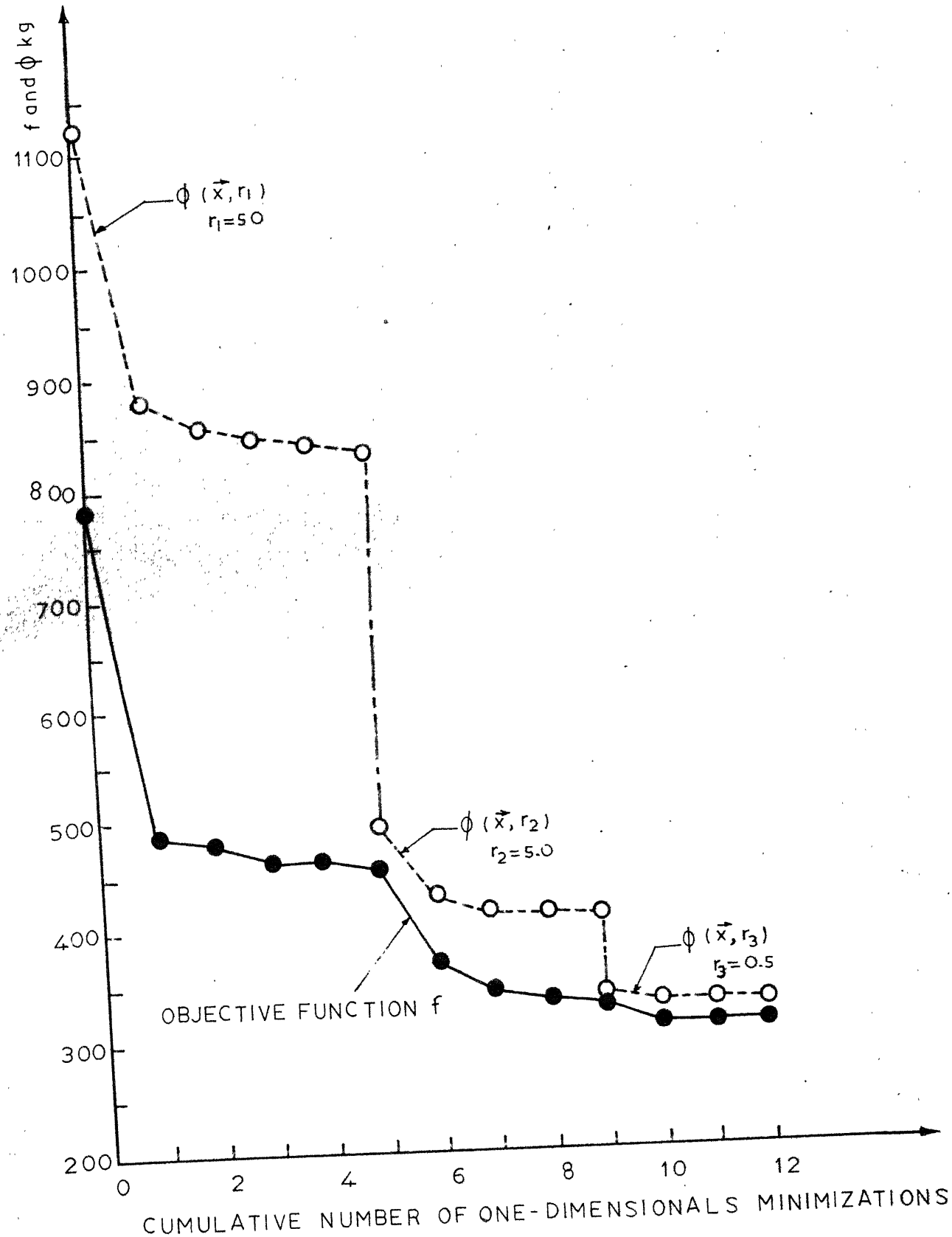

FIG.7.8 PROGRESS OF OPTIMIZATION PATH FOR EXAMPLE 3(b)

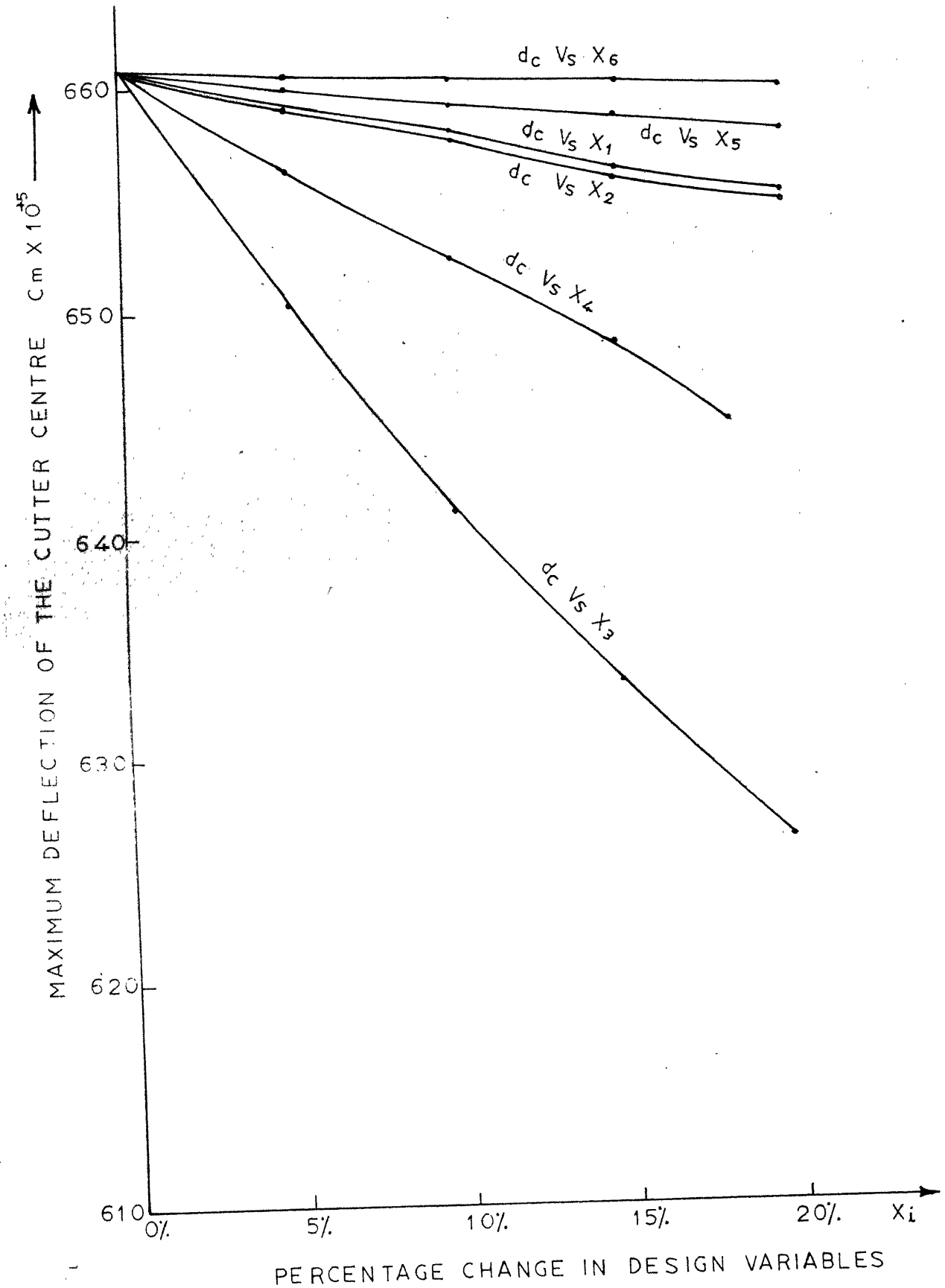

FIG.7·9 MAXIMUM DEFLECTION OF CUTTER CENTRE Vs DESIGN VARIABLE IN HORIZONTAL MILLING MACHINE

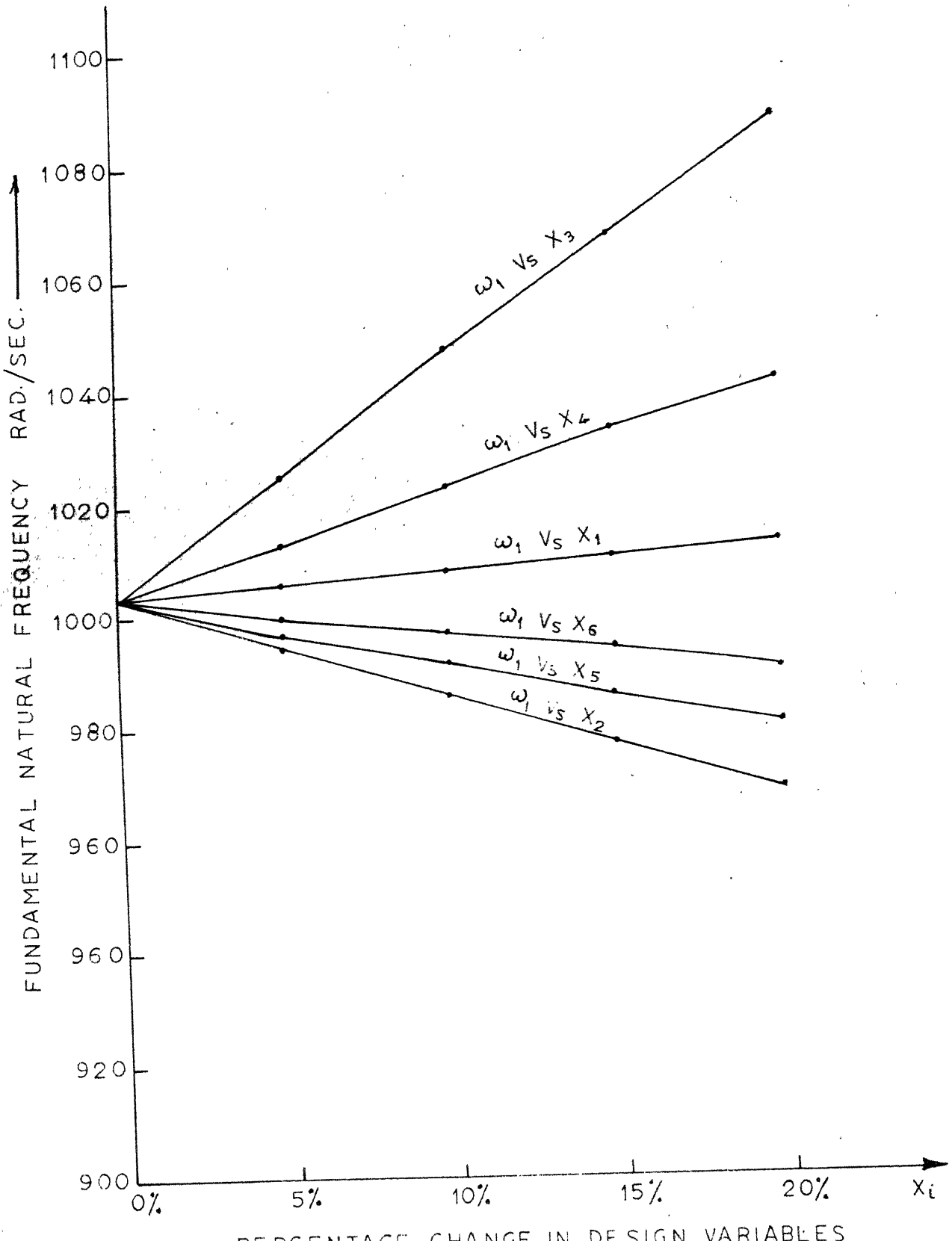

FIG.7.10 FUNDAMENTAL NATURAL FREQUENCY Vs DESIGN VARIABLES IN HORIZONTAL MILLING MACHINE

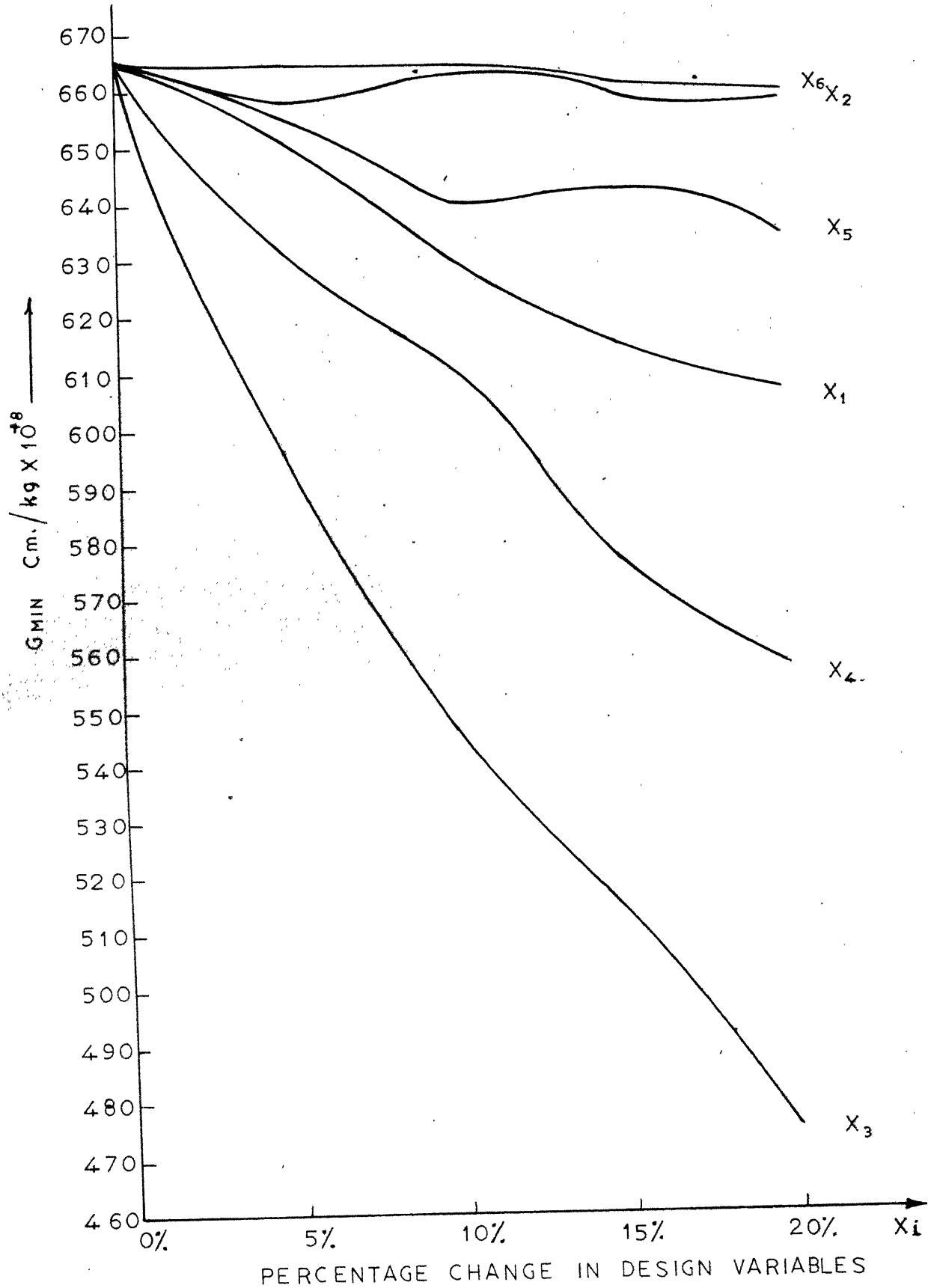

FIG. 7.11 GMIN CURVES Vs DESIGN VARIABLES IN HORIZONTAL MILLING MACHINE.

CHAPTER 8

RELIABILITY ANALYSIS OF MACHINE TOOL STRUCTURES

The conventional approach in design practice, which considers loads, resistances and design variables as deterministic quantities, may be compared to a kind of worst case analysis. In this approach, as an example, when designing a structure for strength, the maximum of loading and the minimum of strength are treated not only as representative of design situations, but also of simultaneous occurrence. The design of a structure for an extremely large load (of rare occurrence) and for an extremely low value of strength (of rare incidence) will be very uneconomical. In such situations, the loads and strengths have to be treated as random variables and the probability of simultaneous occurrence of extreme values of load and strength becomes very important.

In probability (reliability) based design, usually a design is considered to be safe and adequate if the probability of failure of the structure is less than a specified small quantity, say, 10^{-6}. Thus the basic step involved in reliability based design is to analyse the structure for reliability. In this chapter, a method of analysing the reliability of machine tool structures is developed. More specifically, the reliability analysis of horizontal milling machines in various failure modes is considered for illustrating the method.

8.1 CHOICE OF RANDOM VARIABLES

The operating conditions, material properties and modal damping factors vary substantially in machine tool structures. In the present work, the reliability of the milling machine structure considered in example 3 of chapter 7 is evaluated at the initial and optimum designs. The reliability of the structure against the various response quantities of failure modes is found by taking the table height (h), the distance of the cutter centre from arbor support (c), the damping factor (ζ), the Young's modulus of the material of the structure (E), and the load on the cutter and the table (P) as random variables. The response quantities considered are : (1) the maximum static deflection of the cutter centre in any direction, (2) the first natural frequency of vibration, and (3) the minimum negative inphase cross-receptance of the cutter centre relative to the table.

The Location of the table and the cutter centre depend on the size of the work piece. Since the size of the work piece will vary for different jobs, h and c are taken as random variables. From the present knowledge, the modal damping factors of structures, particularly in machine tool structures where joints are involved, cannot be estimated precisely. Therefore modal damping factors (ζ_i) are taken as random variables. In actual practice the material properties vary and hence the Young's modulus (E) is considered as a random variable in this work. Finally the magnitude of the

The probability of failure is given by

$$P_f = P(R < L) = \int_{-\infty}^{\infty} F_R(\ell) \cdot f(\ell) \cdot d\ell$$

$$= 1 - \int_{-\infty}^{\infty} F_L(r) \cdot f_R(r) \cdot dr \qquad (8.1)$$

where $f_X(x)$ and $F_X(x)$ represent the probability density and distribution functions respectively.

If several loads act simultaneously on the structural system as shown in Fig. 8.2(a), the failure probability is given by

$$P_f = 1 - \int_{-\infty}^{\infty} \left[\prod_{j=1}^{p} F_{L_j}(r) \right] f_R(r) \cdot dr \qquad (8.2)$$

If a single member is subjected to several load conditions as snown in Fig. 8.2(b), the probability of failure can be determined from the relation

$$P_f = 1 - \int_{-\infty}^{\infty} \left\{ \prod_{i=1}^{q} \left[1 - F_{R_i}(\ell_i) \right] \right\} f_L(\ell) \cdot d\ell \qquad (8.3)$$

where ℓ_i is the force induced in i^{th} member due to the load ℓ. Since this is a weakest-link chain, the term in braces in Equation 8.3 represents the probability of survival of the chain and is based on all links surviving under the load $L = \ell$. This term is evaluated from the products of probabilities of individual links surviving under the load $L = \ell$. Equation 8.3 is often

approximated as

$$P_f \approx 1 - \prod_{i=1}^{q} (1 - P_{f_i}) \tag{8.4}$$

where P_{f_i} denotes the probability of failure of i^{th} link. Finally the multicomponent, multiload system shown in Fig. 8.2(c) is given by

$$P_f = 1 - \int_{L_1} \int_{L_2} \cdots \int_{L_p} \{ \prod_{i=1}^{q} [1-F_{R_i}(\ell_{im})] \} f_{L_1}(\ell_1)$$

$$f_{L_2}(\ell_2) \cdots f_{L_p}(\ell_p) \cdot d\ell_1 \cdot d\ell_2 \cdots d\ell_p \tag{8.5}$$

where ℓ_{im} is the total force induced in i^{th} member due to the loads $\ell_1, \ell_2, \ldots, \ell_p$. Since the computation of the exact probability of failure is a complex probabilistic problem, Equation 8.4 is often approximated as

$$P_f \approx 1 - \prod_{i=1}^{q} \prod_{j=1}^{p} (1 - P_{f_{ij}}) \tag{8.6}$$

where $P_{f_{ij}}$ denotes the probability of failure of i^{th} member under j^{th} load.

8.3 COMPUTATION OF RELIABILITY IN A PARTICULAR FAILURE MODE

The reliability (R_o) of a system is taken as one minus the probability of failure (P_f). The method of computing the reliability of a system in any particular failure mode is considered in this section.

If R is the resistance and L is the load acting in the specified failure mode the reliability of the system can be analysed as a single member-single load problem. For simplicity the resistance and the load are assumed to be normally distributed so that

$$f_L(\ell) = \frac{1}{\sqrt{2\pi}\ \sigma_L} \exp\ [-\frac{1}{2}\ (\frac{\ell - \bar{L}}{\sigma_L})^2] \qquad (8.7)$$

and

$$f_R(r) = \frac{1}{\sqrt{2\pi}\ \sigma_R} \exp\ [-\frac{1}{2}\ (\frac{r - \bar{R}}{\sigma_R})^2] \qquad (8.8)$$

where $\bar{L}$ and $\bar{R}$ represent the mean values and σ_L and σ_R the standard diviations of L and R respectively. Although Equation 8.1 is applicable, the following simpler procedure is used to find the reliability of the system in this case. By defining a new random variable ξ as

$$\xi = R - L\ , \qquad (8.9)$$

the reliability of the system can be expressed as

$$R_0 = P(\xi \geq 0) = \int_0^\infty f_\xi(\eta)\ d\eta \qquad (8.10)$$

where $f_\xi(\eta)$ is the density function of ξ given by

$$f_\xi(\eta) = \frac{1}{\sqrt{2\pi}\ \sigma_\xi} \exp\ [-\frac{1}{2}\ (\frac{\eta - \bar{\xi}}{\sigma_\xi})^2] \qquad (8.11)$$

where $\bar{\xi}$ is the mean value and σ_ξ is the standard deviation of ξ.

If R and L are independent, the expressions for $\bar{\xi}$ and σ_ξ are given by

$$\bar{\xi} = \bar{R} - \bar{L} \tag{8.12}$$

and

$$\sigma_\xi = \sqrt{\sigma_R^2 + \sigma_L^2} \tag{8.13}$$

Equation 8.10 and 8.11 give

$$R_o = \frac{1}{\sqrt{2\pi}\,\sigma_\xi} \int_o^\infty \exp\left[-\frac{1}{2}\left(\frac{\eta - \bar{\xi}}{\sigma_\xi}\right)^2\right] d\eta \tag{8.14}$$

By defining a standard normal variate Z as

$$Z = \frac{\eta - \bar{\xi}}{\sigma_\xi}, \tag{8.15}$$

Equation 8.14 can be rewritten as

$$R_o = \frac{1}{\sqrt{2\pi}} \int_{Z=z}^\infty \exp\left[-\frac{1}{2} Z^2\right] dZ \tag{8.16}$$

where the lower limit of integration (z) is given by

$$z = -\frac{\bar{\xi}}{\sigma_\xi} = -\left[\frac{\bar{R} - \bar{L}}{\sqrt{\sigma_R^2 + \sigma_L^2}}\right] \tag{8.17}$$

Once the value of z is calculated, the corresponding reliability R_o can be determined from equation 8.16. This value can be obtained more readily from the standard normal tables[78].

In order to find the reliability of a structural system using Equations 8.17 and 8.16, the mean values and standard deviations of the generalized load (L) and the generalized resistance (R) must be known. Since L and R generally depend on several other random design parameters, one has to determine $\bar{L}$, $\bar{R}$, σ_L and σ_R in terms of the means and standard deviations of the random design parameters. In general, if Y is a nonlinear function of several random variables $x_1, x_2, \ldots, x_s$, the approximate values of the mean and the variance of Y can be found by linearizing Y about the mean values of $x_1, x_2, \ldots, x_s$ using Taylor's series expansion. The expressions of $\bar{Y}$ and σ_Y are given by

$$\bar{Y} \approx Y(\bar{x}_1, \bar{x}_2, \ldots, \bar{x}_s) \tag{8.18}$$

and

$$\sigma_Y \approx \left\{ \sum_{i=1}^{s} \left[\frac{\partial Y}{\partial x_i} \Big|_{(\bar{x}_1, \bar{x}_2, \ldots, \bar{x}_s)} \right]^2 \sigma_{x_i}^2 \right\}^{1/2} \tag{8.19}$$

where the random variables $x_1, x_2, \ldots, x_s$ are assumed to have zero correlation.

Since the reliabilities against the response quantities d_c, ω_1 and G_{MIN} are to be found, the partial derivatives of d_c, ω_1 and G_{MIN} with respect to the random design parameters h, c, ζ, E and P (evaluated at the mean values of the design variables) are required. These partial derivatives are found by using a finite difference scheme in this work.

8.4 NUMERICAL RESULTS

The reliability of the horizontal milling machine structure considered in example 3 of the previous chapter is analyzed in each of the failure modes. The partial derivatives of the cutter centre deflection, fundamental natural frequency and the minimum negative cross-receptance of cutter centre relative to the table have been computed by finite difference scheme by taking a 5% variation in the design parameters.

The reliabilities of the machine tool structure are found at the initial and optimum designs of example 3 of chapter 7. The values of the partial derivatives of the response quantities with respect to the design parameters are given in Table 8.1. The reliability results obtained by using a coefficient of variation (V_{x_i}) of 0.05 for all the random design parameters are shown in Table 8.2. From these results, it can be seen that the reliabilities are lower at the optimum design compared to those at the initial design. This is to be expected in this case since the optimum design has been obtained according to deterministic formulation and most of the behaviour constraints (involving the response quantities) tend to reach criticality at the optimum point. If the optimum design is obtained according to probabilistic formulation (using Equations 2.2 of chapter 2), the reliabilities corresponding to the optimum design are expected

to be higher than those corresponding to the initial design.

In many practical problems, one would be interested not only in the reliability of a structure for a particular set of data, but also in knowing how the reliability changes with a variation in the standard deviations of the various design parameters. Hence the variation of reliabilities of the milling machine structure against d_c, ω_1 and G_{MIN} for various coefficients of variation of the design parameters (V_{x_i}) are shown in Figs.8.3, 8.4 and 8.5 respectively. From these figures, it can be seen that the reliability in the deflection failure mode is most sensitive with respect to V_P and least with respect to V_ζ at both initial and optimum designs. The reliability against the fundamental frequency is most sensitive to a change in V_E and least to a change in V_c, V_ζ and V_P. Similarly, the reliability against the response quantity G_{MIN} can be observed to be most sensitive to V_h and least to V_P.

If the machine tool structure is considered as a weakest-link chain, each link representing one particular failure mode, the overall reliability of the system can be calculated from Equation 8.4. This gives the overall system reliability as $(R_o)_{overall} = 0.9989564688$ at the initial design and $(R_o)_{overall} = 0.4816022724$ at the optimum design.

TABLE 8.1 PARTIAL DERIVATIVES OF d_c, ω_1 AND G_{MIN} WITH RESPECT TO THE DESIGN PARAMETERS

	x_i									
	h		c		ζ		E		P	
	AT INITIAL DESIGN*	AT OPTIMUM DESIGN**	AT INITIAL DESIGN	AT OPTIMUM DESIGN	AT INITIAL DESIGN	AT OPTIMUM DESIGN	AT INITIAL DESIGN	AT OPTIMUM DESIGN	AT INITIAL DESIGN	AT OPTIMUM DESIGN
$\frac{\partial d_c}{\partial x_i}$	$+.32\times10^{-3}$	$+.76\times10^{-4}$	$+.56\times10^{-4}$	$-.43\times10^{-4}$	0.0	0.0	$-.44\times10^{-8}$	$-.56\times10^{-8}$	$+.74\times10^{-5}$	$+.95\times10^{-5}$
$\frac{\partial \omega_1}{\partial x_i}$	-1.82	-2.54	0.0	0.0	0.0	0.0	$+.36\times10^{-3}$	$+.33\times10^{-5}$	0.0	0.0
$\frac{\partial G_{MIN}}{\partial x_i}$	$+.29\times10^{-7}$	$+.95\times10^{-7}$	$+.27\times10^{-7}$	$+.93\times10^{-7}$	$-.12\times10^{-4}$	$-.47\times10^{-5}$	$-.57\times10^{-12}$	$-.23\times10^{-11}$	0.0	0.0

*Initial design : $X_1 = 50.0$ cm., $X_2 = 2.8$ cm., $X_3 = 32.0$ cm., $X_4 = 2.8$ cm., $X_5 = 42.0$ cm., $X_6 = 3.0$ cm.

**Optimum design: $X_1 = 50.119$ cm., $X_2 = 0.987$ cm., $X_3 = 28.826$ cm., $X_4 = 0.906$ cm., $X_5 = 41.49$ cm., $X_6 = 0.896$ cm.

TABLE 8.2 RESULTS OF RELIABILITY ANALYSIS WITH RESPECT TO THE VARIOUS RESPONSE QUANTITIES

	AT INITIAL DESIGN*		AT OPTIMUM DESIGN**	
	LOWER LIMIT OF INTEGRATION (z)	RELIABILITY (R_o)	LOWER LIMIT OF INTEGRATION (z)	RELIABILITY (R_o)
d_c	4.30	0.999991467	0.0902	0.535936
ω_1	3.08	0.998964996	1.29	0.901474
G_{MIN}	13.12	0.999999999	2.73	0.996833

*Initial design : X_1 = 50.0 cm., X_2 = 2.8 cm., X_3 = 32.0 cm., X_4 = 2.8 cm., X_5 = 42.0 cm. X_6 = 3.0 cm.

**Optimum design: X_1 = 50.119 cm., X_2 = 0.987 cm., X_3 = 28.826 cm., X_4 = 0.906 cm., X_5 = 41.'49., X_6 = 0.896 cm.

Permissible values : $(\bar{d}_c)_{max}$ = 0.009 cm., $(\bar{\omega}_1)_{min}$ = 850 radians/second, $|\bar{G}_{MIN}|_{max}$ = 0.000003 cm/kg.

Note : Coefficients of variation of all the design variables = 0.05.

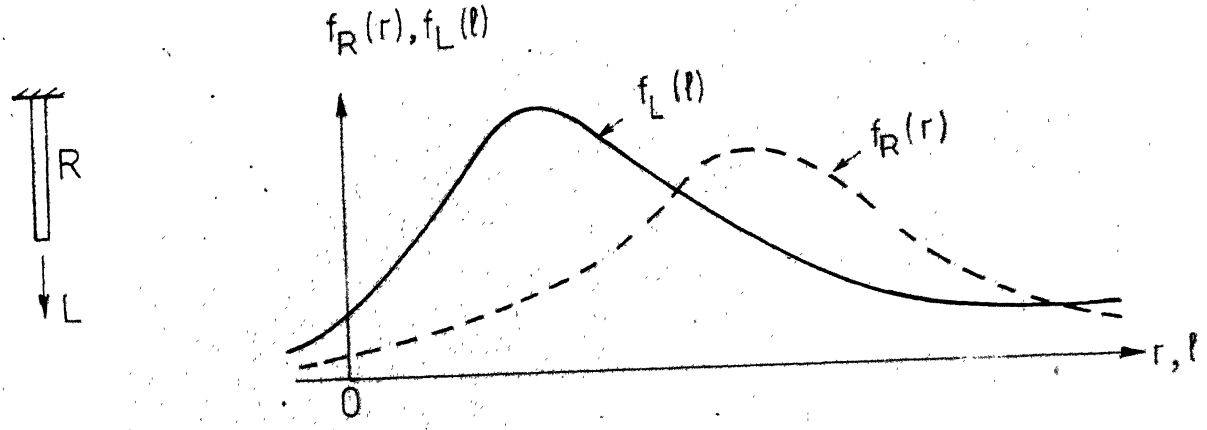

FIG. 8·1 A STRUCTURAL SYSTEM CONSISTING OF ONE MEMBER AND ONE LOAD

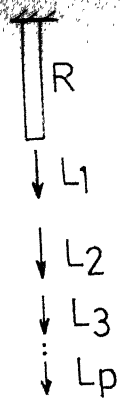

, system consisting
ıe member and p
s

(b) A system consisting of q members and one load

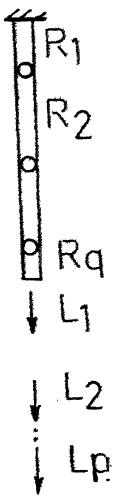

(c) A system consisting of q members and p loads

FIG. 8·2 WEAKEST LINK SYSTEM

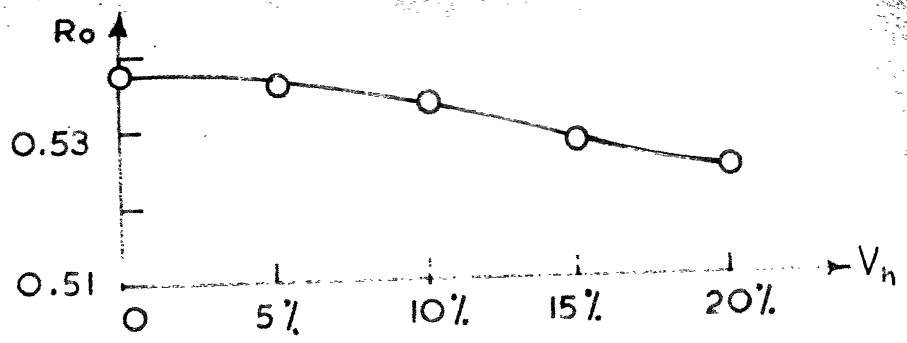

(a)

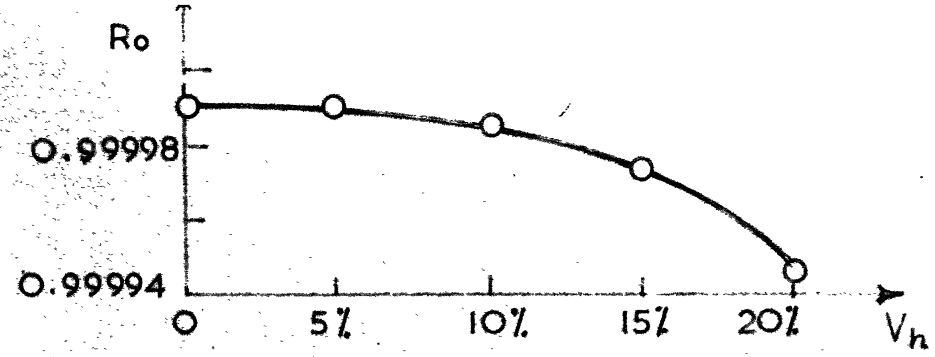

(b)

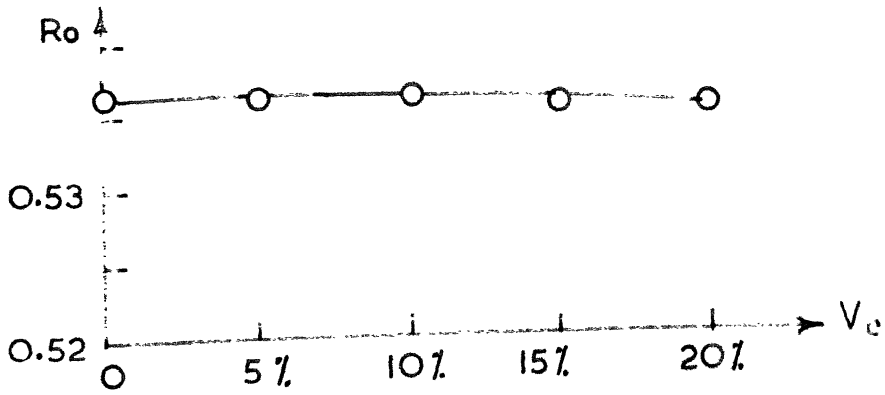

(c)

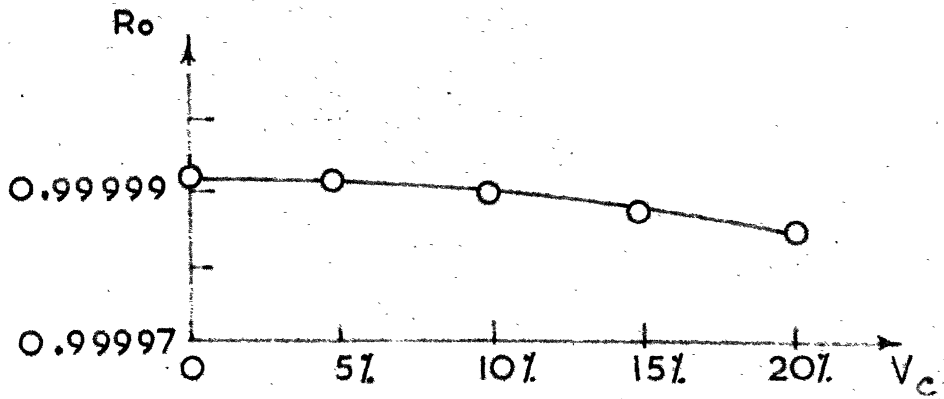

(d)

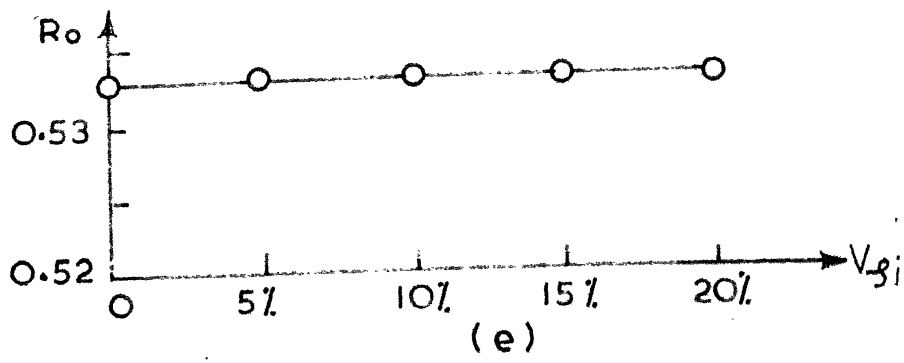

(e)

AT OPTIMUM DESIGN

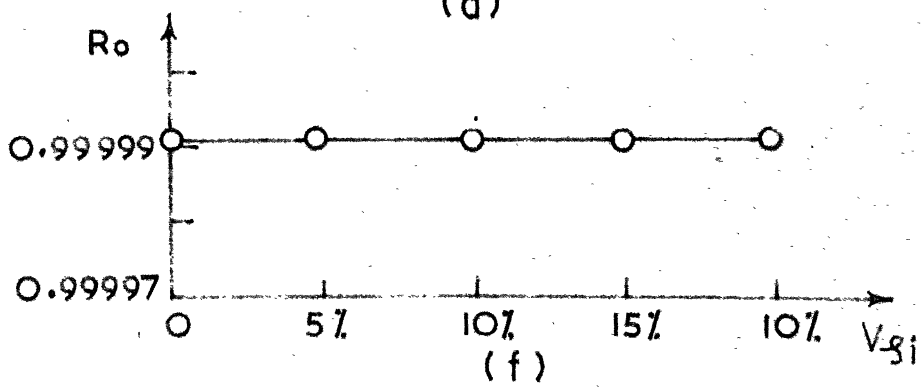

(f)

AT INITIAL DESIGN

FIG·8·3 CONTD.

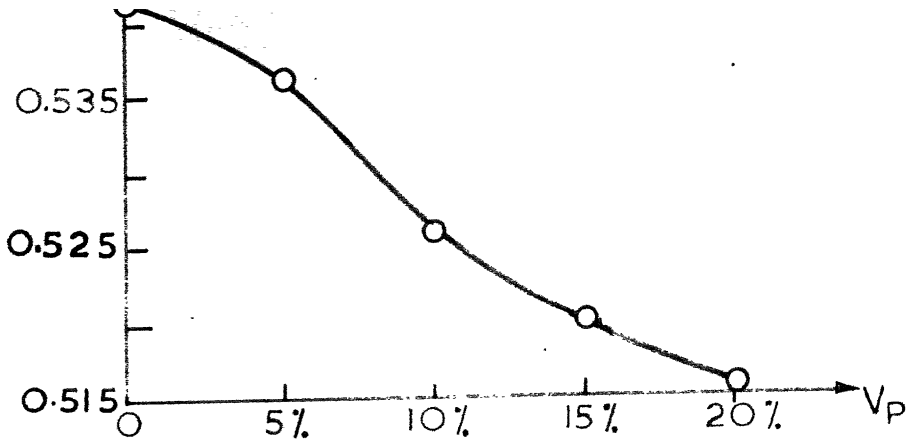

(g)

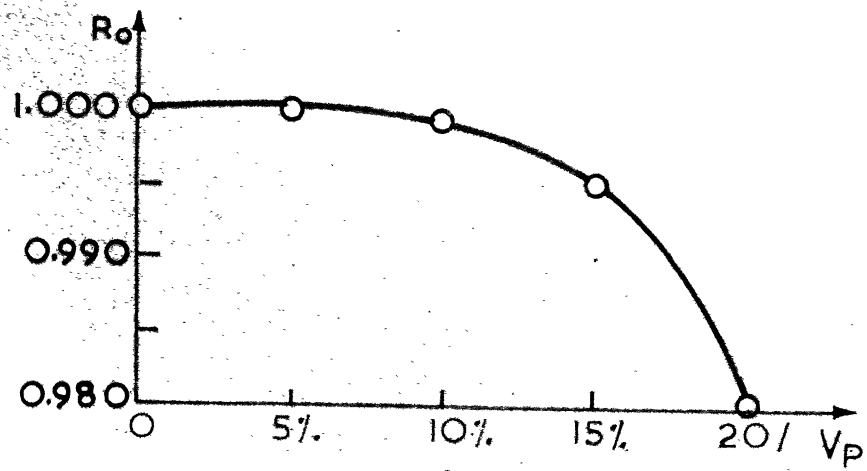

(h)

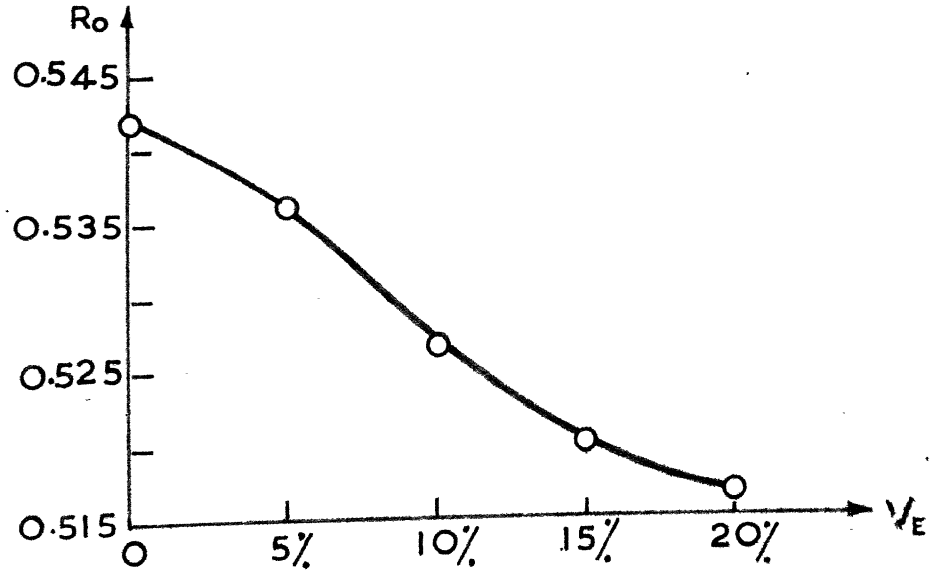

(i)

AT OPTIMUM DESIGN

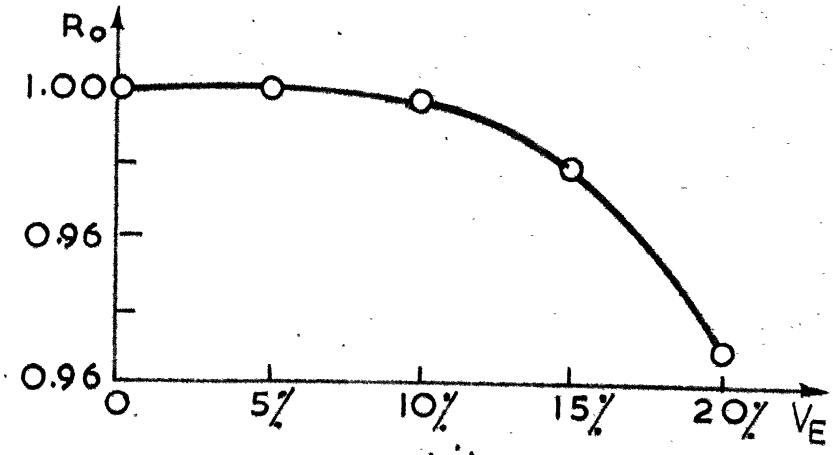

(j)

AT INITIAL DESIGN

FIG·8·3 RELIABILITY CURVES AGAINST DEFLECTIONS

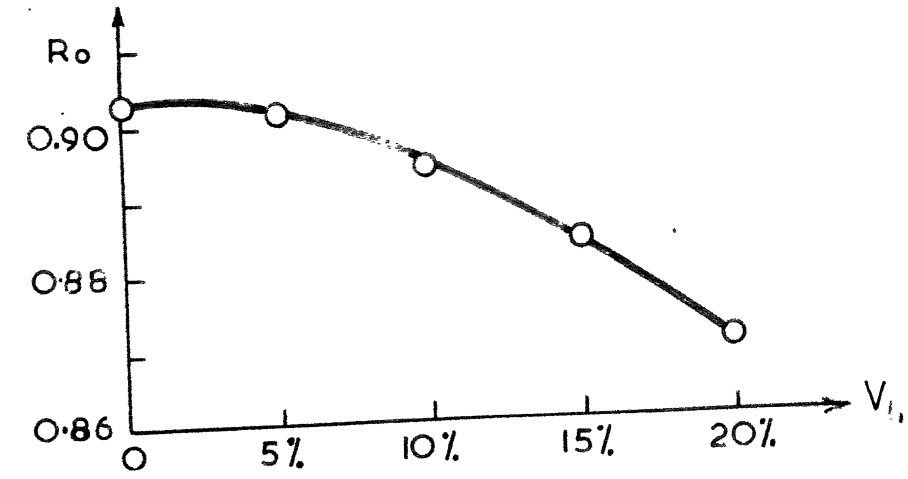

(a)

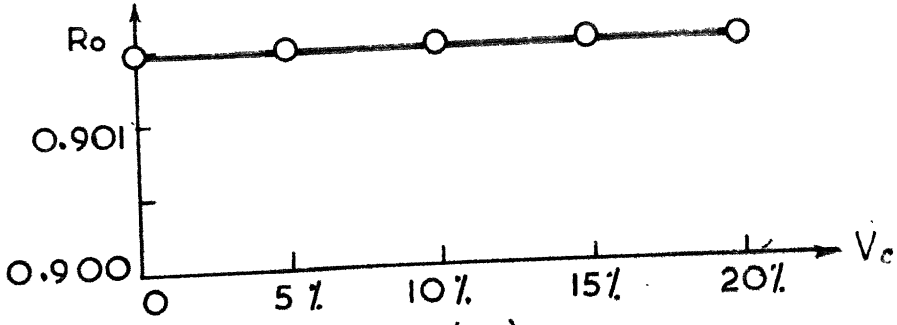

(c)

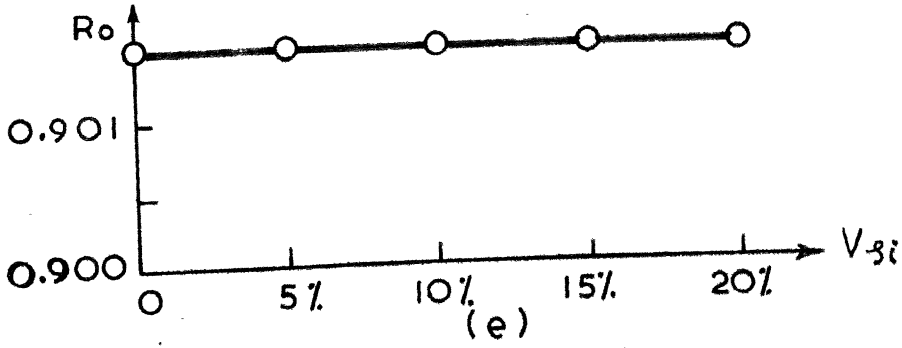

(e)

AT INITIAL DESIGN

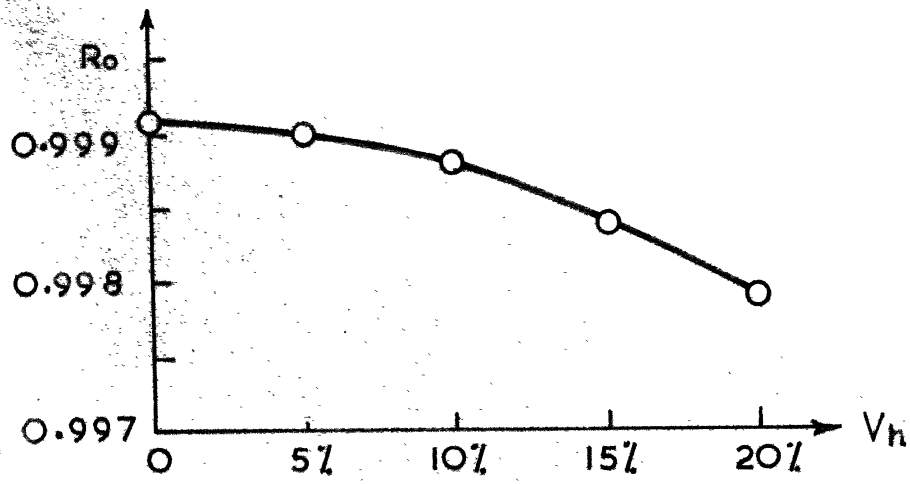

(b)

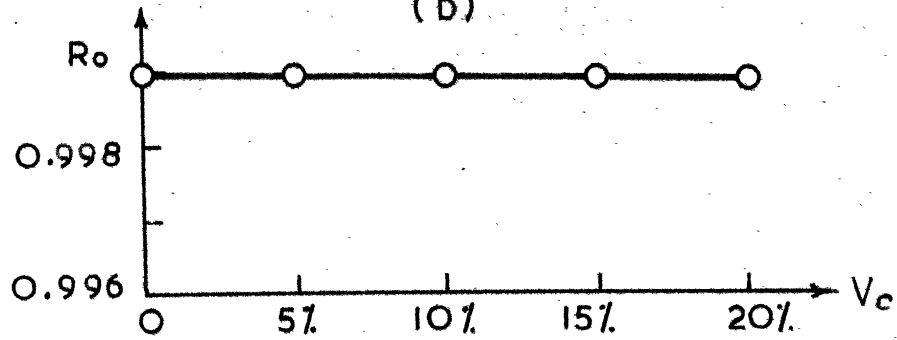

(d)

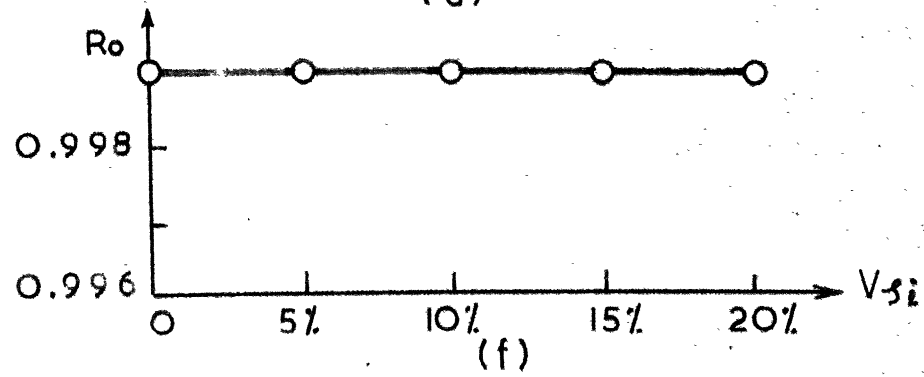

(f)

AT OPTIMUM DESIGN

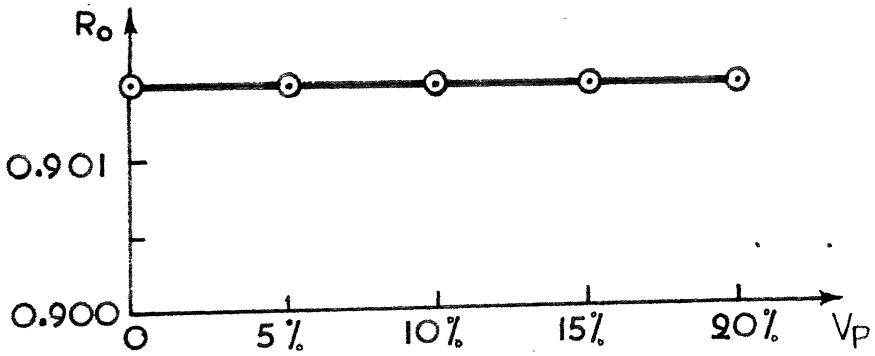

(g)

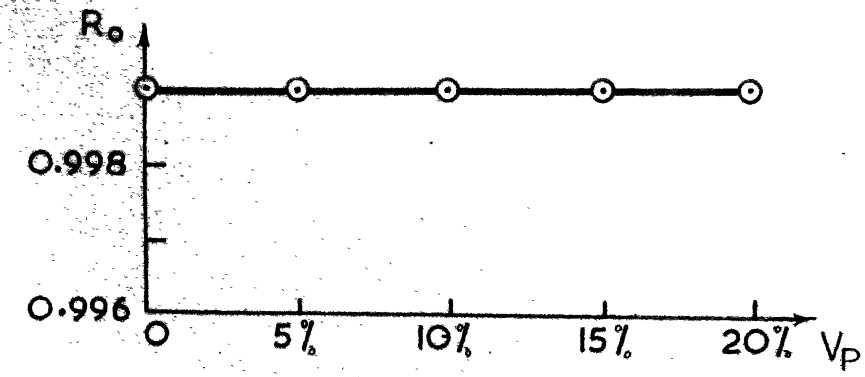

(h)

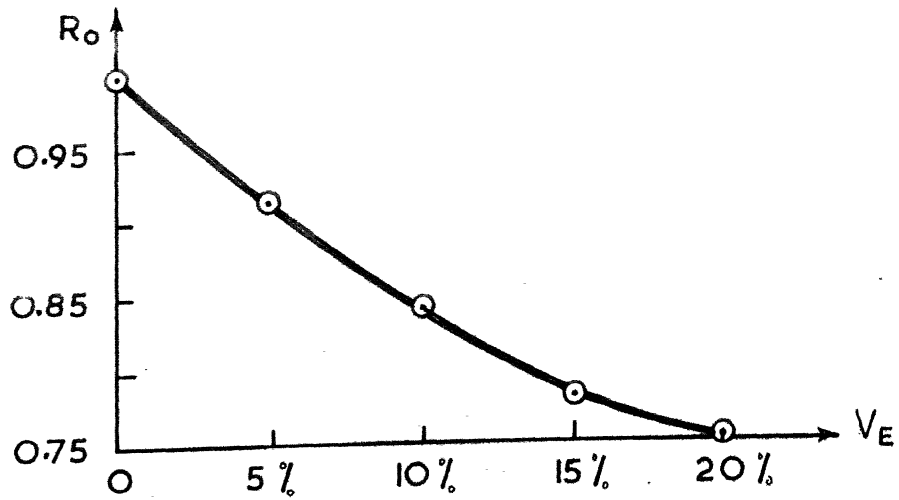

(i)

AT INITIAL DESIGN

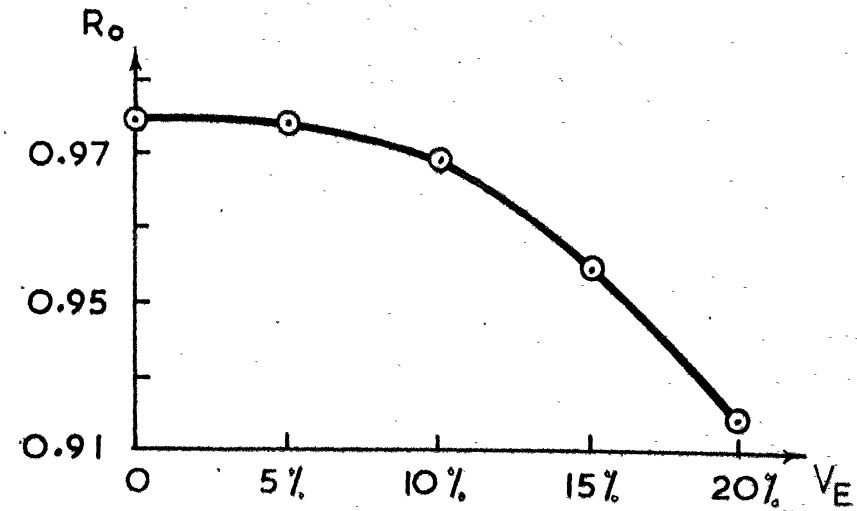

(j)

AT OPTIMUM DESIGN

FIG.8·4 RELIABILITY CURVES AGAINST FIRST NATURAL FREQUENCY

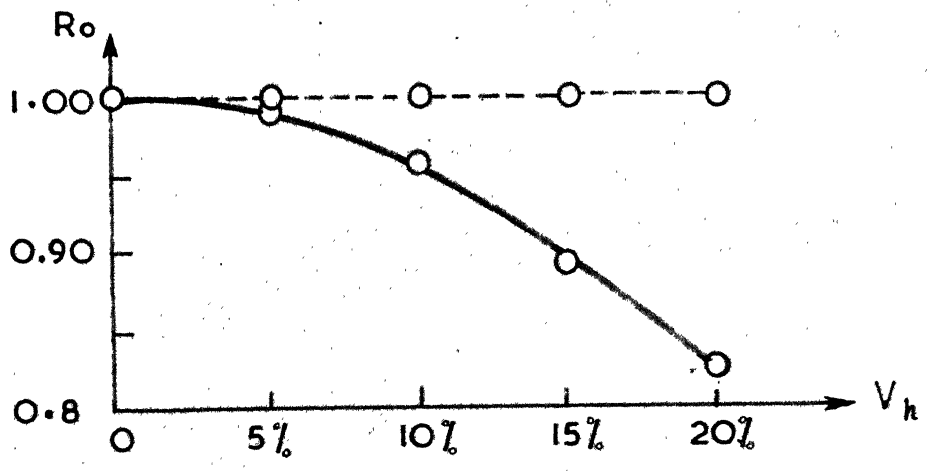
Ro
1.00
0.90
0.8
0
5%
10%
15%
20%
V_h

(a)

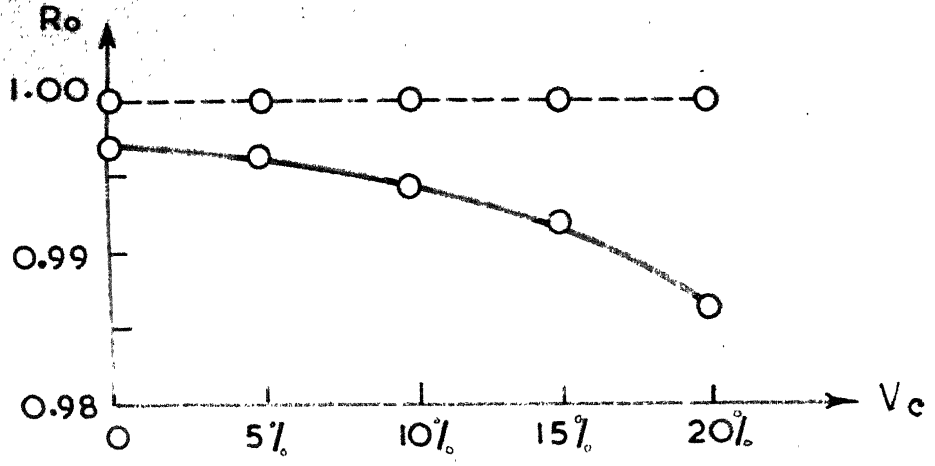
Ro
1.00
0.99
0.98
0
5%
10%
15%
20%
V_c

(d)

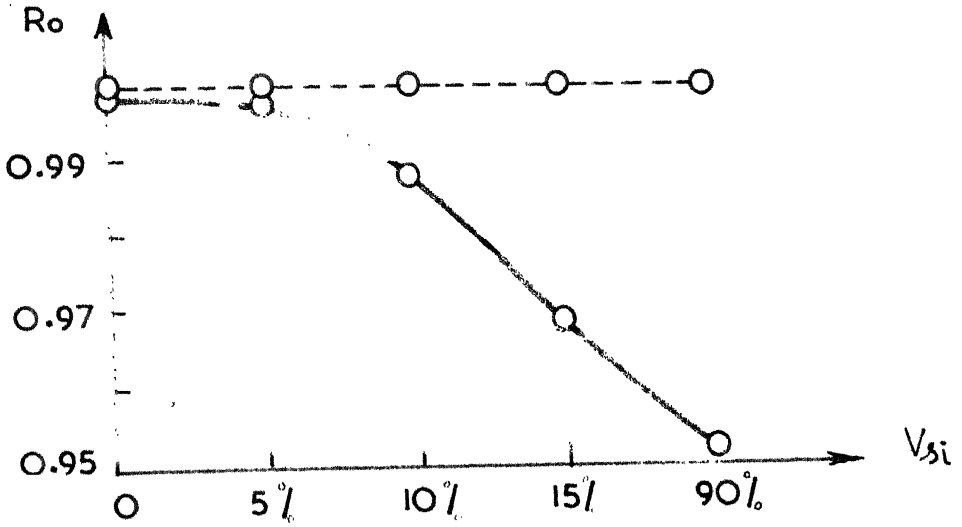
Ro
0.99
0.97
0.95
0
5%
10%
15%
90%
V_{si}

(c)

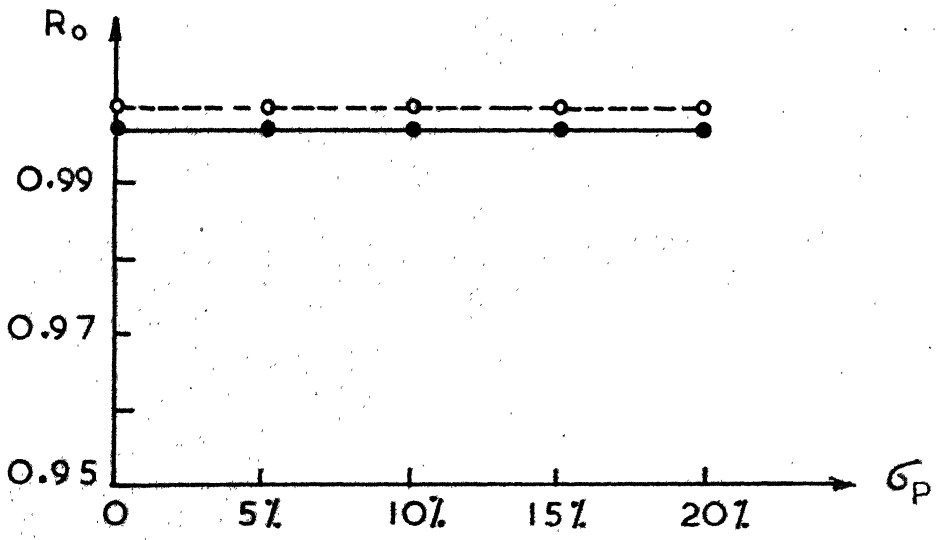

FIG D

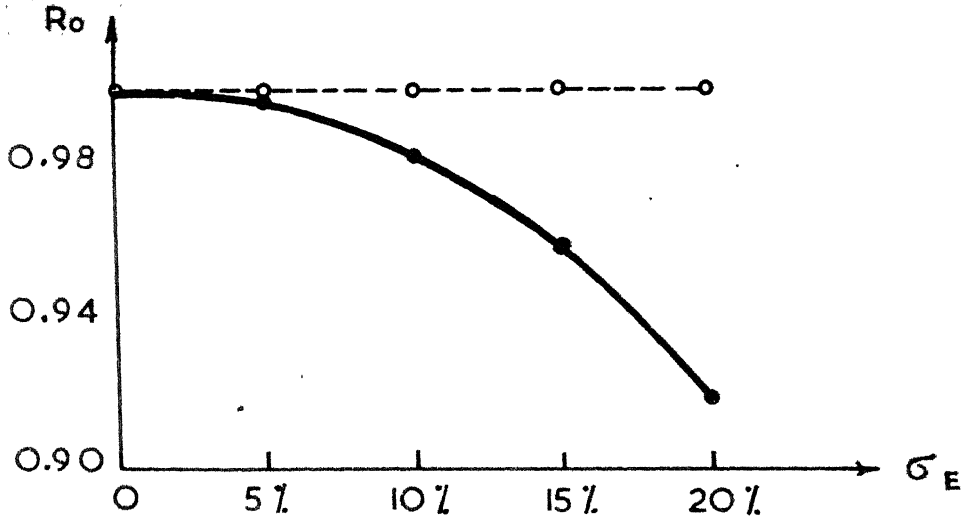

FIG E

---- AT INITIAL DESIGN
—— AT OPTIMUM DESIGN

FIG.8·5 RELIABILITY CURVES AGAINST G_{MIN}

CHAPTER 9

DISCUSSION AND CONCLUSIONS

The results of the example problems presented in chapter 7 demonstrate the feasibility of automated optimum design of machine tool structures with static, dynamic and regenerative chatter stability constraints. The numerical results of chapter 8 indicate the feasibility of reliability analysis of complex machine tool structures. In this chapter, the results given in the previous two chapters are analysed and the conclusions drawn therefrom are enumerated. In designing these complex machine tool structures with multiple behavior constraints several analysis programs have been developed and incorporated into the optimization routine and therefore it is difficult to summarize all the findings. The conclusions drawn from the present study are grouped in section 9.1. Finally suggestions to extend the scope of the design problems are given in section 9.2.

9.1 SUMMARY AND CONCLUSIONS

(1) In the finite element idealisation of Warren type lathe bed and horizontal milling machine structures, triangular plate bending elements and frame elements have been found to be simple and efficient. A moderate number of finite elements have yielded reasonably accurate results. The grouping

of finite elements of the same size, having the same transformation matrix from elemental to global coordinate system, has resulted in a saving of about 20 to 80% of the computer time in generating the global stiffness and mass matrices. In the reanalysis cycle of optimization procedure, the generation of stiffness and mass matrices of the structure is required a number of times and hence the grouping of such elements has resulted in saving of considerable computer time.

(2) The cholesky decomposition of symmetric banded matrices has efficiently been used in solving equilibrium equations and in obtaining a partial solution of eigenvalue problem by Raleigh-Ritz sub-space iteration algorithm. This algorithm solves the eigenvalue problem directly without a transformation to the standard form. This method is the most efficient one for solving a partial eigen solution of large structural systems.

(3) The receptances of the cutter centre relative to the table of horizontal milling machine have been obtained by using modal coordinates assuming the damping matrix as a linear combination of stiffness and mass matrices.

(4) In this work, the geometrical constraints are linear, whereas the behavior constraints and the objective function are non-linear. Hence the constrained optimum design problem is cast as a nonlinear mathematical programming problem. The computational experience shows that the approximate methods used

in the present work for evaluating the gradient and the slope of ϕ-function have been quite efficient and reliable without involving any significant errors. The progress of optimization has been quite smooth without any undue number of optimization steps.

(5) In computing the values of G_{MIN} for regenerative chatter stability in designing milling machine structures, all the possible common cutting conditions have been considered. For an unit amplitude of harmonic forcing, the negative inphase cross receptances have been computed at an interval of 10 radians/second beginning from the first natural frequency to fourth natural frequency of vibration and from these, the minimum value (G_{MIN}) has been found out.

(6) The coupling constants in plain milling operation are required in the design of horizontal milling machine structures for regenerative chatter stability. The coupling constants are obtained, for most common range of cutting conditions, both by the application of basic theory of metal cutting and by using a procedure based on an empirical formula suggested by Vulf. The values obtained from both these methods agree well with each other. The limiting value of the coupling constant (r_{LIM}) has been selected from this analysis.

(7) From the optimum results of lathe bed (example 1), it has been found that the thickness of both the main members and

lacing diagonals decrease as the optimization progressed. At the optimum, the thicknesses are found to be the same and are at their lower bounds. This indicates that the thin structures are preferable for this type of lathe beds. The widths and thicknesses of flanges (stiffners) on main members and lacing diagonals also decreased as the optimization progressed. In example 2, the width of the lathe bed is also included as a design variable and the behavior constraints are taken as nearly active at the initial design. The results show that the width of the lathe bed increased with a corresponding value of the lacing angle as 53.5°. This value of the lacing angle agrees very well with the results obtained by Badauri, Moshin and Thornley who analysed and tested various Warren beams under static torsional loads. It may also be mentioned that the thicknesses of both main members and lacing diagonals decreased approximately at the same rate and at the optimum, their values were same. Therefore, it can be concluded that it is preferable to have equal values of thickness for the main members and lacing diagonals. In designing this type of structures, the machine tool structural designer can adopt this as a general guide line.

(8) The optimization results of the milling machine structure (examples 3a and 3b) show that the thicknesses of the over-arm, the column and the table decreased as the optimization progressed.

Even in horizontal milling machine structures, it can be concluded that thin structures are preferable. The cross sectional areas of the square ribs on the over-arm and its joint with the column also decreased as the optimization progressed. For the same width and depth of cut in plain milling, the static forces on the machine can be reduced by decreasing the feed. Hence the design becomes safer from the static rigidity point of view. However, the same can't be said about the chatter stability of the machine. Before the rated maximum horse power capacity of the machine is reached, the regenerative chatter may develop dependong upon the orientation of the cutting forces and the value of the corresponding coupling constant. Since chatter stability determines the metal removal rate, it becomes essential that the value of the coupling constant be taken for the worst case in designing milling machine structures for chatter stability.

(9) At initial and optimum designs, the reliability analysis of milling machine structures in various failure modes by taking the average height of the table (h), position of the cutter centre (c), modal damping factors (ζ_i), Young's modulus (E) and the loads (P) on the machine as probabilistic quantities. The results show that at optimum design, the reliabilities are very much lower compared to those at the initial design.

This is expected since the behavior quantities are far from the allowable limits at the initial design. According to the results obtained, at initial and optimum designs, the reliability against deflection is more sensitive with respect to σ_P and σ_E. The reliability against deflection with respect to σ_h and σ_c is not as sensitive as with respect to σ_P and σ_E. The reliabilities of the structure, at initial and optimum designs, against ω_1 are more sensitive with respect to σ_E and σ_h. With respect to the variation of other probabilistic quantities (σ_c, σ_{ζ_i} and σ_P), the reliabilities do not change. The reliabilities of the structure at optimum design against G_{MIN} show that the sensitivities will increase with respect to the coefficients of variation of the probabilistic quantities P, c, ζ_i, E and h in increasing order. At the initial design, the reliability against G_{MIN} remained almost constant at 1.

9.2 RECOMMENDATIONS FOR FURTHER WORK

(1) An obvious extension of the present work is to apply the procedure of analysis and automated optimum design to the complete lathe machine structure including the gear box casing, the spindle and its supports. The location and the number of spindle supports and their flexibilities can be included as design variables.

(2) In a milling machine structure, the overall dimensions like the depth of the column at the base, the depth of the column at the top and the width of the machine are very important. It is difficult to summarize the general relationship between these major dimensions from the design example considered in the present work. Therefore, to serve as a general guide for a machine tool structural designer, it is worthwhile to optimize a number of horizontal milling machine structures for various horse power capacities, sizes of work piece and limits on behavior constraints and establish a general relationship between these major dimensions.

(3) In horizontal milling machines the over-arm forms an important part and, therefore, for a given column of the milling machine structure, the over-arm can be further optimized by taking the following quantities as design variables :

i) number of ribs on the structure

ii) cross-sectional shape on the ribs

iii) taper of the over-arm on the sides

iv) taper of the over-arm on the top

v) depth of the over-arm

vi) width of the over-arm.

The analysis can be made either by taking the joint of the over-arm with the column as a flexible support or by idealising the column as a whole by frame elements.

(4) The design of machine tool structures for other criteria like maximization of static rigidity, fundamental natural frequency and regenerative chatter stability can also be studied.

(5) The reliability analysis procedure presented in this work can be extended to cases where the design parameters follow distributions other than normal distribution.

(6) The operating conditions, material and structural properties (damping factors are influenced by the joints of the structure) vary substantially in machine tool structures. Instead of optimizing machine tool structures by taking the most unfavourable cutting conditions and sizes of work piece, the reliability based optimum design of machine tool structures can be attempted to get a more realistic design by considering the operating conditions, material and structural properties as probabilistic quantities.

REFERENCES

The following abbreviations have been used in the names of the journals.

Proceedings	-	Proc.
International	-	Int.
MTDR	-	Machine Tool Design and Research
JIE (INDIA)	-	Journal of Institution of Engineers (INDIA)
Trans. ASME	-	Transactions of American Society of Mechanical Engineers
Proc. IME	-	Proceedings, Institution of Mechanical Engineers, London
JMES	-	Journal of Mechanical Engineering Science
AIAA	-	American Institute of Aeronautics and Austronautics
JSD, ASCE	-	Journal of the Structural Division, Proceedings, ASCE
JEMD, ASCE	-	Journal of the Engineering Mechanics Division, Proceedings, ASCE
JEI, ASME	-	Journal of Engineering for Industry, Transactions, ASME

1. TAYLOR, S. and TOBIAS, S.A., " Lumped Constants Method for the Prediction of Vibration Characteristics of Machine Tool Structures", Proc. 5th Int. MTDR Conference, Sept. 1964, PP. 37-52.

2. COWLEY, A. and FAWCETT, M., "Analysis of Machine Tool Structures by Computing Techniques", Proc. 8th Int. MTDR Conference, 1967, PP. 119-130.

3. BADAURI, M.W., MOSHIN, M.E. and THORNLEY, R.H., "The Static Analysis of Warren Beams Under Torsional and Bending Loads", The Int. Journal of MTDR, Vol. 3,1963, PP. 177-191.

4. THORNLEY, R.H. and HOWES, P.S., "Static and Dynamic Behaviour of Warren Type Machine Tool Structural Elements", JEI, ASME, May 1971, PP. 467-476.

5. PETERS, J., VANHERCK, P., VANDEN, L., WOLF, A.C.H.V., OPITZ H., SCHLEMPER, K., HOSHI, T., TOBIAS, S.A., TAYLOR, S., KOENIGSBERGER, F., and COWLEY, A., "Cooperative Work in Computer Aided Design in the CIRP."

6. COWLEY, A., "Cooperative Work in Computer Aided Design in the CIRP," Seminar on Computer Techniques in Production Engineering Design and Research, Indian Institute of Technology, Madras, India.

7. KOENIGSBERGER, F. and SAID, S.M., "The Production Engineer", 39, 270 (1960).

8. ANDREW, C. and TOBIAS, S.A., " Vibration in Horizontal Milling ", Int. Journal of MTDR, Vol. 2, 1962,PP.369-378.

9. TAYLOR, S., "The Design of Machine Tool Structures Using a Digital Computer," Proc. 7th Int. MTDR Conference, 1966, PP. 369-383.

10. GURNEY, J.P. and TOBIAS, S.A., "A Graphical Analysis of Regenerative Machine Tool Instability", Trans. American Society of Mechanical Engineers, B., Feb., 1962.

11. GURNEY, J.P., "A General Analysis of Two-Degree of Freedom Instability in Machine Tools," JMES, 4, 1962.

12. SWEENEY, G. and TOBIAS, S.A., "An Algebraic Method for the Determination of Dynamic Instability of Machine Tools", Int. Research in Production Engineering, 1963.

13. TLUSTY, J. and POLACEK, M., "Experience with Analysing Stability of Machine Tool Against Chatter," Proc. 9th Int. MTDR Conference, 1968, PP. 521-570.

14. SAID, S.M., "The Stability of Horizontal Milling Machines," Int. Journal of MTDR, Vol. 14, Oct. 1974, PP. 245-265.

15. KOENIGSBERGER, F. and TLUSTY, J., "Machine Tool Structures," Vol.1, Pergamon Press, 1970.

16. YOSHIMURA, M. and HOSHI, T., "Computer Approach to Dynamically Optimum Design of Machine Tool Structures," Proc. 12th MTDR Conference, 1971.

17. FOX, R.L. and KAPOOR, M.P., "Structural Optimization in the Dynamic Response Regime: A Computational Approach," AIAA Journal, Vol.8, No. 10, Oct.1970.

18. McCART, B.R., HANG, E.J. and STREETER, T.D., "Optimal Design of Structures with Constraints on Natural Frequency," AIAA Structural Dynamics and Aeroelasticity Specialist Conference, New Orleans, April 1969.

19. TURNER, M.J., "Design of Minimum Mass Structures with Specified Natural Frequencies," AIAA Journal, Vol. 5, No. 3, March 1967.

20. ZARGHAMEE, M.S., "Optimum Frequency of Structures," AIAA Journal, Vol. 6, No. 4, April 1968.

21. FOX, R.L. and KAPOOR, M.P., "Rates of Change of Eigen Values and Eigen Vectors", AIAA Journal, Vol. 6, No. 12, December 1968.

22. ZARGHAMEE, M.S., "Minimum Weight Design with Stability Constraint," JSD, ASCE, Vol. 96, No. ST , August 1970.

23. SCHMIT, L.A. and THORNTON, W.A., "Synthesis of an Airfoil at Supersonic Mach Number," NASA CR-144,1965.

24. GILES, G.L., "Procedure for Automating Aircraft Wing Structural Design," JSD, ASCE, Vol. 97, No. ST1, January 1971.

25. STROUD, W.J., DEXTER, C.B. and STEIN, M., "Automating Preliminary Design of Simplified Wing Structures to Safety, Strength and Flutter requirements," LWP-961, Langley Research Centre, Hampton, May 1971.

26. RAO, S.S., "Automated Optimum Design of Aircraft Wings to Safety, Strength, Stability, Frequency and Flutter Requirements," Ph.D. Thesis, Case Western Reserve University, Cleveland, October 1971.

27. FARSHI, B. and SCHMIT, L.A., "Minimum Weight Design of Stress Limited Trusses," JSD, ASCE, January 1974.

28. NARASINGAM, M.S. and SRIDHAR RAO, J.K., "Optimization in Trusses Using Optimal Control Theory," JSD, ASCE, May 1975.

29. TWISDALE, L.A. and KHACHATURIAN, N., "Multistage Optimization of Structures," JSD, ASCE, May 1975.

30. FREUDENTHAL, A.M., "Safety and the Probability of the Structural Failure," Trans. ASCE, Vol. 121, 1956.

31. MOSES, F. and KINSER, "Optimum Structural Design with Failure Probability Constraints", AIAA Journal 5, 1152 (1967).

32. MOSES, F. and STEVENSON, J.D., "Reliability Based Structural Design",JSD,ASCE96, 221 (1970).

33. ANG, A.H.S. and CORNELL C.A., "Reliability Bases of Structural Safety and Design", JSD, ASCE, Sept. 1974.

34. RAVINDRA, M.K., LIND, N.C. and SIU, W., "Illustrations of Reliability Based Design," JSD, ASCE, September 1974.

35. MOSES, F., "Reliability of Structural Systems," JSD, ASCE, Sept. 1974.

36. MISCHKE, C., "A Method of Relating Factor of Safety and Reliability", JEI, ASME, Vol. 92, p. 537,1970.

37. RAO, S.S., "A Probabilistic Approach to the Design of Gear Trains," Int. Journal of MTDR, Vol. 14, 1974.

38. Tocher, J.L., "Analysis of Plate Bending Using Triangular Elements," Ph.D. Dissertation, Civil Engineering Department, University of California, Berkeley, 1962.

39. Clough, R.W. and Tocher, J.L., "Finite Element Stiffness Matrices for Analysis of Plate Bending," Proceedings Conference on Matrix Methods in Structural Mechanics, WPAFB, Ohio, October 1965.

40. PRZEMIENIECKI, J.S., " Theory of Matrix Structural Analysis," McGraw-Hill Book Co., New York, 1968.

41. BATHE, K.J. and WILSON, E.L., "Large Eigen Value Problems in Dynamic Analysis," JEMD, ASCE, Dec. 1972.

42. WILLIAM, Y.J., SHIEH, SENG-LIPLEE , and RICHARD, A.P., "Analysis of Plate Bending by Triangular Elements," JEMD, ASCE, October, 1968.

43. HINDUJA, S. and COWLEY, A., "The Finite Element Method Applied to the Deformation Analysis of Thin Walled Columns," Proc. 12th Int. MTDR, Sept. 1971.

44. "Course on Computer Techniques for Design of Machine Structures, Central Machine Tool Institute, Bangalore, India, August, 1973.

45. AIREY, J., and OXFORD, C.J., "On the Art of Milling," Trans. ASME., Vol. 43, 1921, P. 549.

46. PARSONS, F., "Power Required for Cutting Metals," Trans. ASME., Vol. 45, 1923, P. 193.

47. BOSTON, O.W., and KRAUS, C.E., " Elements of Milling," Trans. ASME., Vol. 54, 1932, P. 71 and Vol. 56, 1934, P. 358.

48. MARTELLOTTI, M.E., "An Analysis of the Milling Process- Pt. I", Trans. ASME, Vol. 63, 1941, P. 677.

49. MARTELLOTTI, M.E., "An Analysis of the Milling Process- Pt. II", Trans. ASME, Vol. 67, 1945, P. 233.

50. KOENIGSBERGER, F., and SABBERWAL, A.J.P., "Chip Section and Cutting Force During the Milling Operation," Annalen, C.I.R.P. 1960.

51. SEN, G. C. and BHATTACHARYA, A., "Principles of Metal Cutting," New Central Book Agency, Calcutta, India.

52. OPITZ, H., "Influence of Vibrations on the Life of Tools and on Surface Quality in Milling Operations," Michrotechnic, No. 2, Vol. 12, 1958.

53. SINGH, G.D., BANERJEE, S., CHOWDHARY, S., and BHATTACHARYYA, A., "Analysis of Milling Forces," Pt. 1 and 2, JIE, (India), Vol. 44, No.11, Pt. ME-5, July 1964.

54. MERCHANT, M.E., "Basic Mechanics of the Metal Cutting Process", Journal of Applied Mechanics; Vol. 15, No.9, Sept. 1944.

55. BOSTON, O.W., GILBERT, W.W. and KAISER, K.B., "Power and Forces in Milling SAE 3150 Steel With Helical Cutters," Transactions of ASME, 1937, Vol. 59, P. 545.

56. VULF, A.M., "Theory of Metal Cutting," Text in Russian, Moscow, 1963.

57. ARMAREG, E.J. and BROWN, R.H., "The Machining of Metals", Prentice Hall, Inc. Englewood Cliffs, New Jersey, 1969.

58. KOENIGSBERGER, F., "Design Principles of Metal Cutting Machine Tools", A Pergamon Press Book, The Macmillan Company, New York, 1964.

59. KASIRIN, A.J., "Research in Vibrations in Metal Cutting," Publication of the Academy of Science, U.S.S.R.,Moscow, 1944.

60. ARNOLD, R.N., "Mechanism of Tool Vibrations in Cutting Steel," Proc. IME, Vol. 154, 1956.

61. TLUSTY, J. and POLACEK, M., "The Stability of Machine Tools Against Self-excited Vibrations in Machining," Production Engineering Research Conference, A.S.M.E., Pittsburg, 1963.

62. TOBIAS, S.A. and FISHWICK, W., "The Chatter of Lathe Tools Under Orthogonal Cutting Conditions," Trans.ASME. 80 (1958), P. 1079.

63. TOBIAS, S.A., "Machine Tool vibrations", Glasgow, Blackie and Sons Ltd., 1965.

64. LEE, E.H. and SHAFFER, B.W., "The Theory of Plasticity applied to a Problem of Machining," Trans. A.S.M.E., Vol. 73, 1951.

65. ABULADZE, N.G., "Elements of Mechanics of Metal Cutting", Thesis for Candidate of Science, Georgia Polytechnic Institute, Tbilisi, 1962.

66. HURTY, C. and RUBINSTEIN, M.F., "Dynamics of Structures," Prentice Hall, Inc. Text Book, 1964.

67. HARIHARAN, M., "Optimum Design of Elastic Cable Stayed Structures," Ph.D. Thesis, I.I.T., Kanpur, 1972.

68. ROSEN, J.B., "The gradient Projection method for non-linear programming : Part I : Linear Constraints," SIAM Journal, 9, 514-532, 1961.

69. GOLDFARB, D., "Extension of Davidons' Variable Metric Algorithm to Maximization under Linear Inequality and Equality Constraints," SIAM Journal of Applied Mathematics, 17, 739-764, 1966,

70. ZOUTENDIJK, G., "Method of Feasible Directions," Elsevier, Amsterdam, 1960.

71. FIACCO, A. and McCORMICK, G.P., "The Sequential Unconstrained Minimization Technique for Nonlinear Programming, A Primal-Dual Method," Journal of Management Science, Vol. 10, No. 2, January 1964,

72. FLETCHER, R. and POWELL, M.,J.D., "A Rapidly Convergent Descent Method for Minimization," Computer Journal (British), Vol. 6, 1963.

73. BOX, M.J., "A Comparision of Several Current Optimization Methods and the use of Transformations in Constrained Problems," Computer Journal (British), Vol.9, 1966.

74. FOX, R.L., "Optimization Methods for Engineering Design", Addison, Wesley Publishing Company, Reading, Massachussets, 1971.

75. FOX, R.L., "Constraint Surface Normals for Structural Synthesis Techniques," AIAA Journal 3 (8) 1965.

76. KAPOOR, M.P., "Automated Optimum Designs of Structures under Dynamic Response Restrictions," Ph.D. Thesis, Case Western Reserve University (1969).

77. IMDAD IMAM, SANDOR, G.N. and KRAMER, S.N., "Deflection and Stress Analysis in High Speed Planar Mechanisms with Elastic Links," JEI, ASME, May 1973.

78. ANG, A.H.S. and TANG, W.H., "Probability Concepts in Engineering Planning and Design ", Volume 1 Basic Principles, John Wiley & Sons, Inc., New York 1975.

APPENDIX A

ELEMENT STIFFNESS AND MASS MATRICES

A.1 ELEMENTAL STIFFNESS AND MASS MATRICES OF A TRIANGULAR PLATE BENDING ELEMENT

In deriving the elemental stiffness matrix [K] for a triangular plate bending element (shown in Fig. A. 1), when both in plane and bending stiffnesses are considered, equations 3.1, 3.2 and 3.3 of chapter 3 are used. From equations 3.1 and 3.2, the in-plane stiffness matrix $[K]_p$ of the element will result in a 6 x 6 matrix in local coordinate system. The matrix $[K]_p$ can be written as follows:

$$[K]_{p\ (6x6)} = \begin{bmatrix} [S_{11}]_p & [S_{12}]_p & [S_{13}]_p \\ (2x2) & (2x2) & (2x2) \\ [S_{21}]_p & [S_{22}]_p & [S_{23}]_p \\ (2x2) & (2x2) & (2x2) \\ [S_{31}]_p & [S_{32}]_p & [S_{33}]_p \\ (2x2) & (2x2) & (2x2) \end{bmatrix} \quad (A.1)$$

For in-plane analysis, the relationship between the nodal dis - placements and forces of an element can be written as :

$$\begin{bmatrix} P_{x_1} \\ P_{y_1} \\ P_{y_2} \\ P_{x_3} \\ P_{y_3} \end{bmatrix} = [K]_p \begin{bmatrix} u_1 \\ v_1 \\ u_2 \\ v_2 \\ u_3 \\ v_3 \end{bmatrix} \qquad (A.2)$$

where u_i and v_i indicate the components of displacement of node $i(i=1,2,3)$ parallel to the local x-and y-axes respectively. Similarly P_{x_i} and P_{y_i} denote the components of force at node $i(i=1,2,3)$ parallel to the x-and y-axes respectively. Notice that the suffix 'p' has been used to indicate the in-plane stiffness matrix in equation (A.1).

Similarly a relation between the forces and displacements corresponding to the bending of the plate (obtained from equation 3.3 of chapter 3) can be written as :

$$\begin{bmatrix} P_{z_1} \\ M_{x_1} \\ M_{y_1} \\ P_{z_2} \\ M_{x_2} \\ M_{y_2} \\ P_{z_3} \\ M_{x_3} \\ M_{y_3} \end{bmatrix} = [K]_b \begin{bmatrix} w_1 \\ x_1 \\ y_1 \\ w_2 \\ x_2 \\ y_2 \\ w_3 \\ x_3 \\ y_3 \end{bmatrix} \qquad (A.3)$$

where $[K]_b$ is the bending stiffness matrix in the local coordinate system. Here w_i and P_{z_i} indicate the components of displacement and force parallel to z axis at node i, and M_{x_i} and M_{y_i} represent the generalized forces corresponding to θ_{x_i} and θ_{y_i} at node i respectively (i = 1,2,3) the suffix 'b' has been used to denote the bending stiffness matrix.

The order of the bending stiffness matrix, $[K]_b$, is 9 x 9 and it can be written in the following form :

$$[K]_b = \begin{bmatrix} [S_{11}]_b & [S_{12}]_b & [S_{13}]_b \\ (3x\ 3) & (3x\ 3) & (3x\ 3) \\ [S_{21}]_b & [S_{22}]_b & [S_{23}]_b \\ (3x\ 3) & (3x\ 3) & (3\ x3) \\ [S_{31}]_b & [S_{32}]_b & [S_{33}]_b \\ (3x\ 3) & (3x\ 3) & (3x\ 3) \end{bmatrix} \qquad (A.4)$$

In the analysis of three dimensional structures, both in-plane and bending stiffnesses have to be combined. In combining these stiffnesses the following points are taken into account:

i) For small displacements, the in-plane and bending stiffnesses are uncoupled,

and ii) the in-plane rotation θ_z (rotation about the local z- axis) is not necessary for a single element.

However, θ_z and its conjugate force M_z have to be considered in the analysis by including appropriate number of zeroes to obtain the elemental stiffness matrix (for the purpose of assembling several elements). Therefore to obtain the elemental stiffness matrix [K], the in-plane and the bending stiffnesses are combined as shown below :

$$
[K] = \left[\begin{array}{cccc|cccc|cccc}
[S_{11}]_p & & & & [S_{12}]_p & & & & [S_{13}]_p & & & \\
\multicolumn{4}{c|}{} & \multicolumn{4}{c|}{} & \multicolumn{4}{c}{} \\
\hline
\multicolumn{4}{c|}{} & \multicolumn{4}{c|}{} & \multicolumn{4}{c}{} \\
\multicolumn{4}{c|}{} & \multicolumn{4}{c|}{} & \multicolumn{4}{c}{} \\
\multicolumn{4}{c|}{} & \multicolumn{4}{c|}{} & \multicolumn{4}{c}{} \\
\hline
[S_{21}]_p & & & & [S_{22}]_p & & & & [S_{23}]_p & & & \\
\multicolumn{4}{c|}{} & \multicolumn{4}{c|}{} & \multicolumn{4}{c}{} \\
\hline
\multicolumn{4}{c|}{} & \multicolumn{4}{c|}{} & \multicolumn{4}{c}{} \\
\multicolumn{4}{c|}{} & \multicolumn{4}{c|}{} & \multicolumn{4}{c}{} \\
\multicolumn{4}{c|}{} & \multicolumn{4}{c|}{} & \multicolumn{4}{c}{} \\
\hline
[S_{31}]_p & & & & [S_{32}]_p & & & & [S_{33}]_p & & & \\
\multicolumn{4}{c|}{} & \multicolumn{4}{c|}{} & \multicolumn{4}{c}{} \\
\hline
\multicolumn{4}{c|}{} & \multicolumn{4}{c|}{} & \multicolumn{4}{c}{} \\
\multicolumn{4}{c|}{} & \multicolumn{4}{c|}{} & \multicolumn{4}{c}{} \\
\multicolumn{4}{c|}{} & \multicolumn{4}{c|}{} & \multicolumn{4}{c}{} \\
\hline
\end{array}\right]
$$

(A.5)

A.2 TRANSFORMATION TO GLOBAL COORDINATE SYSTEM

The stiffness matrix derived above (equation A.5) is with reference to the local coordinate system shown in Fig. A.1. In the analysis of complex structures having finite elements with different orientations, it becomes necessary to transform the local stiffness matrix to a common set of coordinates known as the global coordinate system. This can be achieved with the help of a transformation matrix, $[\lambda]$. The global stiffness matrix, $[K]_G$, of an element can be written as :

$$[K]_G = [\lambda]\ [K]\ [\lambda]^T \qquad (A.6)$$

where $[\lambda]^T$ represents the transpose of $[\lambda]$.

The transformation matrix is given by

$$\underset{(18 \times 18)}{[\lambda]} = \begin{bmatrix} [L] & & \\ & [L] & \\ & & [L] \end{bmatrix} \qquad (A.7)$$

where [L] is given by

$$\underset{(6\times6)}{[L]} = \begin{bmatrix} \ell_1 & m_1 & n_1 & 0 & 0 & 0 \\ \ell_2 & m_2 & n_2 & 0 & 0 & 0 \\ \ell_3 & m_3 & n_3 & 0 & 0 & 0 \\ 0 & 0 & 0 & \ell_1 & m_1 & n_1 \\ 0 & 0 & 0 & \ell_2 & m_2 & n_2 \\ 0 & 0 & 0 & \ell_3 & m_3 & n_3 \end{bmatrix} \qquad (A.8)$$

where ℓ_1, m_1 and n_1 represent the direction cosines of the local x-direction with respect to the X, Y and Z direction of the global coordinate system respectively. Similarly the suffixes '2' and '3' represent the direction cosines of the local y and z directions.

The elemental (consistent) mass matrix can be derived in a similar manner. However, in the present work, the lumped mass matrix, by neglecting the rotary inertia properties, is used for obtaining the eigen solution. This simplifying approximation effected considerable savings in computer storage and time at the expense of insignificant loss of accuracy in the eigen solution.

A 3 ELEMENTAL STIFFNESS AND MASS MATRICES OF A FRAME ELEMENT

The elemental stiffness and mass matrices of a frame element given in reference 40 have been used in the present work.

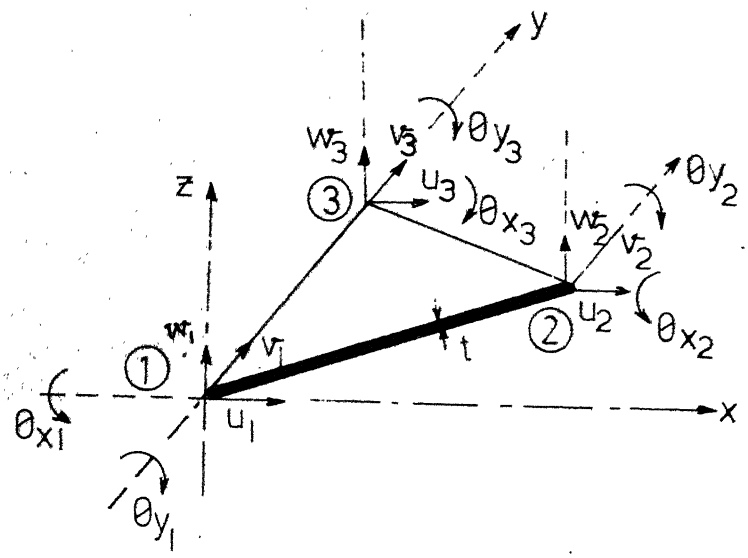

G. A.1 IN-PLANE AND BENDING DISPLACEMENT IN LOCAL COORDINATE SYSTEM

APPENDIX B

DESCRIPTION OF THE COMPUTER PROGRAM

The main computer program for the optimization of machine tool structures is written in FORTRAN IV language and it consists of 18 subroutines. Initially the computer program is perfected on IBM 7044 (at Indian Institute of Technology, Kanpur) and the final optimization results are obtained on IBM 370/155 computer at Indian Institute of Technology, Madras.

B.1 PURPOSE OF THE SUBROUTINES

(1) GSM : To generate the stiffness and mass matrices for a triangular plate bending element and frame element in a banded form.

(2) CBAND: To obtain the cholesky decomposition of symmetric banded matrices. This routine stores only the upper triangular band of the decomposed matrix and the diagonal of the matrix is stored in the first colurm.

(3) ZOLF : To solve the equilibrium equations from the upper triangular band of the decomposed stiffness matrix.

(4) BASIC : To obtain the partial eigen solution of a structure by Rayleigh-Ritz sub-space iteration technique. It calls routine EIGEN for solving the generalized Ritz problem.

(5) EIGEN : To compute the eigen values and eigen vectors of the generalized Ritz problem by power method.

(6) MATINV: To find the inverse of a real matrix.

(7) MATMUL: To multiply two real matrices.

(8) BAMMUL: To multiply two real banded matrices.

(9) RESP : To find the frequency response by the modal superposition technique.

(10) FTN : To compute the ϕ - function by exact method.

(11) FTNZ 2: To compute the ϕ -function by approximate method (making use of the expressions for the rates of changes of eigen values and eigen vectors).

(12) OBFEVA: To evaluate the objective function.

(13) GRADN : To calculate the gradient of ϕ-function by evaluating the response quantities by approximate method.

(14) SCAQUA: To evaluate scalar quantities for obtaining response quantities by rates of changes of eigen values and eigen vectors.

(15) STRESS : To compute the stress in different finite elements.

(16) MINIM4 : To implement the Davidon-Fletcher-Powell variable metric method of unconstrained minimization. It calls the one dimensional minimization routine STEPX2

(17) STEPX2 : It implements one-dimensional search method by cubic interpolation.

(18) SLOPE2 : To evaluate the slope of ϕ - function $(S^T.\nabla\phi)$.